# Analysis of 3D Shape Measurement for Fringe Projection Profilometry based Intraoral Scanner



**A Dissertation Defense #2**

**By**

**Furqan Ullah**

**December 13, 2013**

**Dissertation Chair: Park Kang, Ph.D.**

**Department of Mechanical Engineering**

**Myongji University**

**South Korea**

# Dissertation Committee

명지대학교
MYONGJI UNIVERSITY



**Kye Han Rhee, Ph.D.**
**(Chair)**

**Kang Park, Ph.D.**
**(Member)**

**Soo Jin Lee, Ph.D.**
**(Member)**

**Seungjae Min, Ph.D.**
**(Member)**

**Ji Hyun Yang, Ph.D.**
**(Member)**

# Outlines

명지대학교
MYONGJI UNIVERSITY

- Motivation and Objectives
- Introduction
  - What is a 3D Scanner?
  - What is Structured Light Technology?
  - What is Fringe Projection Technique?
  - Why we need an Intraoral Scanner?
- Implementation of Previous Work and Improvements
- Analysis of 3D Shape Measurement System Models
- Development of 3D Intraoral Scanner
- Development of a Real-time SMDFP System
- Development of a Real-Time Virtual 3D Scanner
- Development of Computer Software
- Conclusions
- Videos

# Ultimate Objective



**The ultimate objective of this dissertation is to develop a complete 3D intraoral scanning system, and a general purpose computer-aided scanning software for the analysis of 3D shape measurement systems.**

명지대학교
MYONGJI UNIVERSITY

# Dissertation Goals

- **Goals**
  - **Analysis of 3D shape measurement in order to develop an intraoral scanner**
  - **Development of a general purpose computer-aided 3D scanning software**

- **In order to achieve the goals, the following tasks has been implemented and completed:**
  - **Investigate the issues and problems in the development of an intraoral scanner**
  - **Improve the existing method and develop new approaches for acquiring the accurate point cloud data**
  - **Develop a real-time virtual 3D scanner in order to analyze different kinds of 3D scanning system models and to verify the proposed methods and algorithms**
  - **Develop a SMDFP system in order to test and verify the scanning methodology**
  - **Improve the various existing algorithms that involve in the pre and post processing**

# What is a 3D Scanner?



**A device that collects information on the shape of a real-world object and converts it to digital data named “point cloud” that can be used to construct a digital 3D model.**



Real-world Object ⇨ 3D Scanner ⇨ Point cloud ⇨ Digital 3D model

?

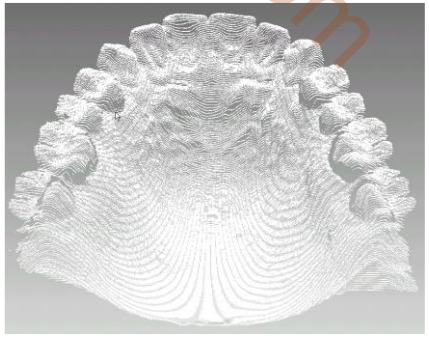

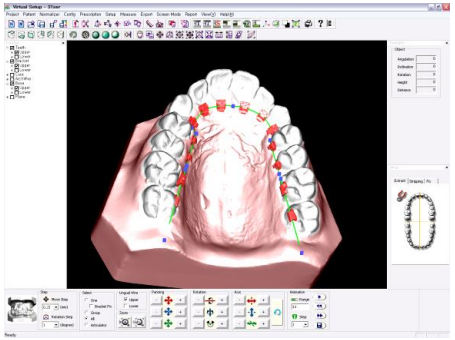

명지대학교
MYONGJI UNIVERSITY

# What is Structured Light Technology?

**Structured light is the process of projecting a known pattern of pixels (often grids or horizontal bars) on to a scene.** *(Wikipedia)*



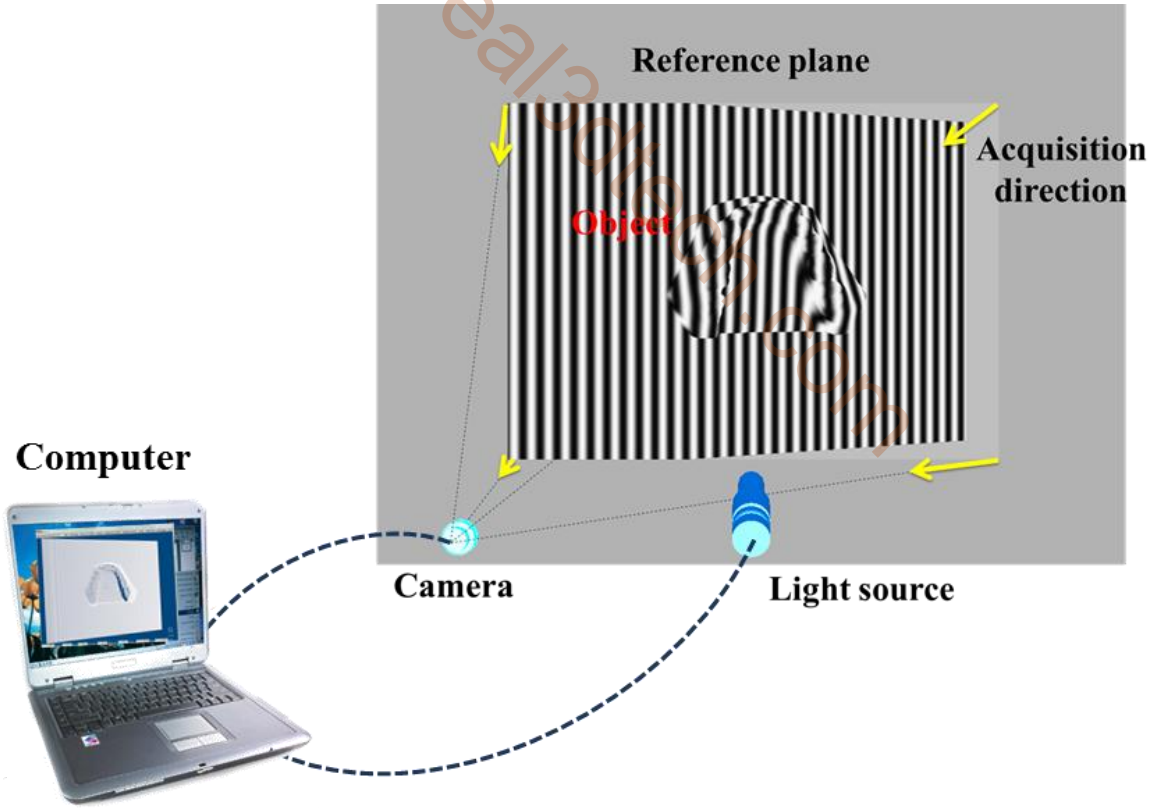

# What is Fringe Projection Technique?

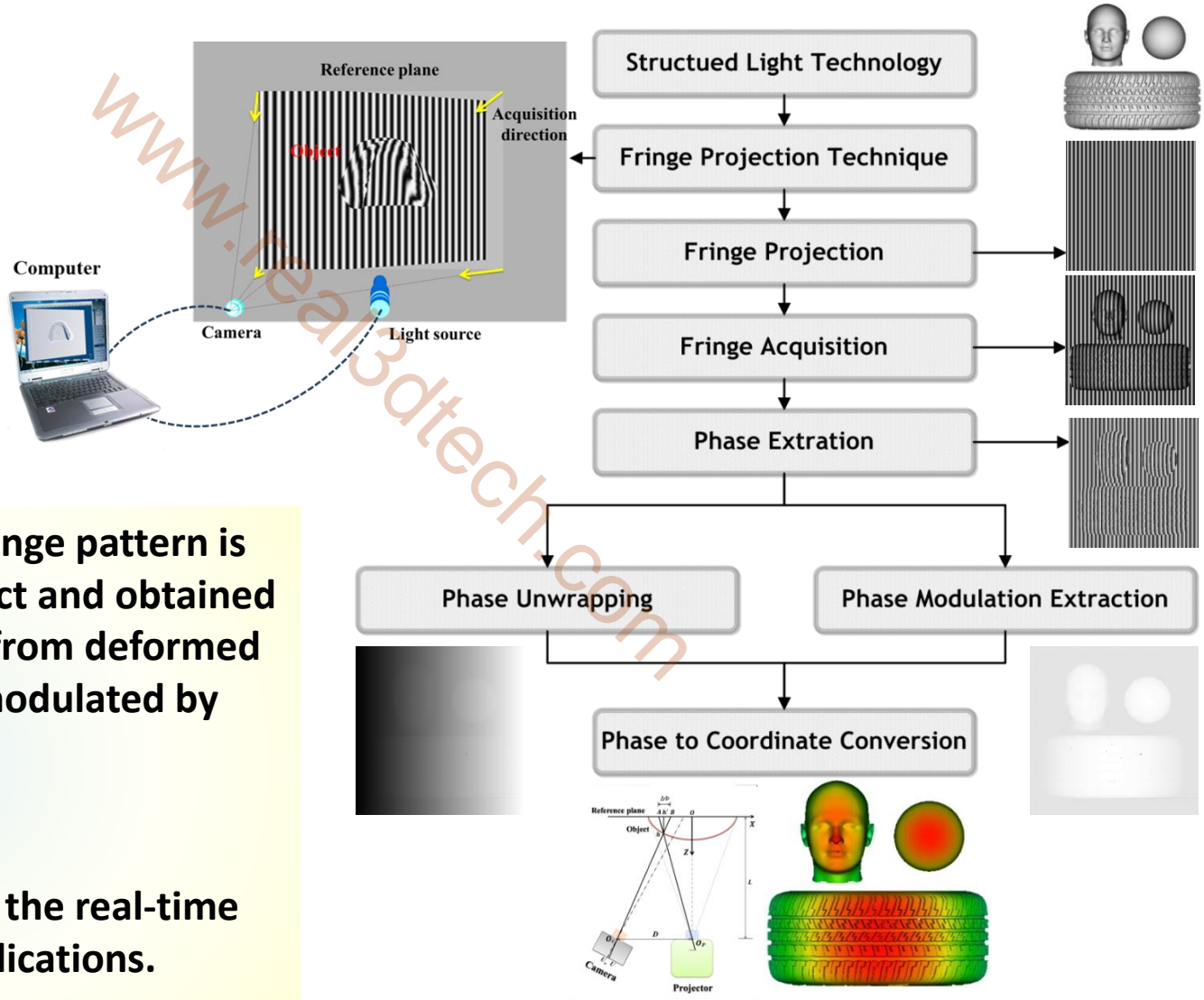




**In this technique, the fringe pattern is projected onto the object and obtained the height of an object from deformed fringe image, which is modulated by the object surface.**

**Increasingly popular for the real-time and high resolution applications.**

명지대학교 MYONGJI UNIVERSITY

# Applications of Structured Light 3D Scanners

- Precision shape measurement for production control (e.g. turbine blades)
- Reverse engineering (obtaining precision CAD data from existing objects)
- Volume measurement (e.g. combustion chamber volume in motors)

- Classification of grinding materials and tools
- Precision structure measurement of grinded surfaces
- Radius determination of cutting tool blades

- Skin surface measurement for cosmetics and medicine
- Body shape measurement
- Wrinkle measurement on cloth and leather

- Forensic science inspections
- Measurement of topography of solar cells
- Road pavement structure and roughness



*Source: Wikipedia*

명지대학교
MYONGJI UNIVERSITY

# Why we need an Intraoral Scanner?

❖ No need to make a plaster model


Tray Selection


Dispensing Materials


Setting of Materials


Disinfection

Shipping

❖ Handy and fast Intraoral Scanner


Intra Oral Scanning

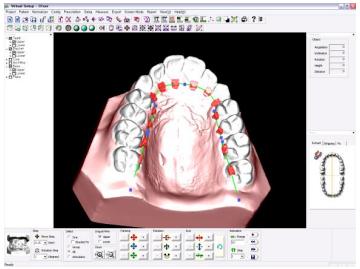
3D Dental Model

Treatment Planning

Operation Planning

Prosthetic Appliance

❖ Should be small, light, and accurate

# Existing Intraoral Scanners

**Only ten intraoral scanning devices for restorative dentistry are available all over the world**

| Country | Intraoral Scanning devices |
|---|---|
| **USA** | 4 |
| **Israel** | 2 |
| **Germany** | 2 |
| **Italy** | 1 |
| **Denmark** | 1 |
| **South Korea** | **?** |

**Only four are commercially available**

| No. | Companies |
|---|---|
| 1 | CEREC® – by Sirona Dental System GMBH (DE) |
| 2 | iTero – by CADENT LTD (IL) |
| 3 | E4D – by D4D TECHNOLOGIES, LLC (US) |
| 4 | Lava™C.O.S. – by 3M ESPE (US) |
| 5 | IOS FastScan – by IOS TECHNOLOGIES, INC. (US) |
| 6 | DENSYS 3D – by DENSYS LTD. (IL) |
| 7 | DPI-3D – by DIMENSIONAL PHOTONICS INTERNATIONAL, INC. (US) |
| 8 | 3D Progress – by MHT S.p.A. (IT) and MHT Optic Research AG (CH) |
| 9 | DirectScan – by HINT - ELS GMBH (DE) |
| 10 | Trios – by 3SHAPE A/S (DK) |



Ref: Silvia L., Giordano F., Ari K., Michele C., Lapo G., Luciano B., "A Comparative Analysis Of Intraoral 3d Digital Scanners For Restorative Dentistry," The Internet Journal of Medical Technology, Vol. 5, No. 1, 2011.

# The Fringe Pattern

**A fringe pattern can be considered as a sinusoidal signal fluctuation in two-dimensional space.**

$$I(i,j,t) = a(i,j)\left[1 + b(i,j)\cos\Phi(i,j)\right] + n(i,j)$$

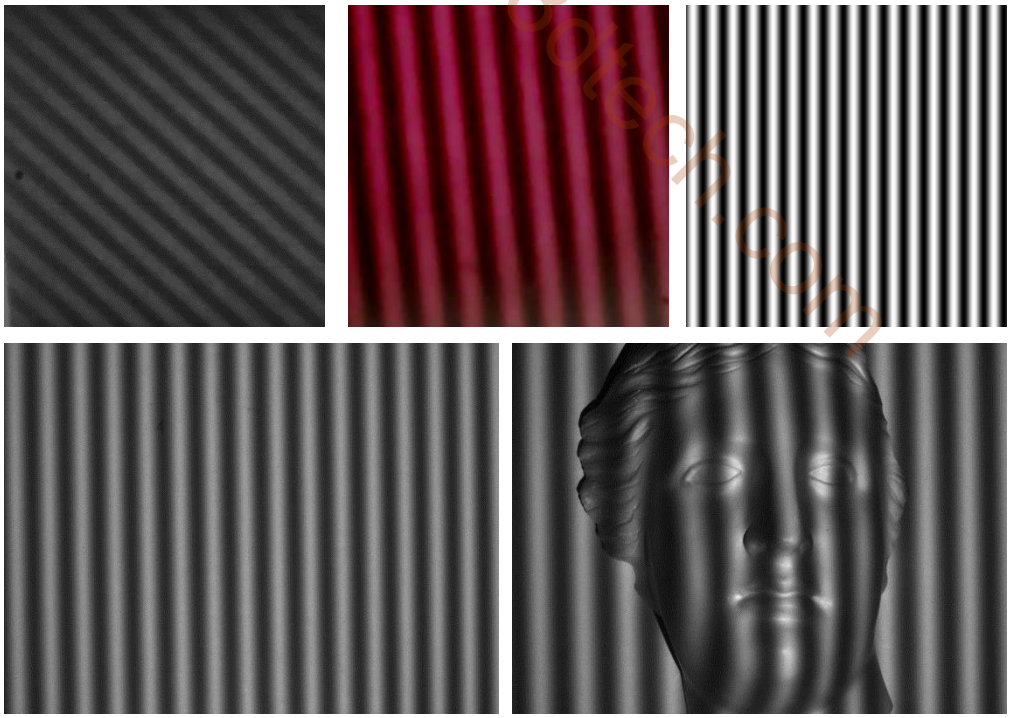

# Phase-Shifting Method



**The phase-shifting interferometry (PSI) method was first introduced by Bruning et al in 1974.**



***Basic equation:*** $$I(i,j,t) = a(i,j) + b(i,j)\cos\left[\Phi(i,j) + \delta(t)\right]$$

**There are several methods for phase extraction such as**
**2-step, 1+2 step,**
**3, 4, 5, step,**
**6, 7, 8, … step,**

**Carré Algorithm for Unknown Phase-shifts.**

**Most Common Sources of Errors**

- **Incorrect phase shift between data frames**
- **Vibrations**
- **Sensors non-linearity**
- **Quantization errors**
- **Stray reflections**
- **Intensity fluctuations**
- **Frequency stability**

# 3-Step Phase-Shifting Method

**The minimum number of patterns will be three.**



***Three equations:***

$$I_1(i,j) = a(i,j) + b(i,j)\cos[\Phi(i,j) - \delta]$$

$$I_2(i,j) = a(i,j) + b(i,j)\cos[\Phi(i,j)]$$

$$I_3(i,j) = a(i,j) + b(i,j)\cos[\Phi(i,j) + \delta]$$

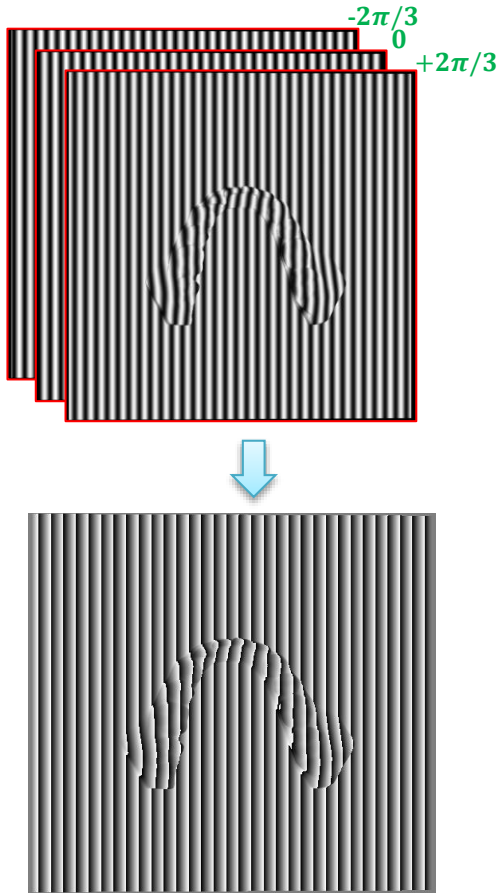


***Wrapped Phase Map:***

$$\Phi(i,j) = \tan^{-1}\left[\sqrt{3}\,\frac{I_1(i,j) - I_3(i,j)}{2I_2(i,j) - I_1(i,j) - I_3(i,j)}\right]$$

# 4-Step Phase-Shifting Method

## Most common and widely used algorithm in PSI



***Four equations:***

$$I_1(i,j) = a(i,j) + b(i,j)\cos[\Phi(i,j)]$$
$$I_2(i,j) = a(i,j) + b(i,j)\cos[\Phi(i,j) + \pi/2]$$
$$I_3(i,j) = a(i,j) + b(i,j)\cos[\Phi(i,j) + \pi]$$
$$I_4(i,j) = a(i,j) + b(i,j)\cos[\Phi(i,j) + 3\pi/2]$$

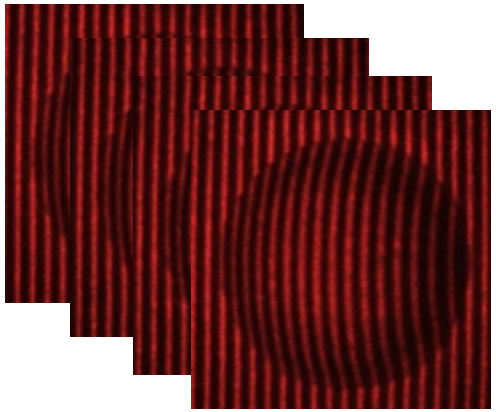

***Wrapped Phase Map:***

$$\Phi(i,j) = \tan^{-1}\left[\frac{I_4(\mathrm{i},\mathrm{j}) - I_2(\mathrm{i},\mathrm{j})}{I_1(\mathrm{i},\mathrm{j}) - I_3(\mathrm{i},\mathrm{j})}\right]$$

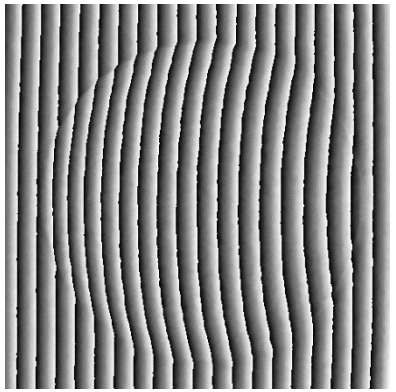

# 5-Step Phase-Shifting Hariharan Algorithm

**A very popular five-step algorithm offer advantages in reduced uncertainties in the phase calculation, reduced sensitivity to phase-shifter calibration, and robust to detuning.**



***The 5-phase stepped interferograms with a phase shift of π/2.***

***Wrapped Phase Map:***

$$\Phi(i,j) = \tan^{-1}\left[\frac{2\{I_4(\mathrm{i},\mathrm{j}) - I_2(\mathrm{i},\mathrm{j})\}}{I_1(\mathrm{i},\mathrm{j}) - 2I_3(\mathrm{i},\mathrm{j}) + I_5(\mathrm{i},\mathrm{j})}\right]$$

# Two-dimensional Phase-Unwrapping Method



**A linear unwrapped phase can be obtained by adding or subtracting 2π according to the phase jump ranging from –π to +π or vice versa.**



**Challenging issues involved in the computation of the linear phase**

- Discontinuities and noise in the observed image, which may cause large changes in the measured data
- Dark or low intensity area in the image, which makes the unwrapping equation difficult or sometime impossible to solve
- Inconsistencies in the unwrapping process when following different paths
- Phase jumps and Undersampling

***Relationship between the wrapped and unwrapped phases.***

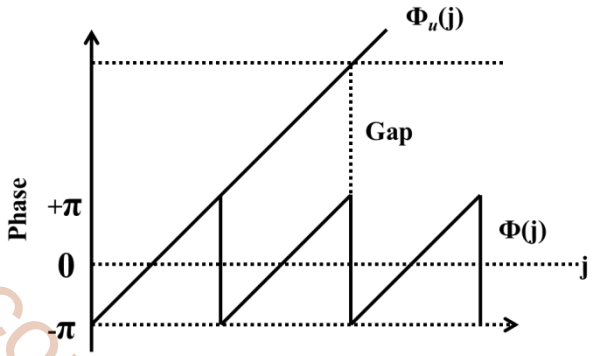


$$\Phi_u(i,j) = \Phi(i,j) + 2\pi k(i,j)$$

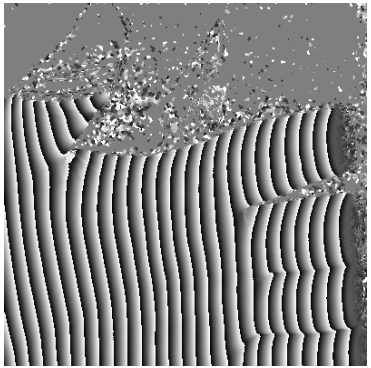

# Two-dimensional Phase-Unwrapping Method



***Comparison of different phase unwrapping algorithms***

***Residues Removal Filter:***

$$r = PG[k+1,k] + PG[k+1+N,k+1] + PG[k+N,k+1+N] + PG[k,k+N]$$

*If (r>0.001 || r <-0.001)*
*discard pixel k*



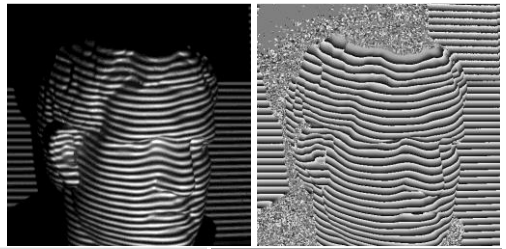

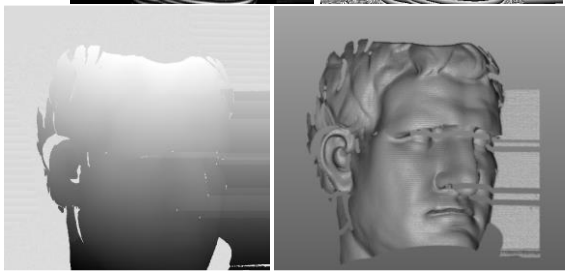

***Linear***

**Virtual Simulation**

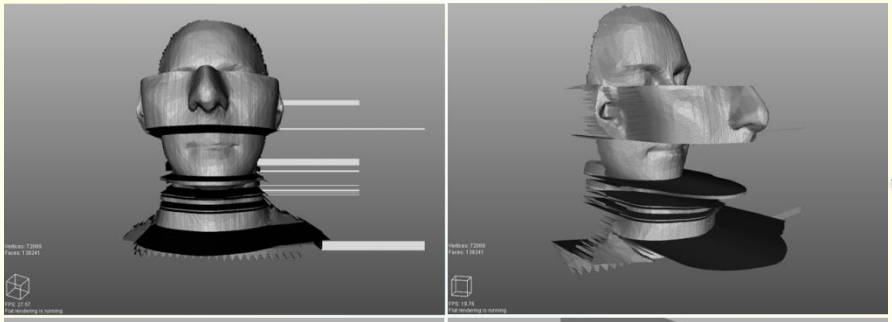

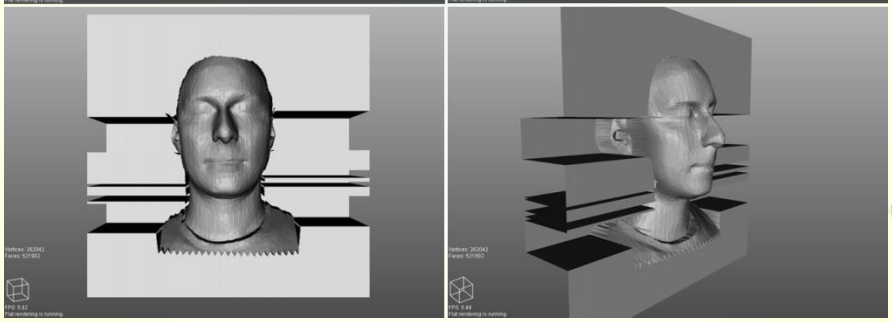

***Flood-fill without Quality Map***

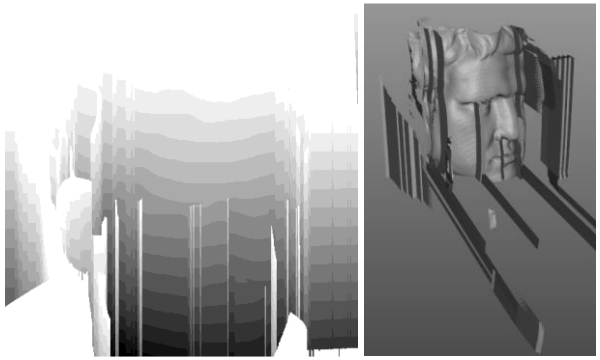

***Path-following Quality Guided***

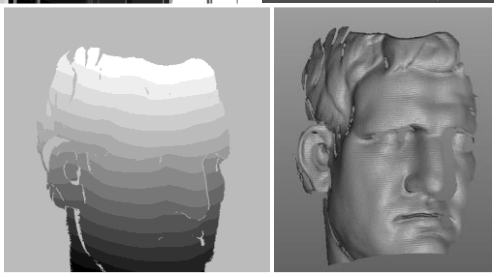

# Two-Dimensional Carrier Removal Method



***After obtaining the unwrapped phase map from the wrapped phase, in general, we need to remove the fringe relation carrier phase component in order to accurately estimate the 3D shape of the object.***

***Reference Subtraction Approach***

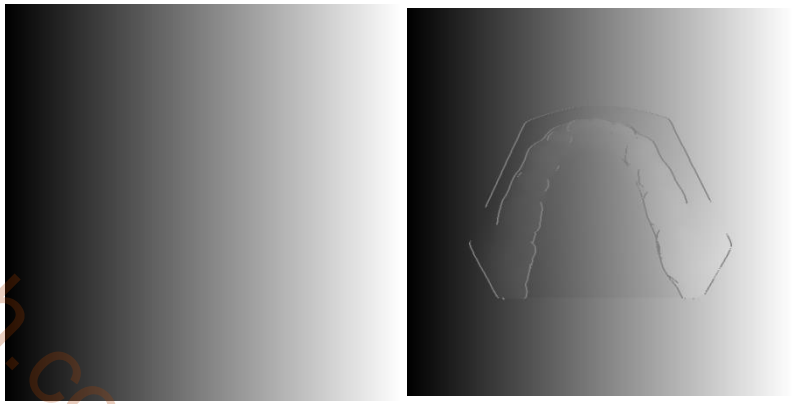

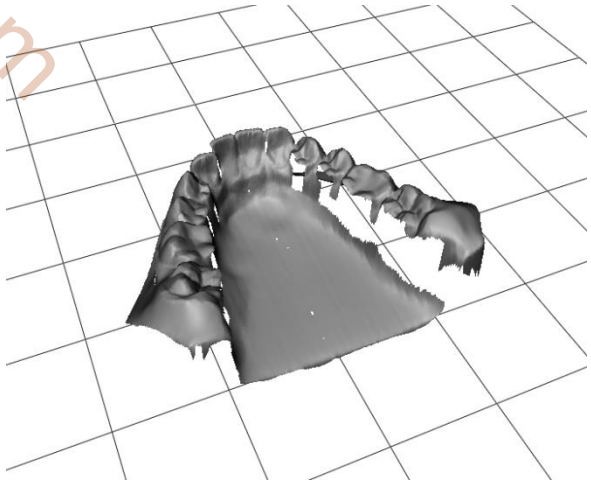

**Linear and non-linear carrier removal techniques**

- ❖ spectrum-shift approach
- ❖ average-slope approach
- ❖ plane-fitting approach
- ❖ reference-subtraction approach
- ❖ phase-mapping approach
- ❖ series-expansion approach

# Mathematical Models for 3D Measurement Systems

## Collimating Illumination based Model

**Geometry relationship of the SMFP model proposed by Srinivasan et. al. in 1984.**



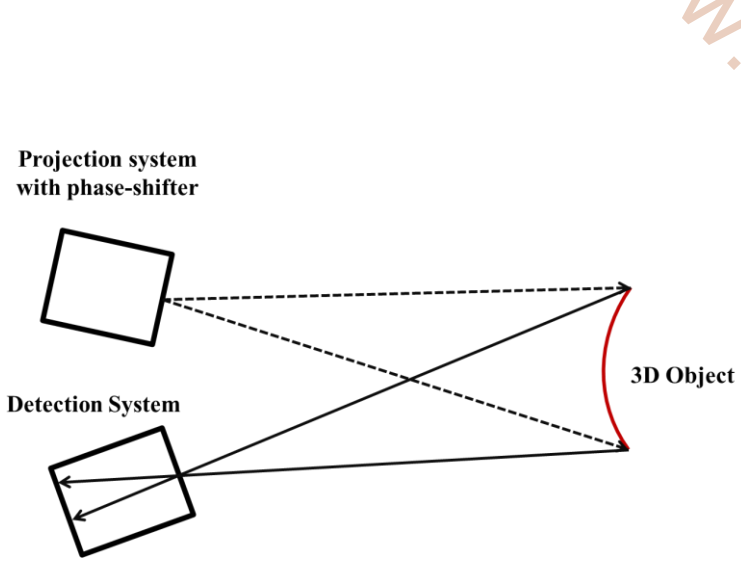


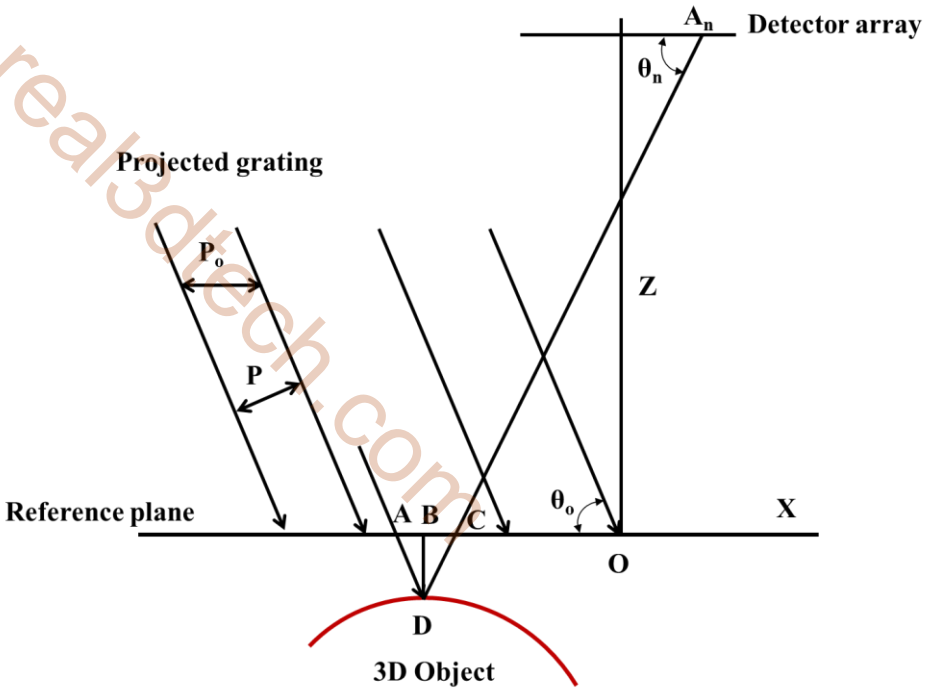


$$AC = \frac{P_o}{2\pi}\Phi_{CD}$$

$$BD = \frac{AC\tan\theta_o}{1+\tan\theta_o/\tan\theta_n}$$

# Mathematical Models for 3D Measurement Systems



## Non-Collimating Illumination based Model

**Geometry relationship of the SMFP model proposed by Takeda et. al.**



$$\omega_o = \frac{\omega_p \cos\theta}{G_p}$$

$$h_y = \frac{L\Delta\Phi_y}{\Delta\Phi_y - \omega_o D}$$

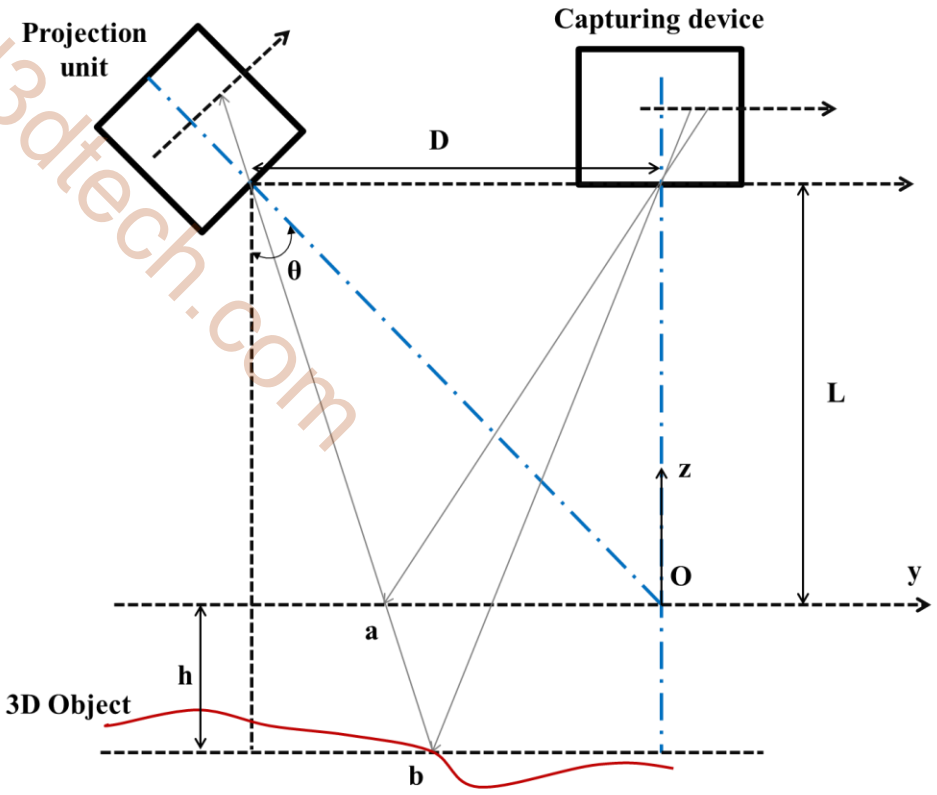

# Parameter Estimation (Camera Model)



**The process to obtain the true coordinates can be assumed as rigid-body transformation, perspective projection through pinhole, and radial and tangential distortions.**

# 3D Registration and Merging

***Registration:***

***-Improved using rigid body Landmark Transform-***

- ***Curvature calculation at each source point***
- ***Reject irrelevant points***
- ***Recalculate and update point normal***
- ***Check iteration ending criteria***
- ***Comparison of normal of source and target***

***Merging:***

**The integration of multiple scanned surfaces is called Mesh Merging.**

***Types:***

**Surfaces and Volumetric merging**

- ***Construct voxels***
- ***Compute distance map***
- ***Extract Iso-Surface***

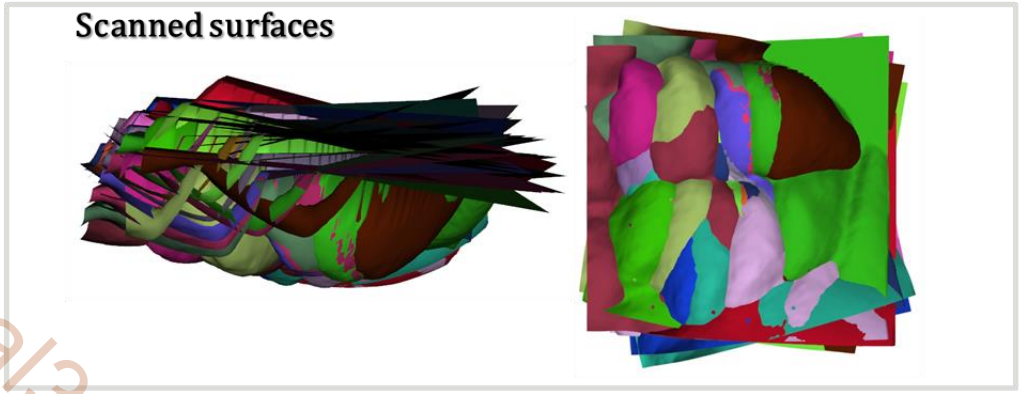


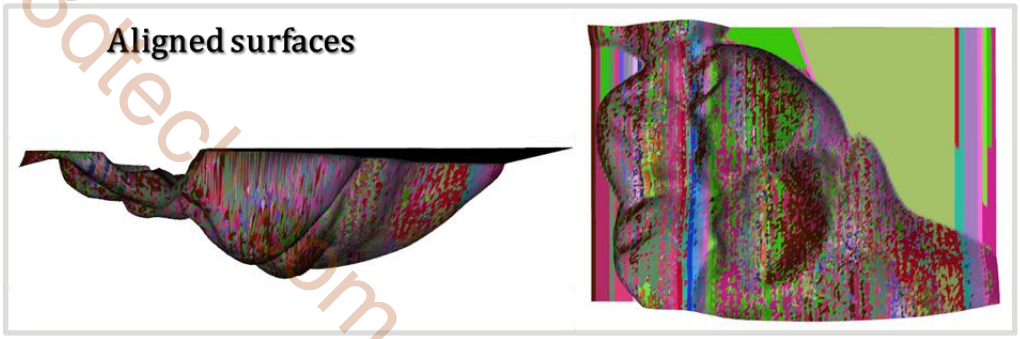


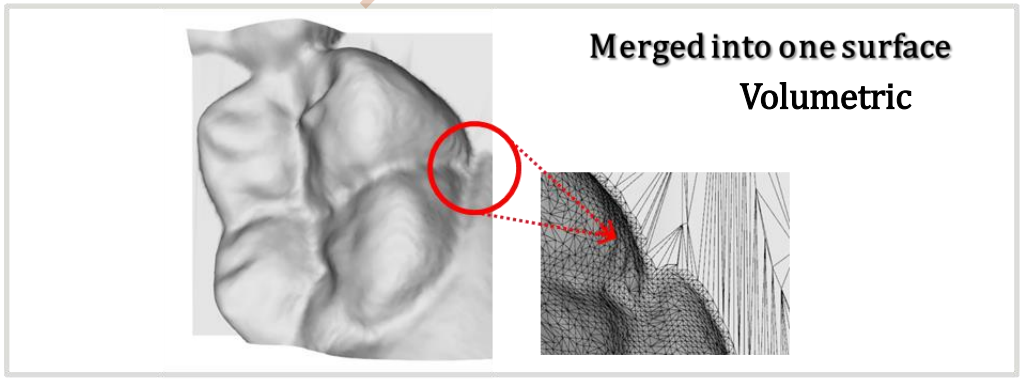

# Surface Denoising and Smoothing Methods



***There can be two general goals to perform smoothing algorithms, the first goal is denoising the measured data and second is to design high-quality fair surfaces.***

***Comparison results of various algorithms:***

a) *Raw data*
b) *Conventional Laplacian filter with five iterations*
c) *Improved Laplacian smoothing filter with five iterations*
d) *Desbrun's algorithm with five iterations*
e) *Mean filter with fifty iterations*
f) *Median filter with fifty iterations*
g) *Taubin's filter with ten iterations*
h) *Two-step fairing algorithm*
i) *SUSAN smoothing*

# Elimination of Outliers



***Outlier can be referenced to points that are out of range and unreliable, long, and thin triangles.***



*Some algorithms that work on point clouds and can also be extended to meshes are*

- ***Range algorithm (it discards out of range points)***
- ***Statistical removal algorithm (it discards points based to spherical density criteria)***
- ***Radius outlier algorithm (it discards points based on number of neighbors they have)***

## *Unreliable mesh removal Criteria*

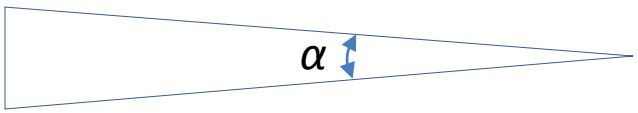


***Based on edge angle***

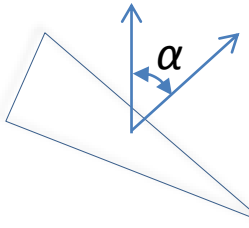


***Based on normal angle***

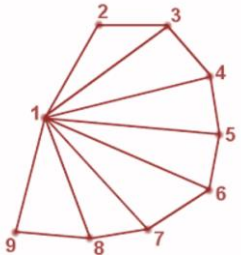


***Based on number of neighbors***

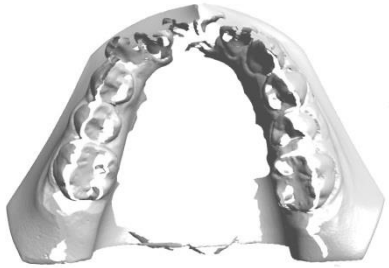

# Mathematical Models of SMFP Systems



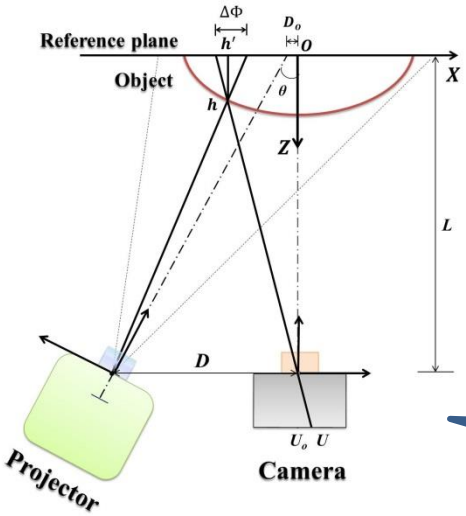


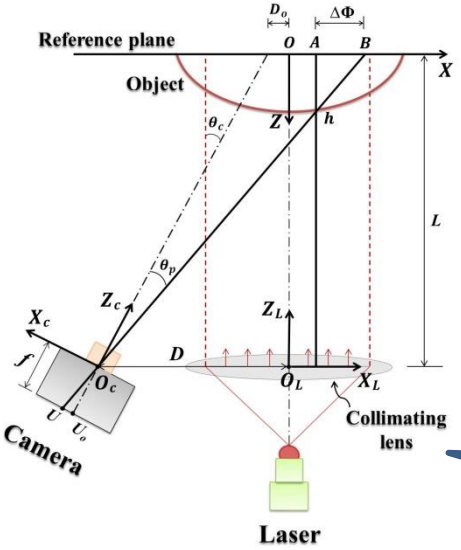


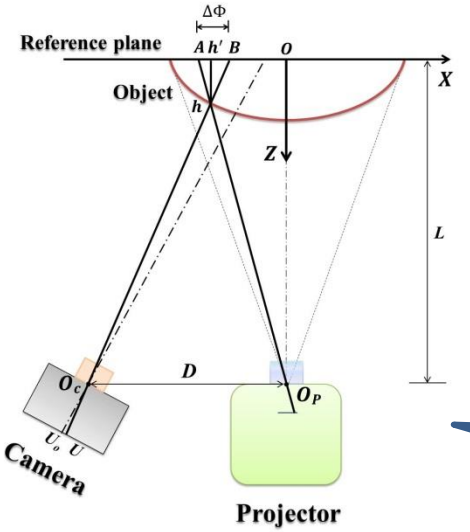


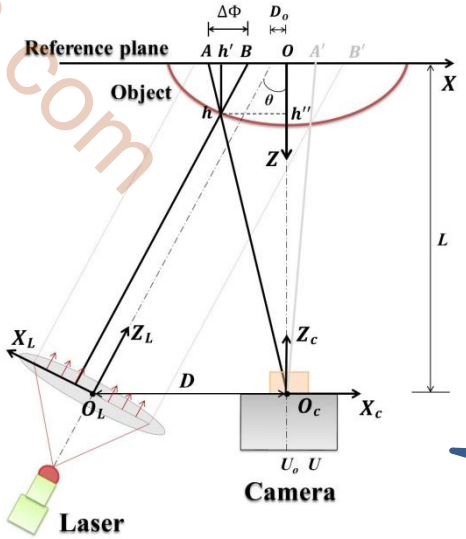

# Case # 1 (calculation of X, Y, Z)

$$\theta = \tan^{-1}\left(\frac{D - D_o}{L}\right)$$

***Assume the fringe pitch is p, then***

$$\Delta\Phi = \frac{P}{2\pi}\left[\Phi_{obj}(i,j) - \Phi_{ref}(i,j)\right]$$

***Height of the object at point h:***

$$Z_h = \overline{hh'} = \frac{\Delta\Phi}{sin\theta}$$

***Since, the camera is aligned with the axis of the object, therefore, the coordinates (X, Y) is considered to be proportional to the imaging index (i, j).***

***Therefore:***

$$X_h = (U - U_o)\delta$$

$$Y_h = (V - V_o)\delta$$

***where δ is the pixel size in mm.***

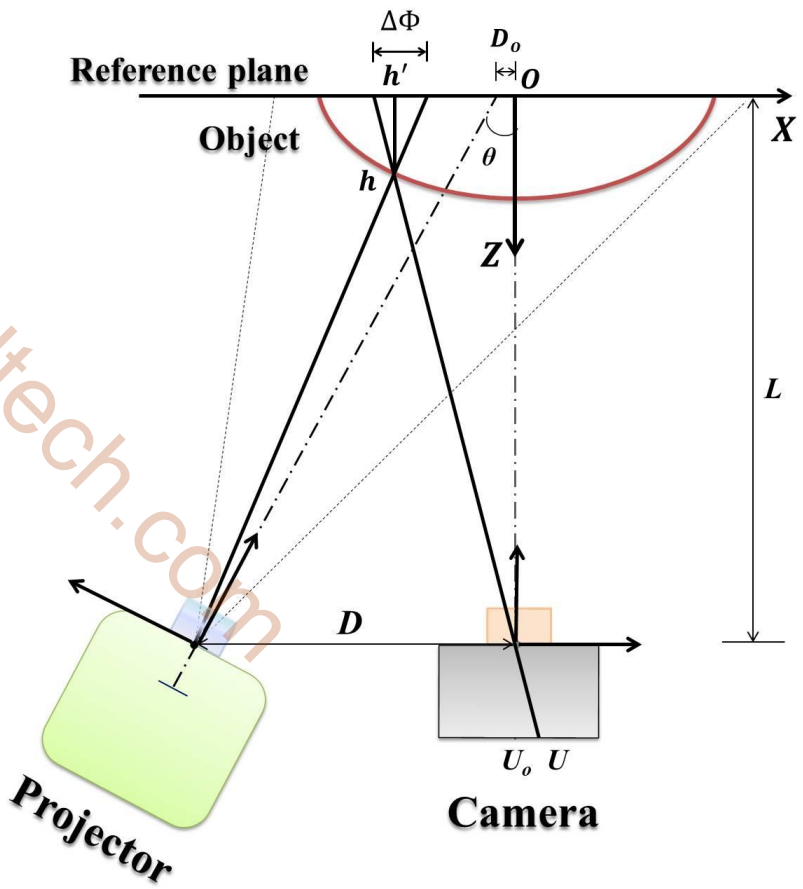

# Case # 1

***Due to the proportionality of the imaging index (i, j) and the object coordinates (X, Y), the geometric relationship to retrieve the height of the object can also be expressed by:***

$$Z_h(x,y) = a\left(\Delta\Phi(x,y)\right)^2 + b\left(\Delta\Phi(x,y)\right) + c$$

***And***

$$Z_h(x,y) = K(x,y)\,\Delta\Phi(x,y)$$

***where a, b, c are the fit parameters and K is the calibration constant for that specific pixel.***

# Case # 2 (calculation of Z)

***Since, $\Delta O_P O_c h$ and $\Delta hAB$ are similar, we have:***

$$\frac{\overline{O_c O_P}}{\overline{hO_P}} = \frac{\overline{AB}}{\overline{hh'}}$$

$$\frac{D}{L - \overline{hh'}} = \frac{\Delta\Phi}{\overline{hh'}}$$

***Height of the object at point h:***

$$Z_h = \overline{hh'} = \frac{L\Delta\Phi}{D + \Delta\Phi}$$

***Since, the camera is not aligned with the axis of the object, therefore, the coordinates (X, Y) is not considered to be proportional to the imaging index (i, j).***

***So***

$$X_h = ?$$

$$Y_h = ?$$

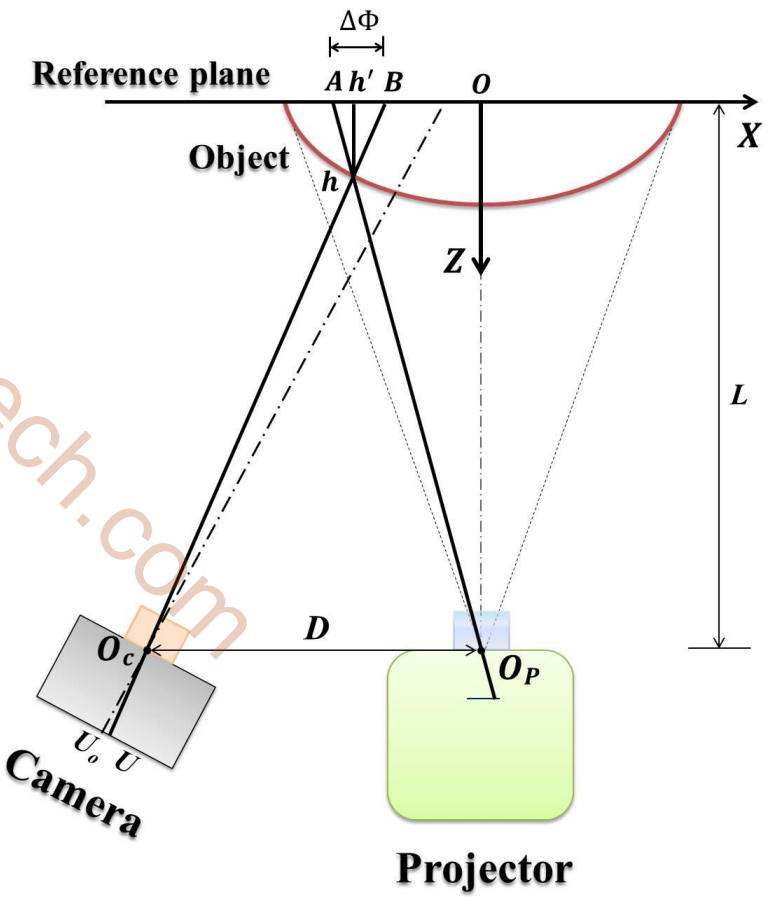

# Case # 2 (calculation of X, Y)

$$X_A = \frac{P}{2\pi}\left(\Phi_A - \Phi_O\right)$$

***Since, $\Delta OO_PA$ and $\Delta h'hA$ are similar:***

$$\frac{X_A}{L} = \frac{X_A - X_h}{Z_h}$$

***Thus, the accurate X coordinate of point h can be written as:***

$$X_h = X_A\left[1 - \frac{Z_h}{L}\right]$$

***Since, the vertical fringe patterns are projected onto the object, therefore, the height of the object is independent of the $Y_h$ coordinate.***

$$Y_h = (V - V_o)\delta$$

***where δ is the pixel size in mm.***

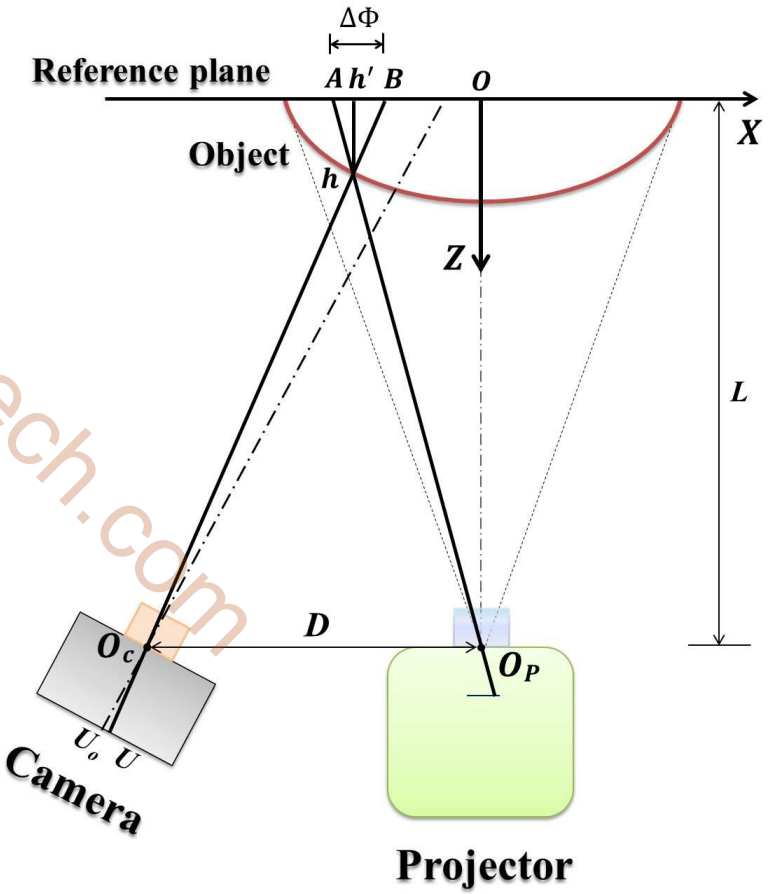

# Case # 3 (calculation of Z)

$$\overline{Ah} = \frac{\Delta\Phi}{\tan(\theta_c + \theta_p)}$$

***And***

$$\tan\left(\theta_c + \theta_p\right) = \left[\frac{L\left(U - U_o\right) + f\left(D - D_o\right)}{f\,L - \left(U - U_o\right)\left(D - D_o\right)}\right]$$

***Height of the object at point h:***

$$Z_h = \overline{Ah} = \Delta\Phi\left[\frac{f\,L - \left(U - U_o\right)\left(D - D_o\right)}{L\left(U - U_o\right) + f\left(D - D_o\right)}\right]$$

***Since, the camera is not aligned with the axis of the object, therefore, the coordinates (X, Y) is not considered to be proportional to the imaging index (i, j).***

***So***

$$X_h = ?$$

$$Y_h = ?$$

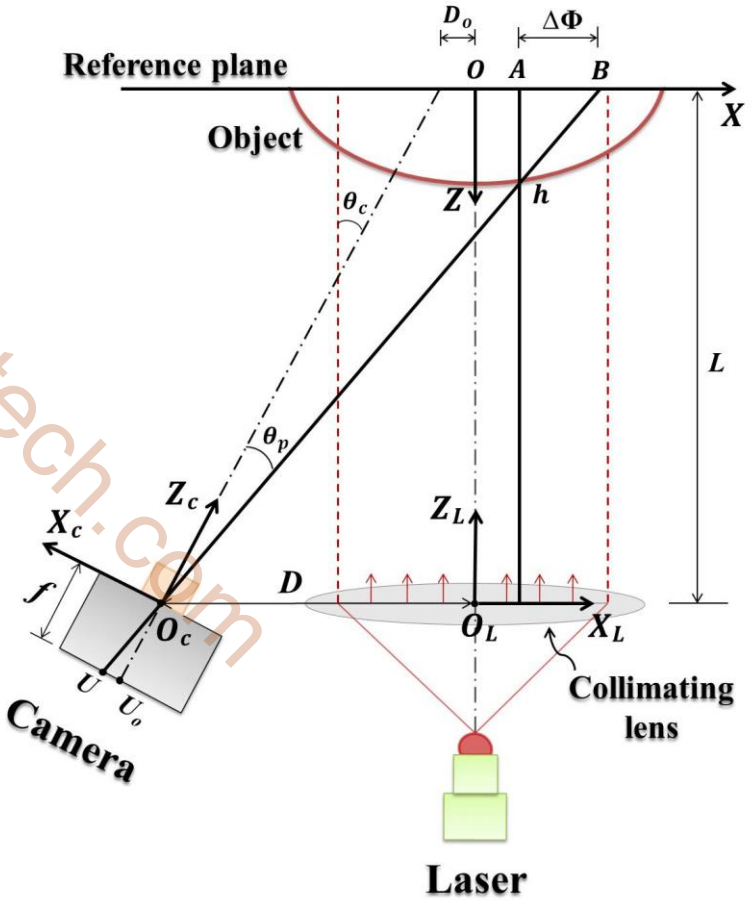

# Case # 3 (calculation of X)

$$X_{A'} = \frac{P_R}{2\pi}\left[\Phi_{A'} - \Phi_O\right]$$

***$P_R$ is the pitch of captured phase-shift fringe patterns when X is negative.***

***Since, $\Delta h'G'O_c$ and $\Delta h'A'B'$ are similar:***

$$\frac{\overline{O_cG'}}{\overline{G'A'} - \overline{h'A'}} = \frac{\overline{A'B'}}{\overline{h'A'}}$$

***And***

$$\frac{D - X_{A'}}{L - Z_h} = \frac{\overline{A'B'}}{Z_h}$$

$$\overline{A'B'} = Z_h\left[\frac{D - X_{A'}}{L - Z_h}\right]$$

***The difference between measured and calculated phase depths can be written as:***

$$\varepsilon_R = \Delta\Phi - \overline{A'B'}$$

***Thus, X coordinate of point h' can be expressed by:***

$$X_{h'} = \frac{P}{2\pi}\left[\left(\Phi_{h'} + \varepsilon_R\right) - \Phi_O\right]$$

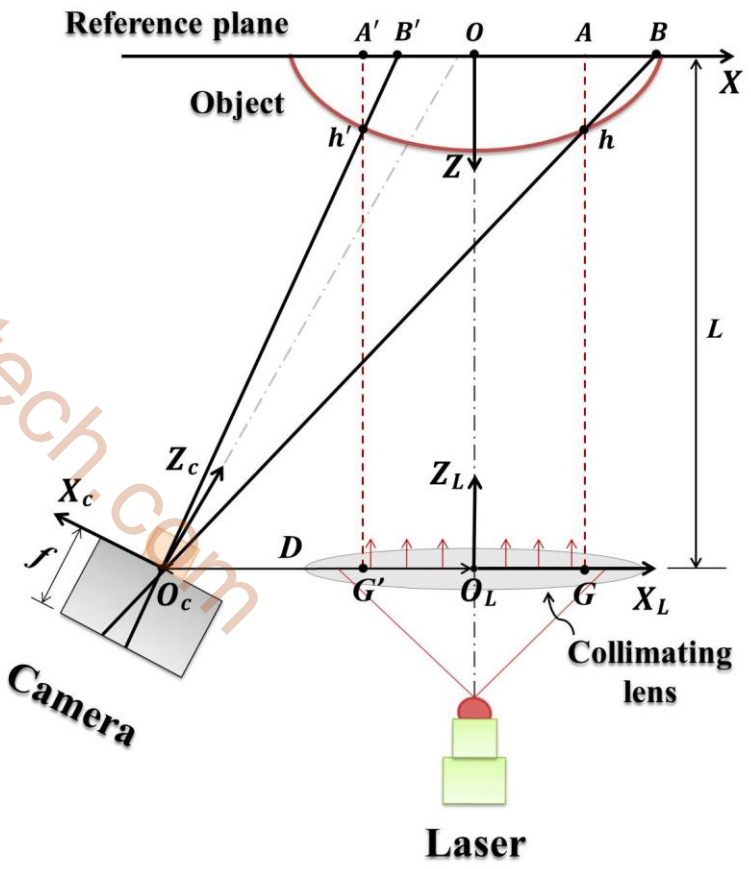

# Case # 3 (calculation of X)

$$X_A = \frac{P_L}{2\pi}\left[\Phi_A - \Phi_O\right]$$

***$P_L$ is the pitch of captured phase-shift fringe patterns when X is positive.***

***Since, $\Delta hGO_c$ and $\Delta hAB$ are similar, we have:***

$$\overline{AB} = Z_h\left[\frac{D + X_A}{L - Z_h}\right]$$

$$\varepsilon_{R'} = \Delta\Phi - \overline{AB}$$

***Thus, X coordinate of point h can be expressed by:***

$$X_h = \frac{P}{2\pi}\left[\left(\Phi_h + \varepsilon_{R'}\right) - \Phi_O\right]$$

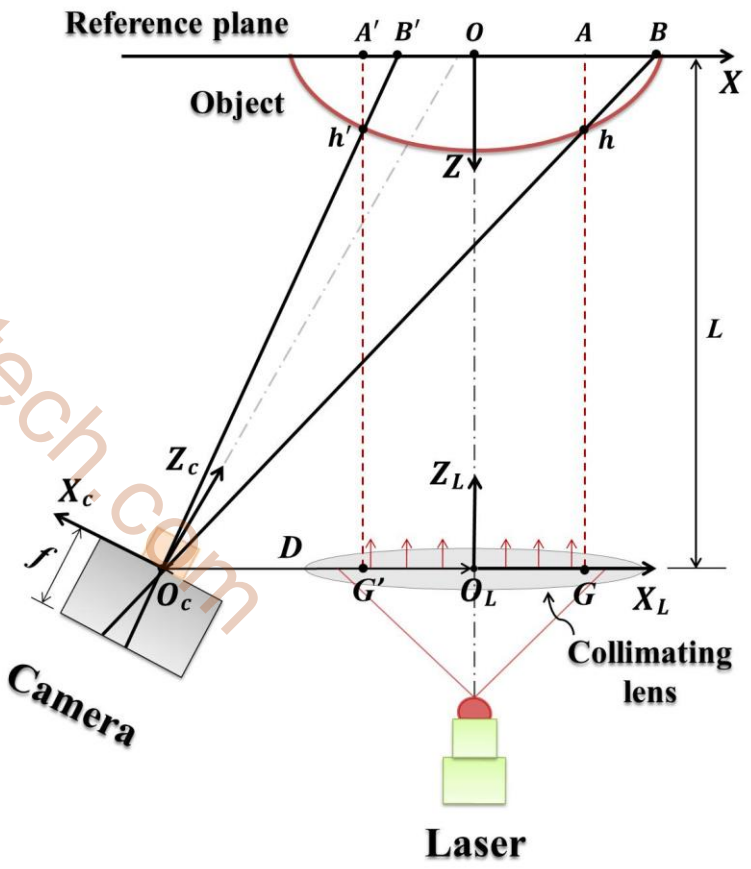

# Case # 3 (calculation of Y)

***Since, $\Delta O_cVU$ and $\Delta O_cFB$ are similar, we have:***

$$\frac{\overline{VU}}{\overline{O_cU}} = \frac{\overline{FB}}{\overline{O_cB}}$$

$$\overline{O_cU} = \frac{\overline{O_cO'}}{\cos\theta_p} = \frac{f}{\cos\theta_p}$$

***And***

$$\overline{O_cB} = \frac{L}{\cos(\theta_c + \theta_p)}$$

$$Y_F = \overline{FB} = \frac{L(V - V_o)\cos\theta_p}{f\cos(\theta_c + \theta_p)}$$

***Since, $\Delta O_cFB$ and $\Delta hFE$ are similar, we have:***

$$\overline{FE} = \left[\frac{Z_h}{L}\right]\overline{FB}$$

***Finally, $Y_h$ can be determined by:***

$$Y_h = \overline{EB} = \overline{FB} - \overline{FE} = Y_F\left(1 - \frac{Z_h}{L}\right)$$

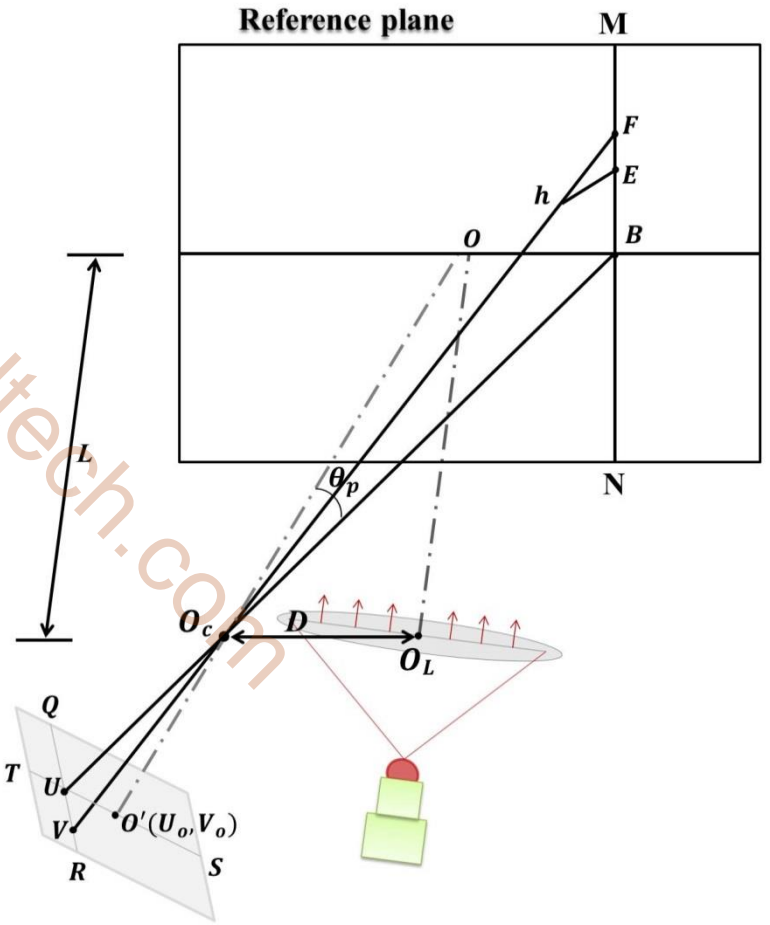

# Case # 4 (calculation of Y, Z)



***Height** of the object at point h:*

$$Z_h = \overline{hh'} = \frac{\Delta\Phi}{sin\theta}$$

***Since, the vertical fringe patterns are projected onto the object, therefore, the height of the object is independent of the $Y_h$ coordinate.***

$$Y_h = (V - V_o)\delta$$

***where δ is the pixel size in mm.***

***But***

$$X_h = ?$$

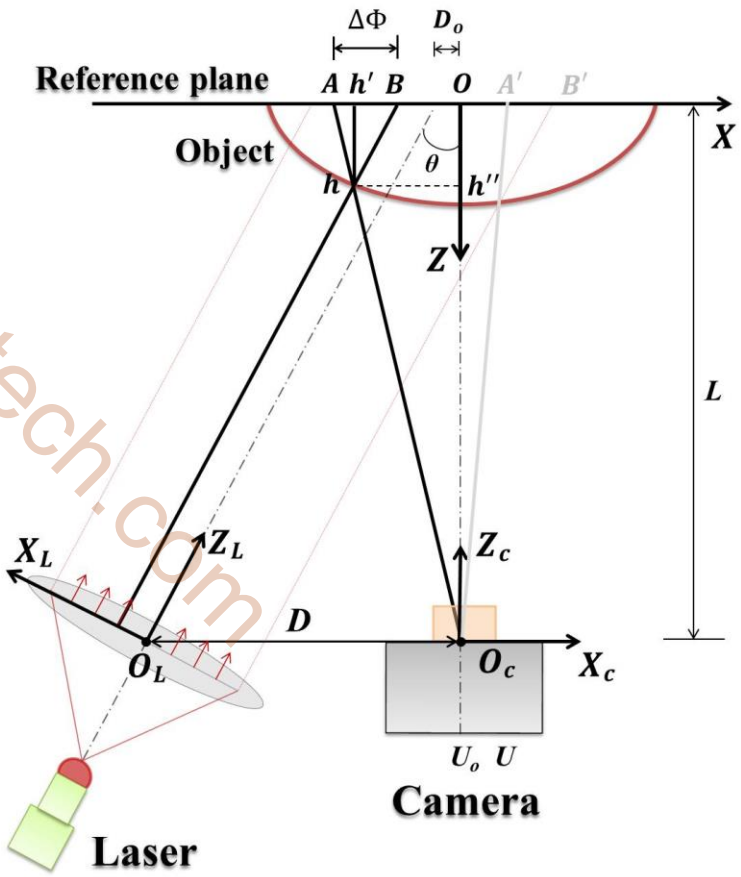

# Case # 4 (calculation of X)

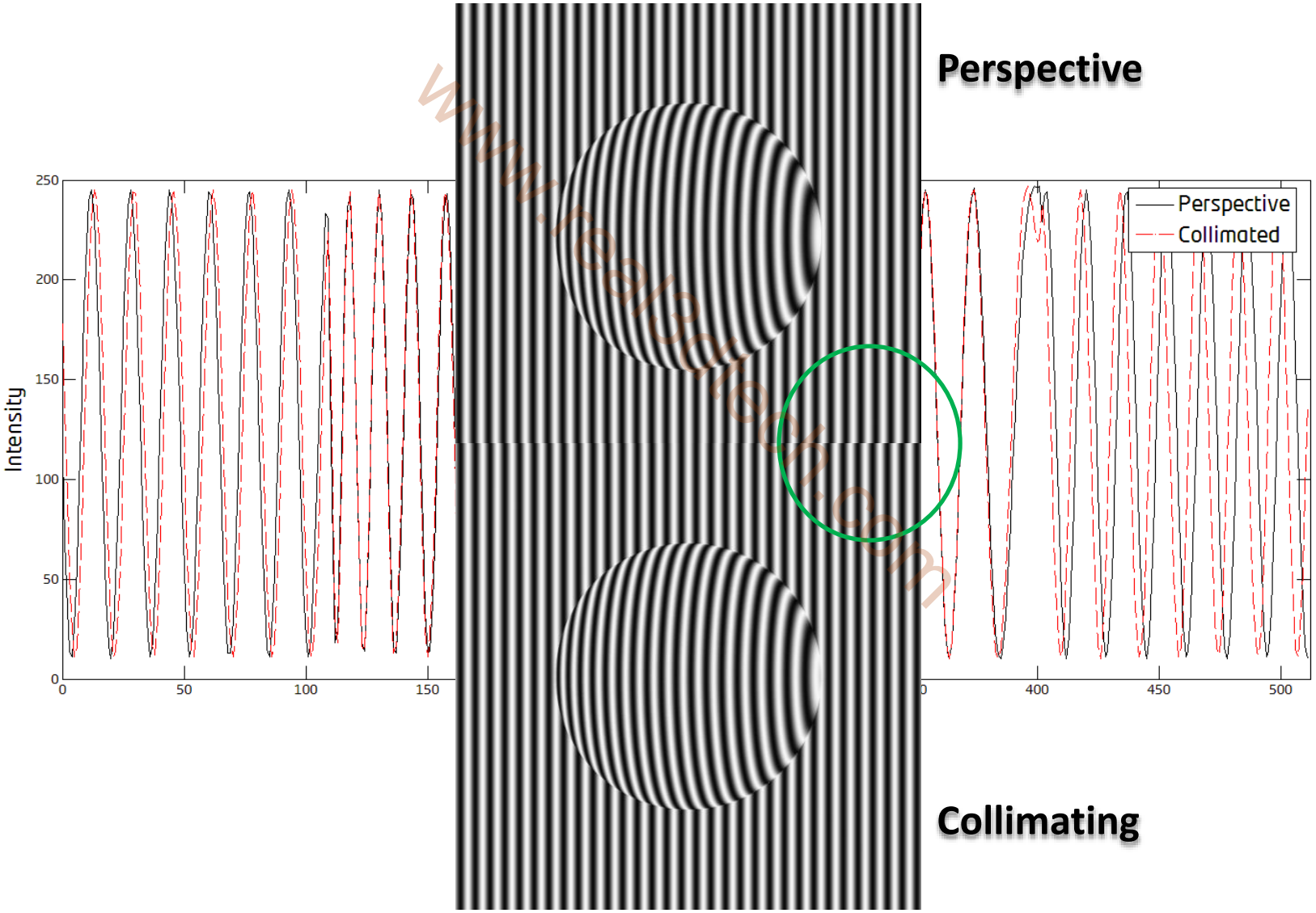

# Case # 4 (calculation of X)

$$X_B = \frac{P_R}{2\pi}\left[\Phi_B - \Phi_O\right]$$

***Since, $\Delta$ hh''$O_c$ and $\Delta$ Ah'h are similar:***

$$\overline{Ah'} = \frac{\overline{hh''}\,\overline{hh'}}{\overline{OO_c} - \overline{Oh''}}$$

$$\overline{h'B} = \overline{hh'}\tan\theta$$

***And***

$$\overline{AB} = \overline{Ah'} + \overline{h'B}$$

$$\overline{AB} = Z_h\left[\frac{X_B}{L - Z_h} + \tan\theta\right]$$

***The difference between measured and calculated phase depths can be written as:***

$$\varepsilon_R = \Delta\Phi - \overline{AB}$$

***Thus, X coordinate of point h can be expressed by:***

$$X_h = \frac{P}{2\pi}\left[\left(\Phi_B + \varepsilon_R\right) - \Phi_O\right]$$

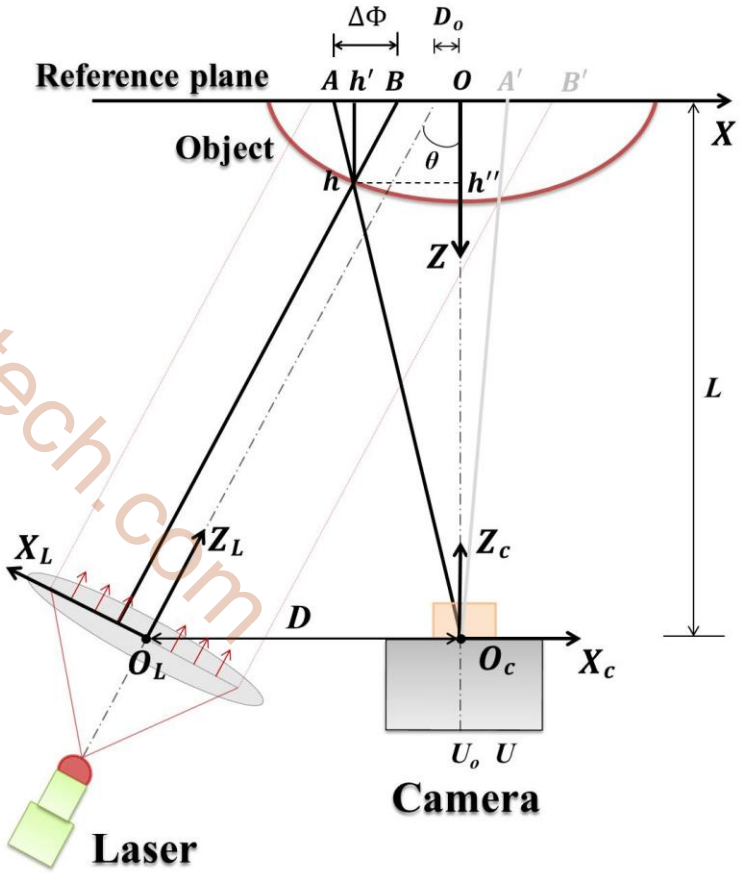

# Verification by Computer Simulation



4-step phase shifting

Wrapped phase map

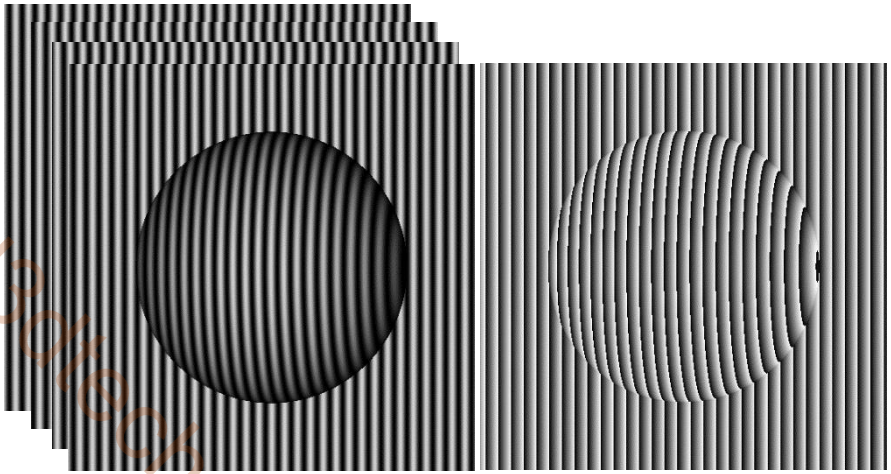

**Setup**

- Image size 512 x 512 pixels
- 4-step phase shifting
- Quality guided phase unwrapping
- Reference-subtraction approach

- Real-time Virtual 3D Scanner platform

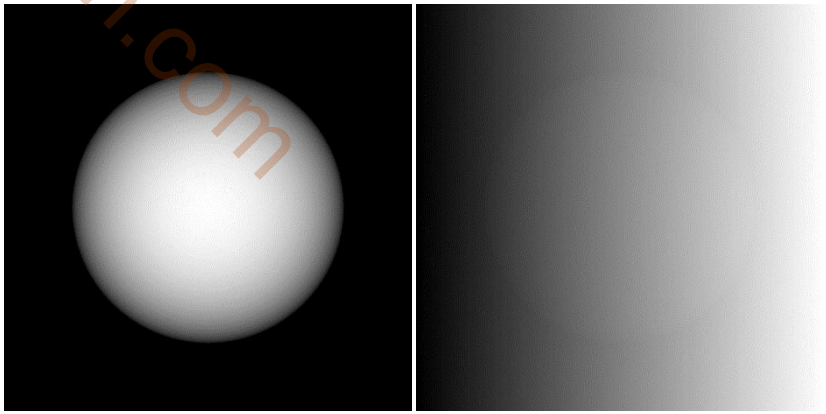

Depth map

Unwrapped phase map

# Results of Case # 1 & 2



Case # 1

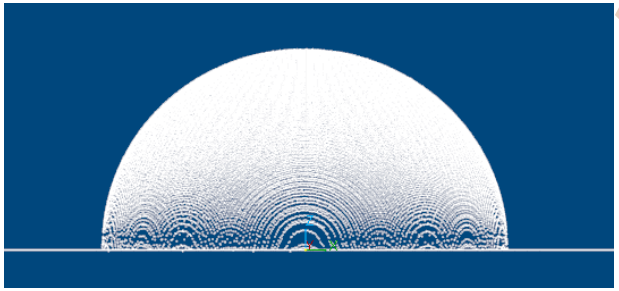

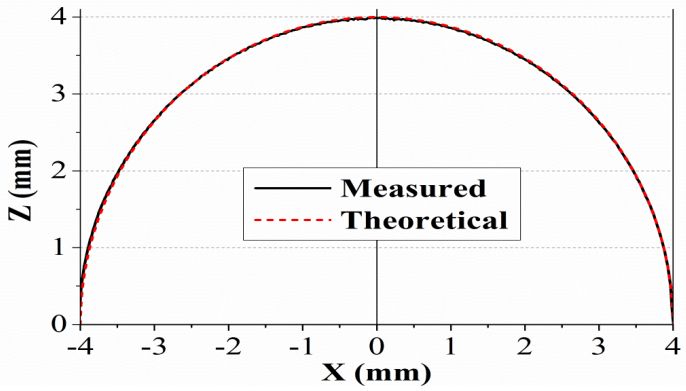


RMS difference = 0.001 mm

Case # 2

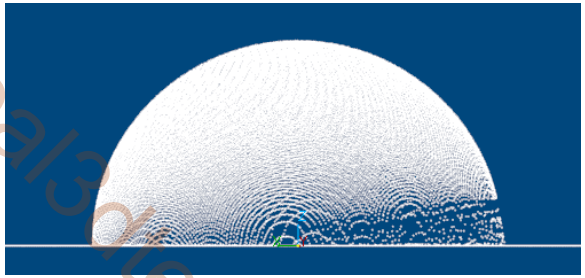

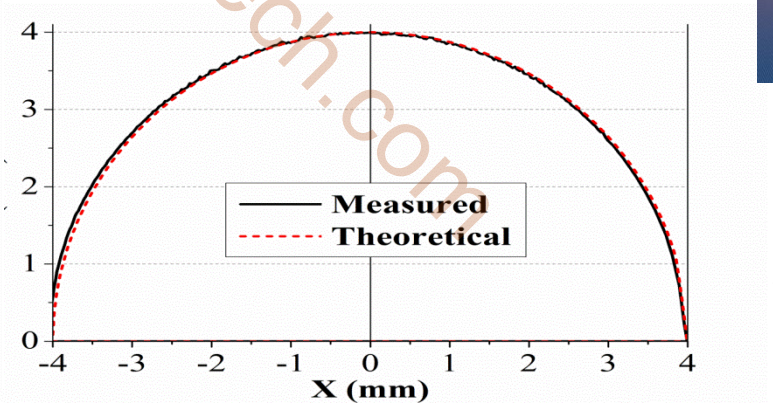


RMS difference = 0.0015 mm

Measured 3D sphere

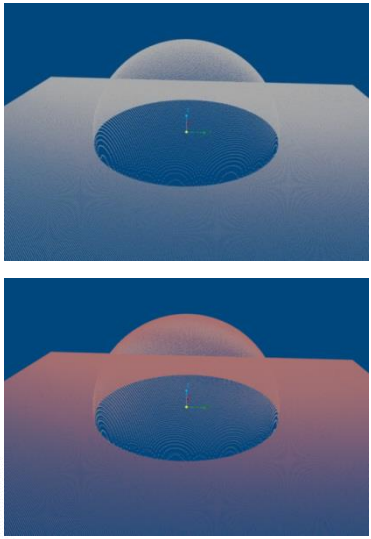

*Comparison: Measured and theoretical half spheres are rendered in a same window*

# Results of Case # 3 & 4

## Reconstruction results without using our method

Case # 3

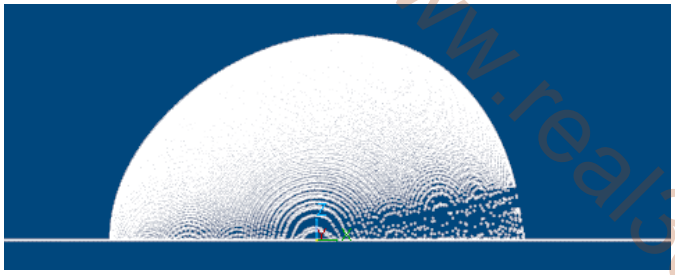

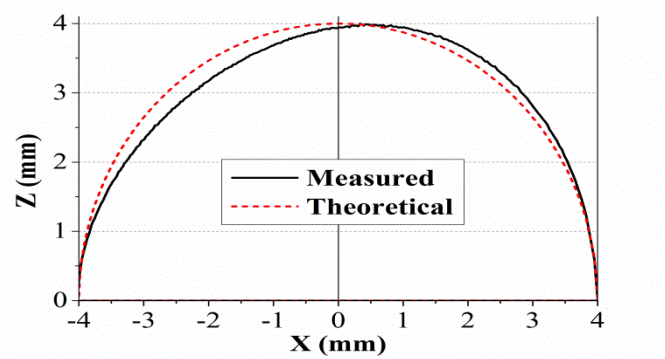


Case # 4

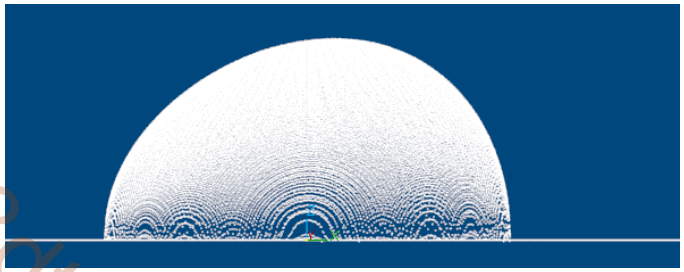

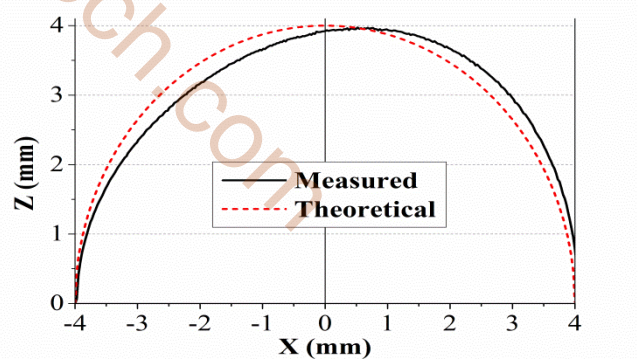




*The tilted shape profile or nonlinear distortion can be observed in illustrations due to the collimating effect on captured phase-shifted fringe pattern images.*

# Results of Case # 3 and 4

## Reconstruction results with using our method



Case # 3

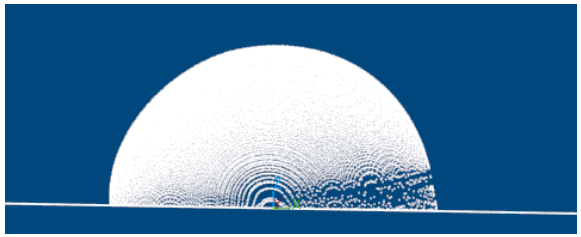

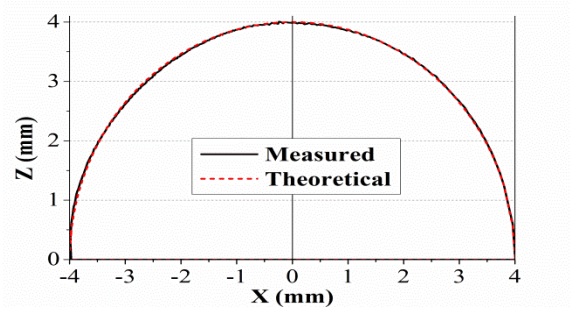


RMS difference = 0.0018 mm

Case # 4

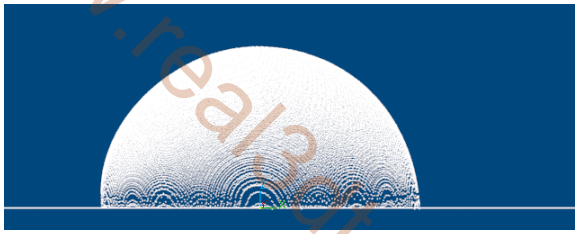

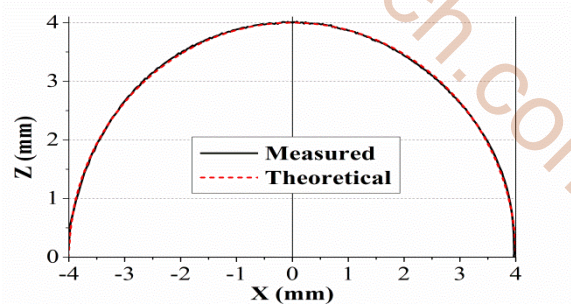


RMS difference = 0.0013 mm

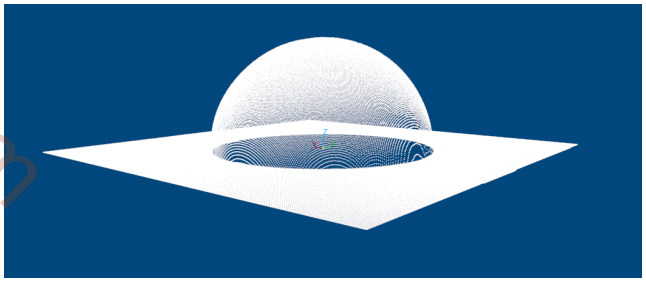

# Reconstruction results with using our method

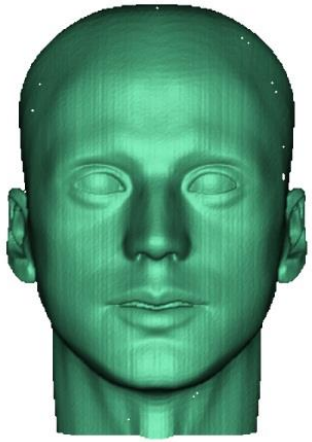

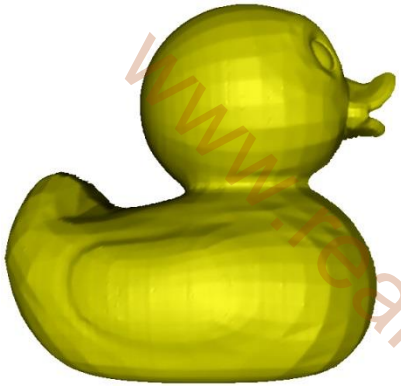

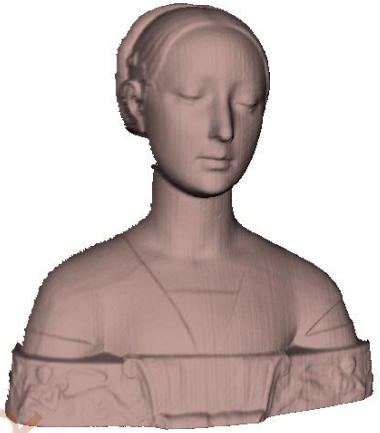

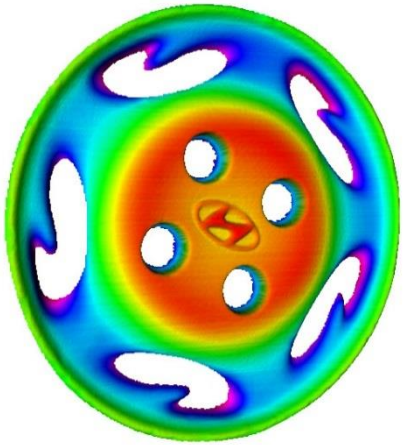

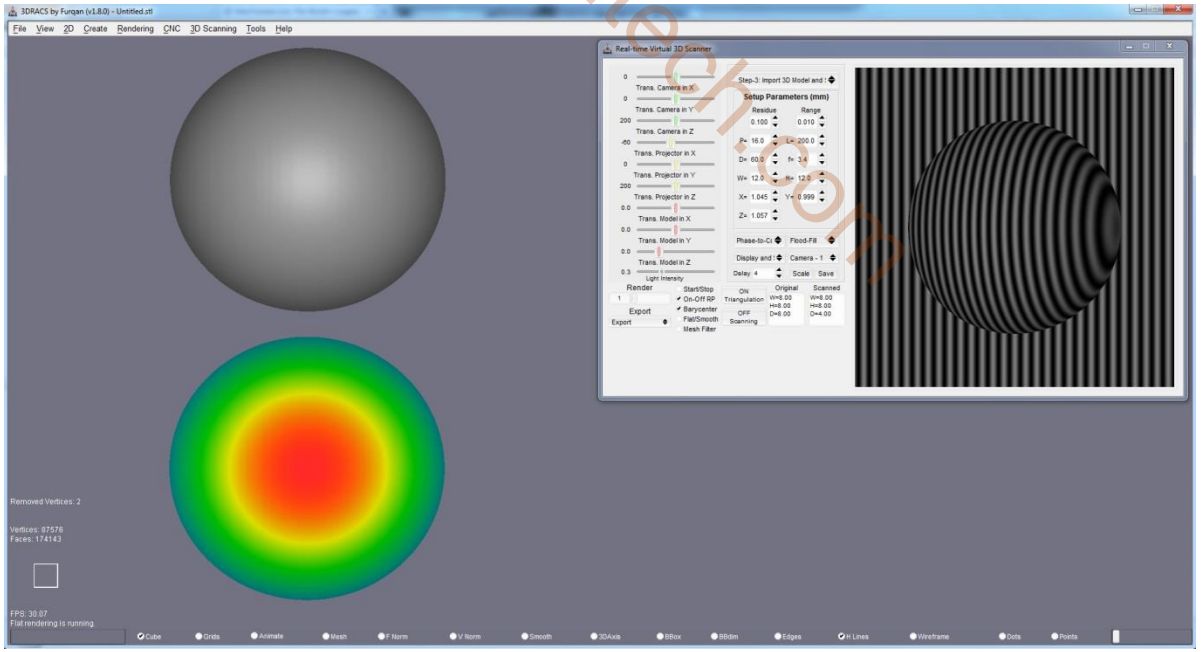

# Introduction

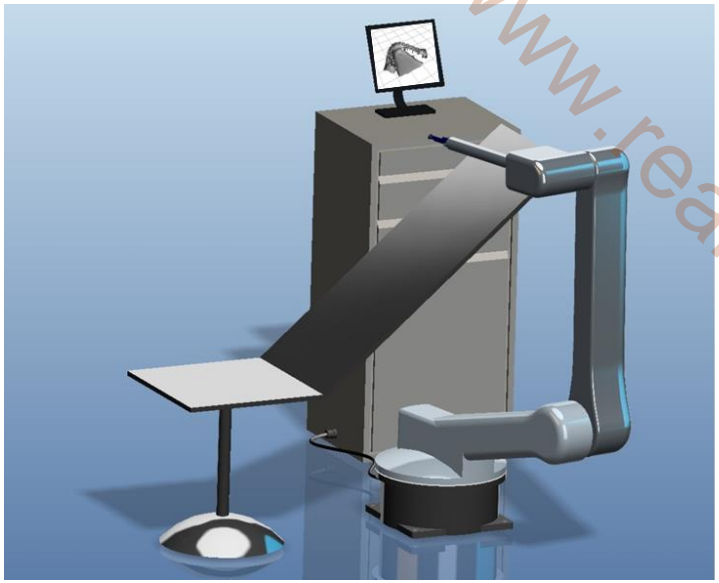

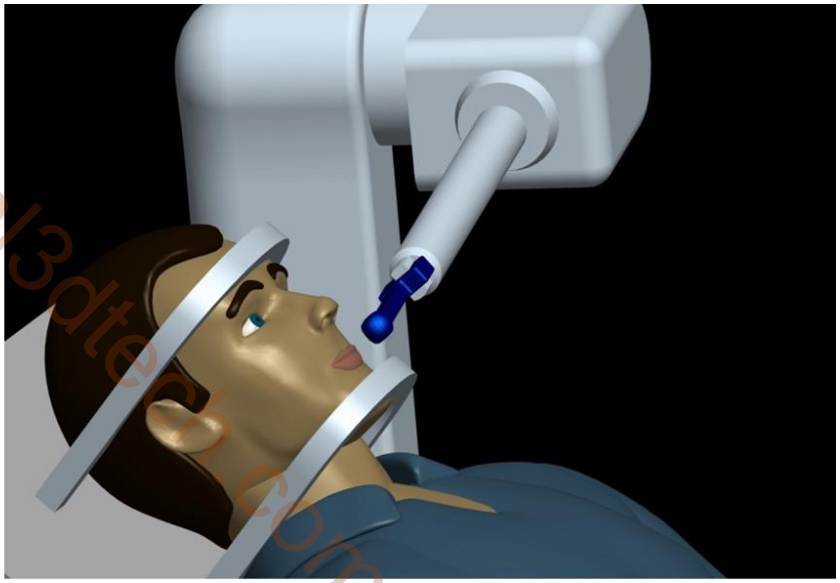

# Design of the 1st Device

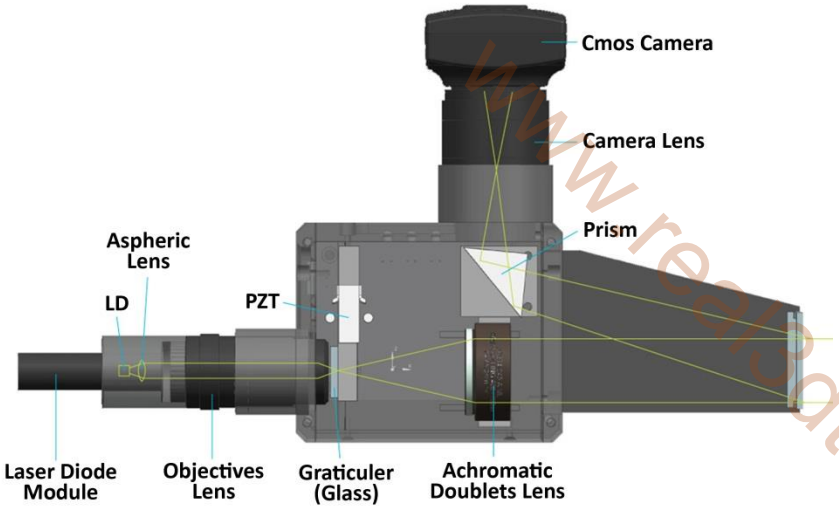


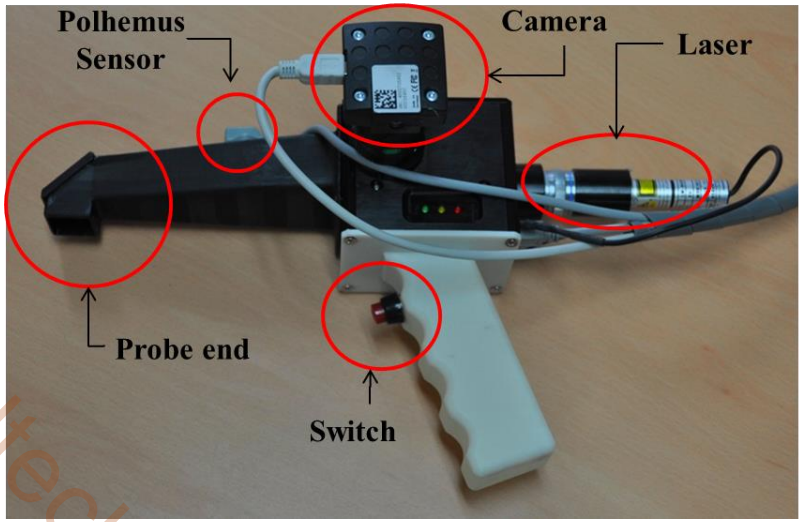


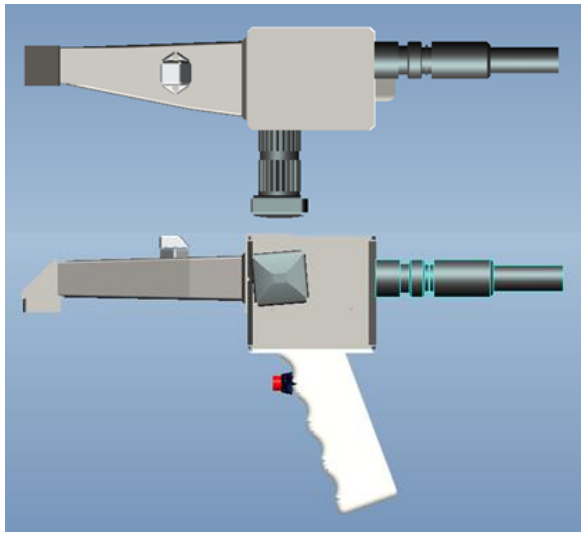

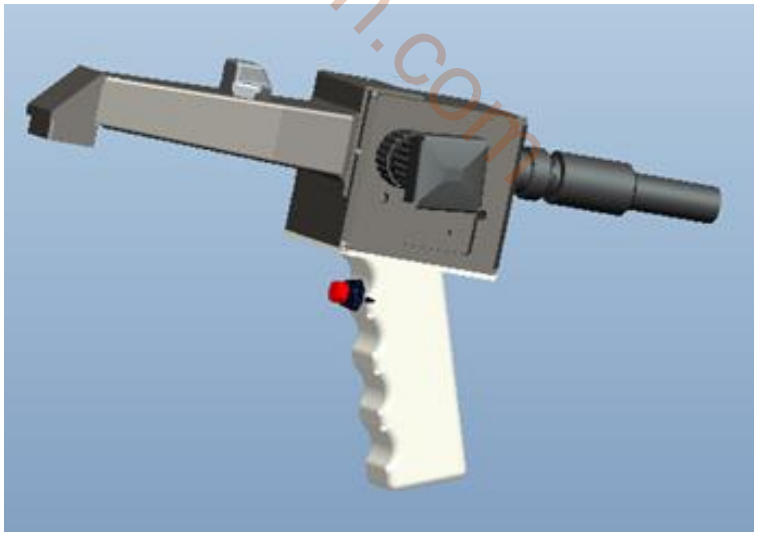

# Optical System Architecture of the 1st Device

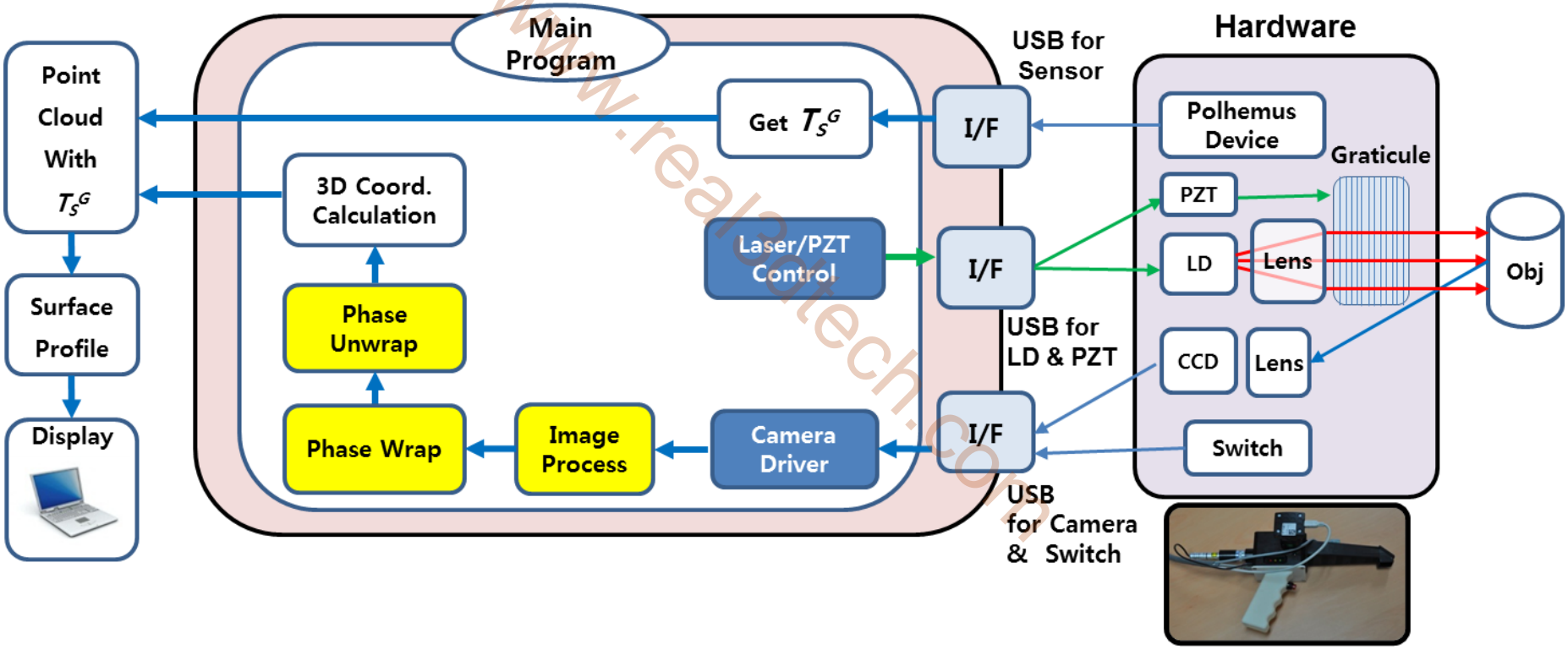

# Piezoelectric Transducer vs Phase Shifts (1st Device)

***Due to the mechanical nature of the PZT transducer, the relationship between phase shifts and the PZT step becomes non-linear.***



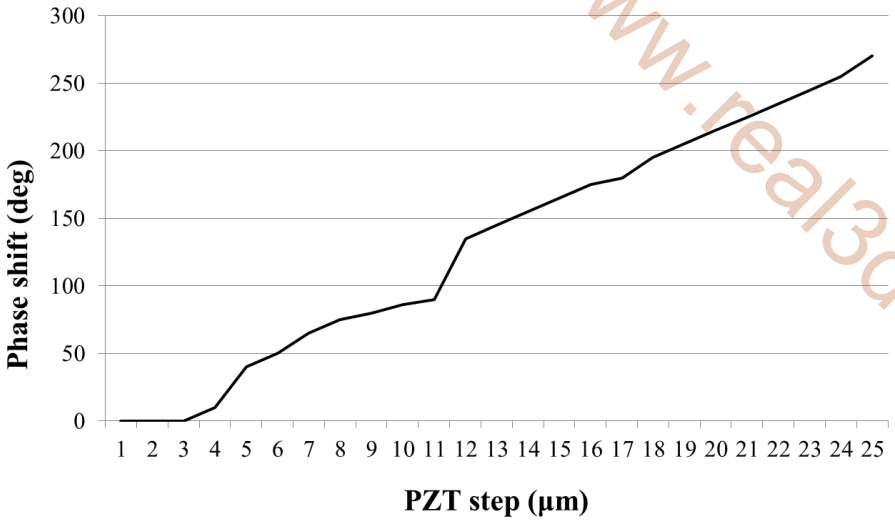


| PZT step (μm) | Phase shift (deg) |
|---|---|
| **5** | 0 |
| **11** | 90 |
| **17** | 180 |
| **25** | 270 |

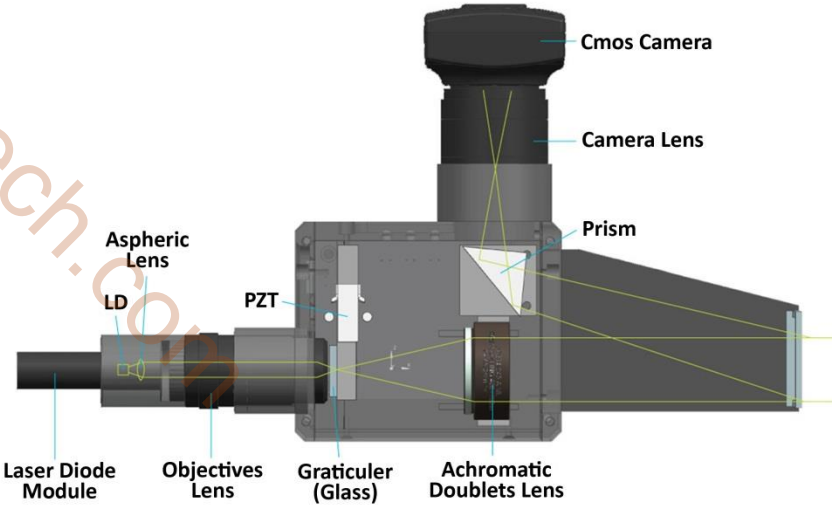

# Camera Calibration (1st Device)

**We prosed a Jig for Camera Calibration**

**It can provides, Easiness, Accurate center point of the checkerboard, Uniform intensity of light on the captured image by using the backlight, and Lesser cost.**



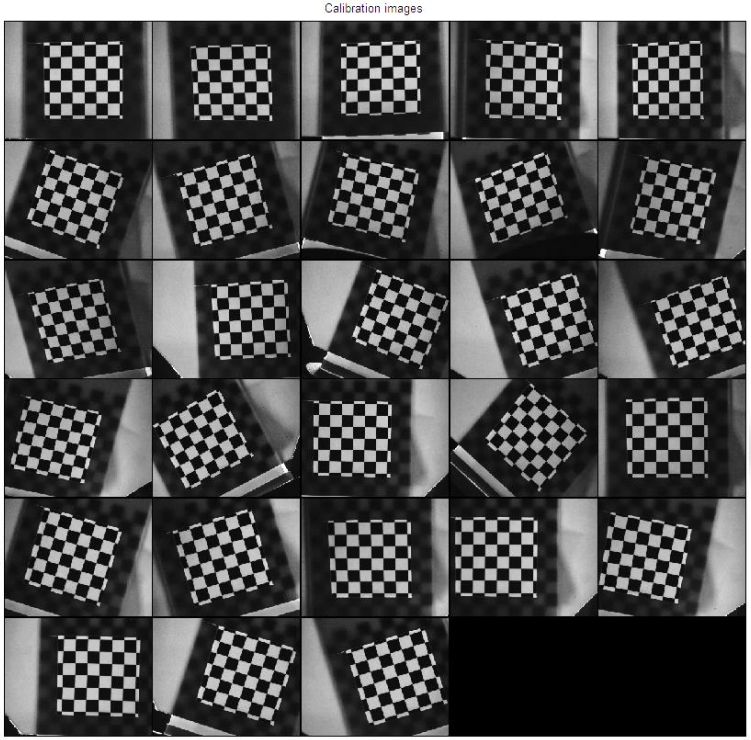


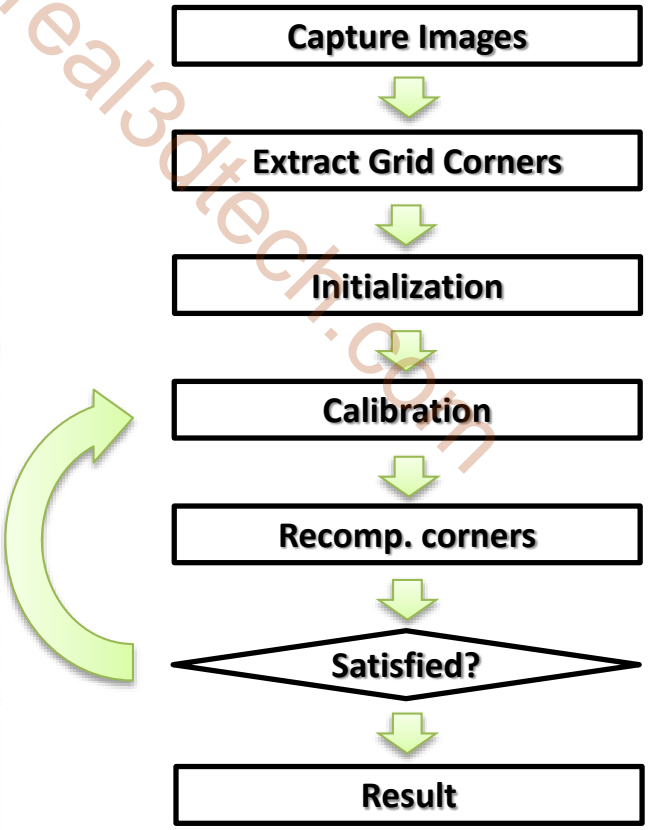


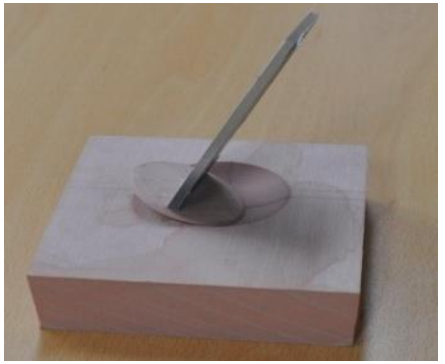

# Measurement Results of Calibration Jig (1st Device)

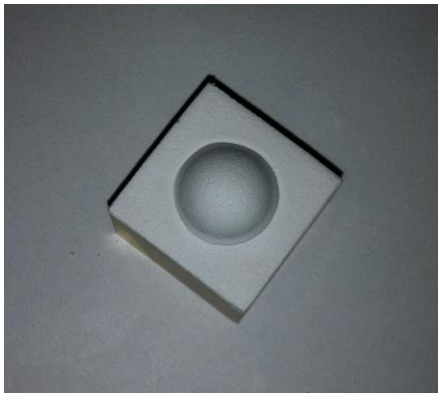

*Calibration jig*

*Intraoral scanner*



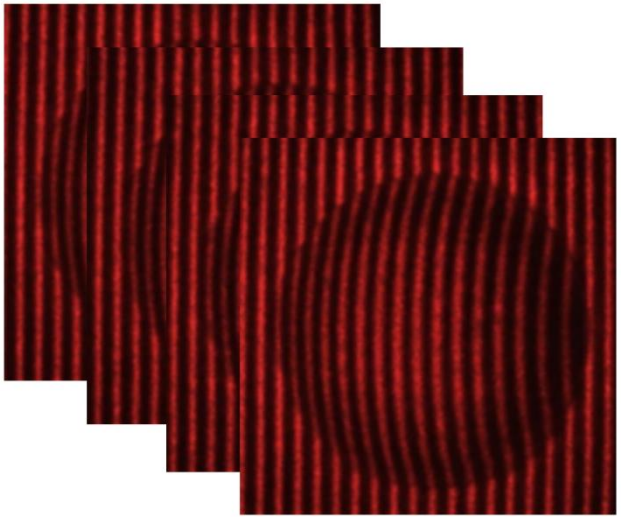

*Captured images*

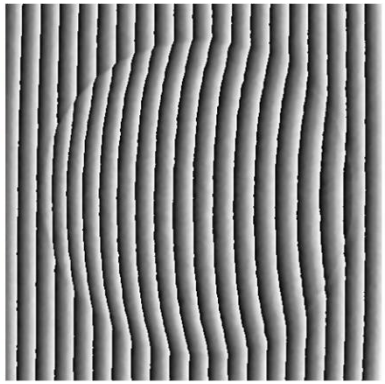

*Image processing*

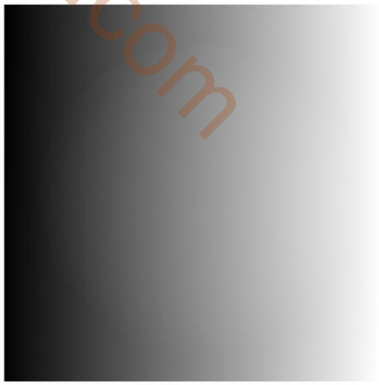

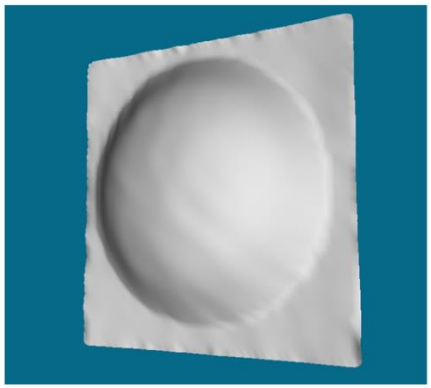

*Reconstructed surface*

# Measurement Results of Calibration Jig (1st Device)

*15x15x15 mm Cube + ϕ10mm Ball*

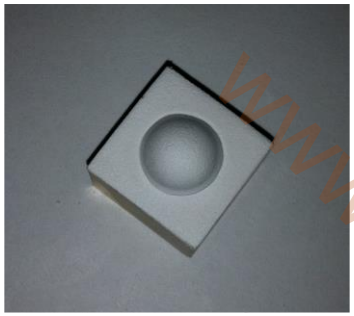

*Painted Jig*

*Plaster Scanning Jig*

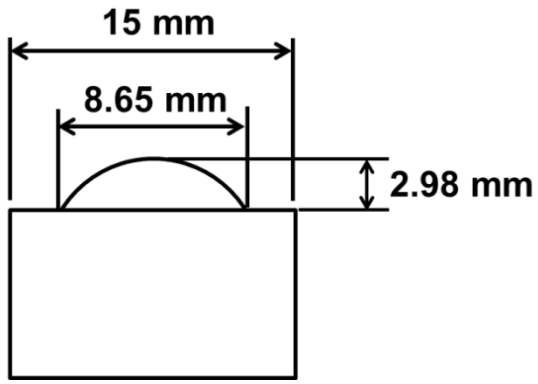


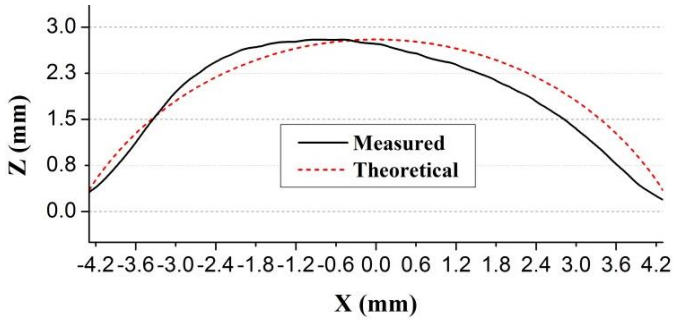


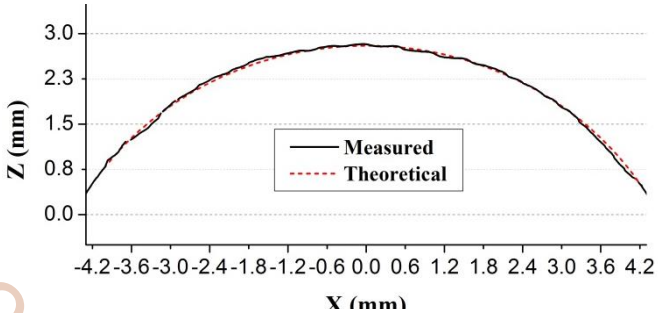


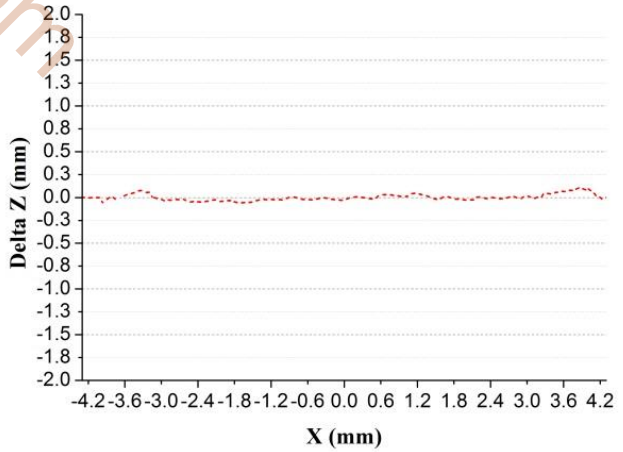


***Maximum measured error: ± 0.07 mm***

***Accuracy: ± 0.035 mm***

# Measurement Results of Dental Tooth(1st Device)

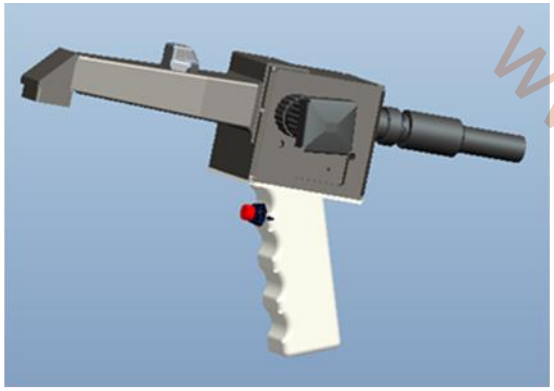

Intraoral scanner

Experiment within
a narrow space

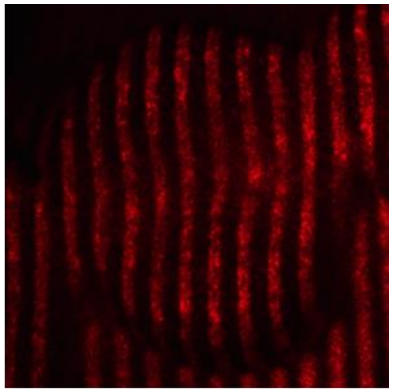

Fringe pattern

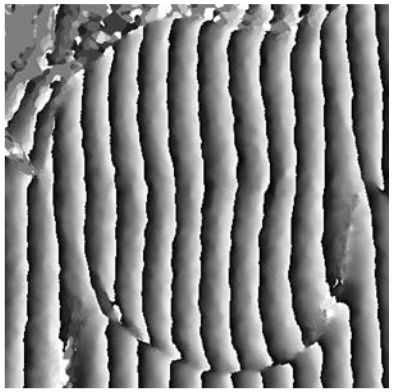

Wrapped phase

Unwrapped phase

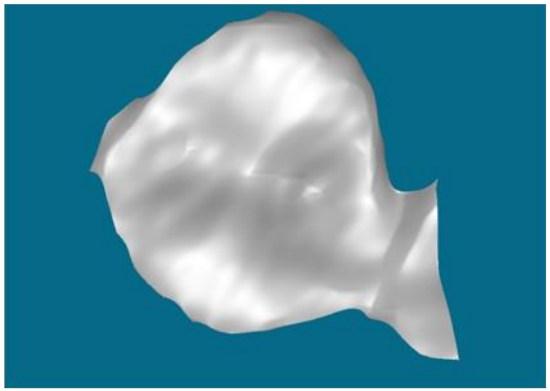

Reconstructed Shaded Tooth

# Issues with the 1st Device

*Inaccurate phase shifts*

*Reconstructed Tooth model*

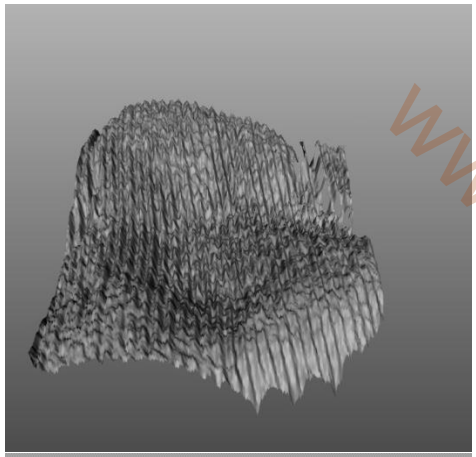

*Inaccurate phase shifts verified by computer simulation*

*Reconstructed virtual object*

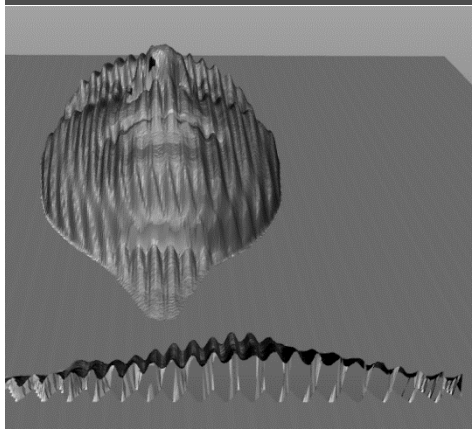

*Fixed platform*

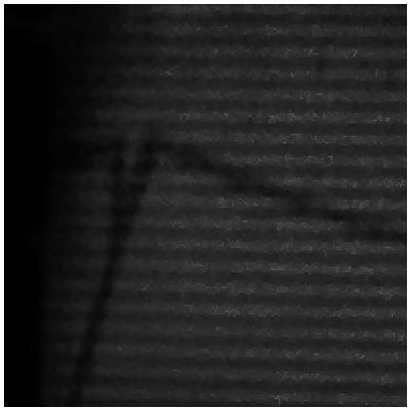

*Low illumination*

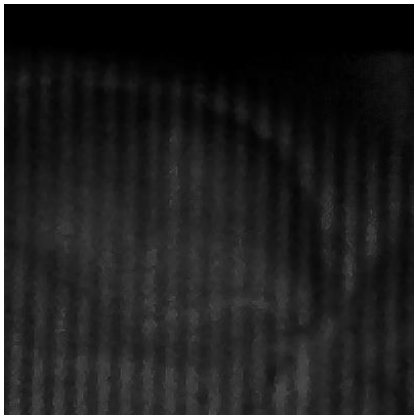



**Issues**

- Low illumination
- Low power hardware
- Camera control
- Inaccurate phase shifts
- PZT
- Fixed platform

# Design of the 2nd Device

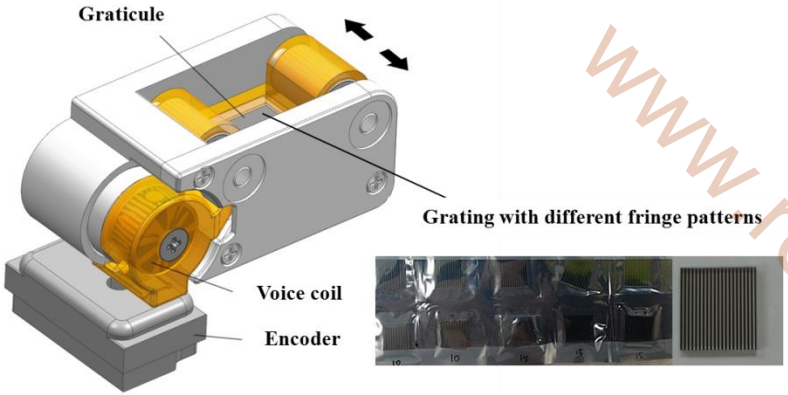


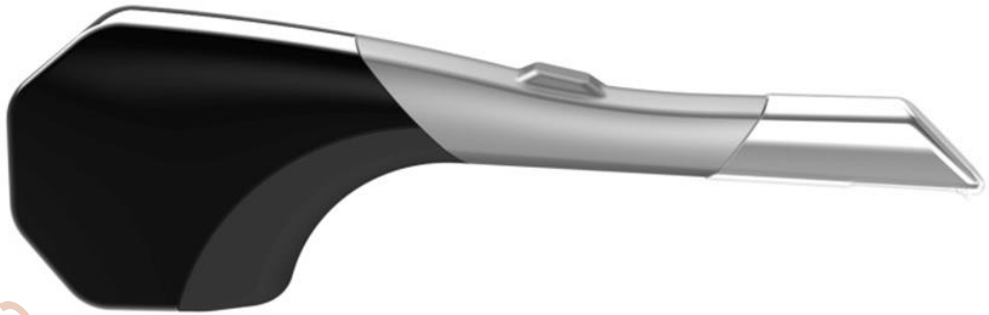

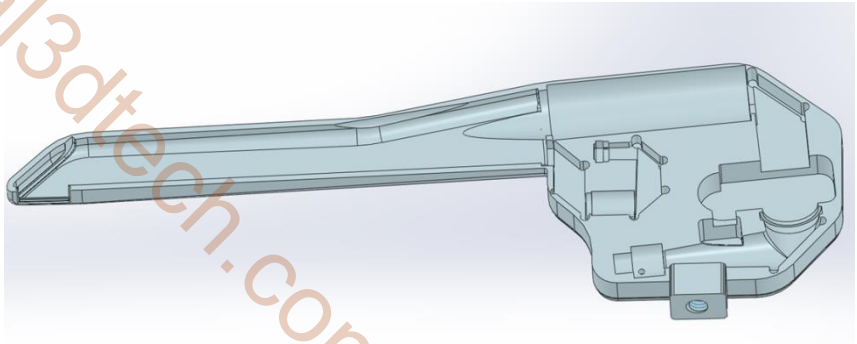

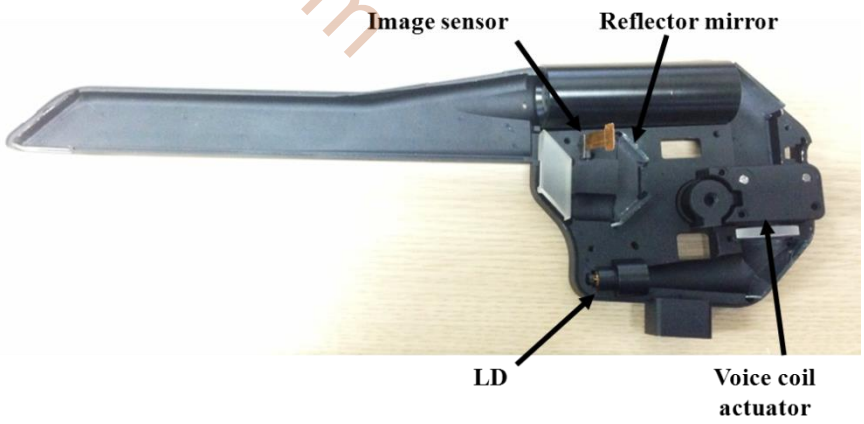


**Improvements**

- Overall design
- LD light source
- CMOS image sensor
- Voice coil actuator (VCA)
- Grating
- Optical lenses

# Issues with the 2nd Device

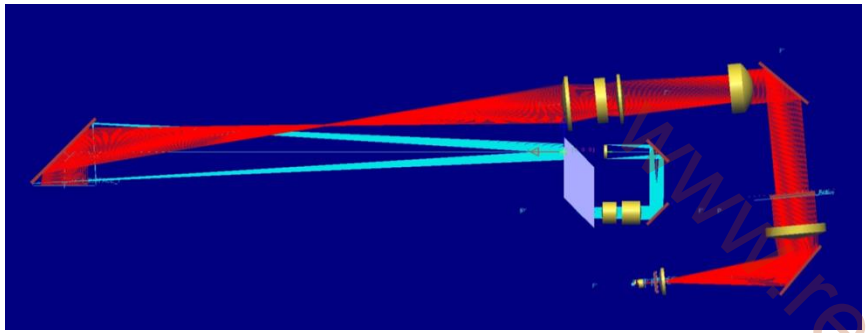

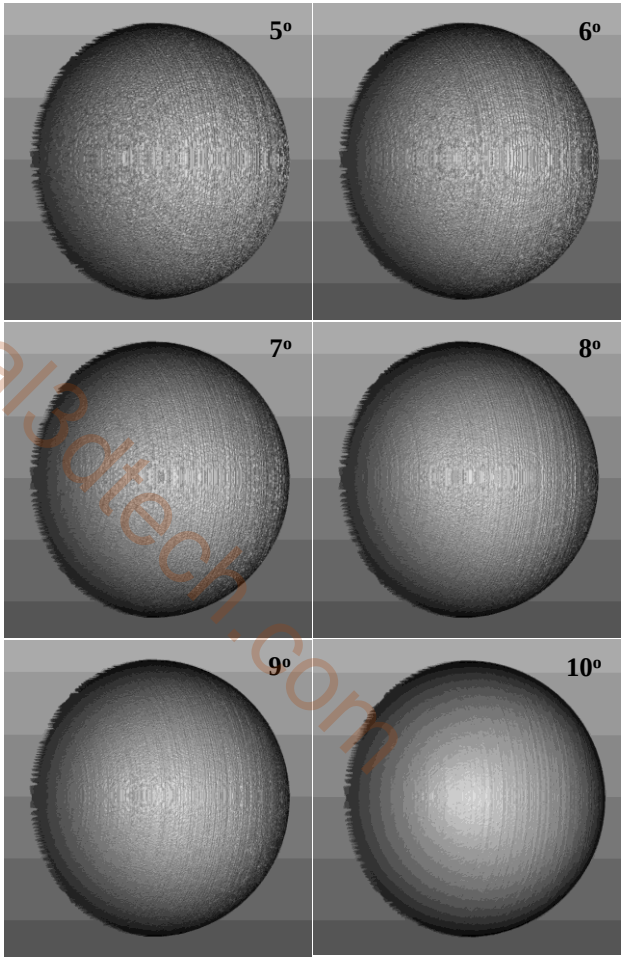


*Verified with computer simulation*

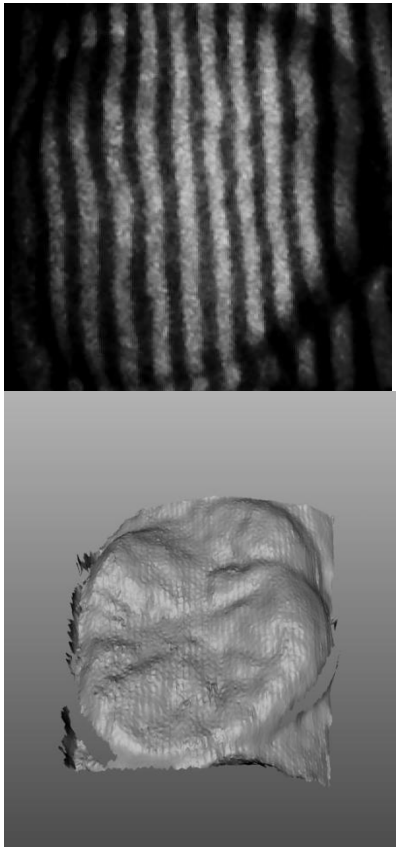

*Optical measurement*



**Issues**

- 5° degree angle between the D (ray of sensor) and L (ray of light source) is not enough to measure surfaces with nice results
- Low power LD
- Hardware temperature goes higher with the long time running

# Design of the 3rd Device

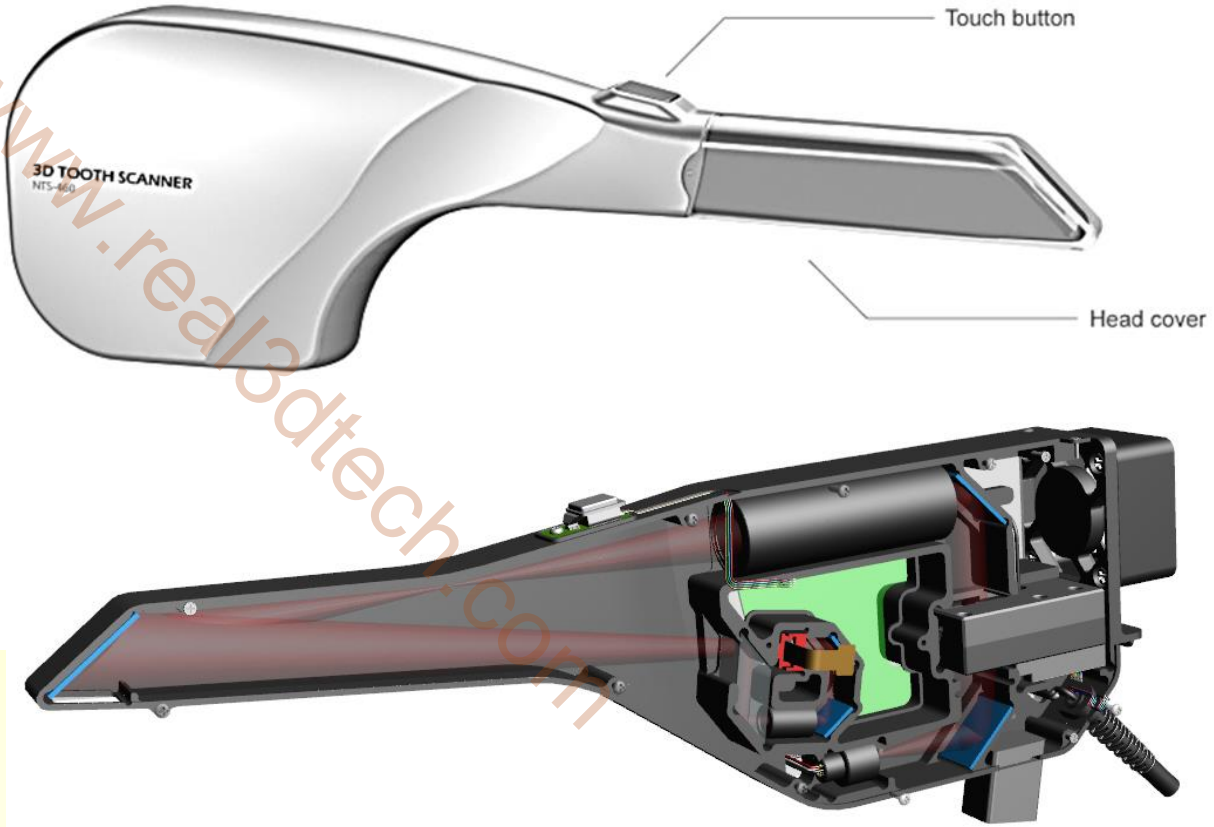




**Improvements**

- Hardware temperature control with a cooling fan
- Visible high power LED as a new light source
- Increase the angle between the sensor and LED ray

명지대학교
MYONGJI UNIVERSITY

# Measurement Results using the 3rd Device

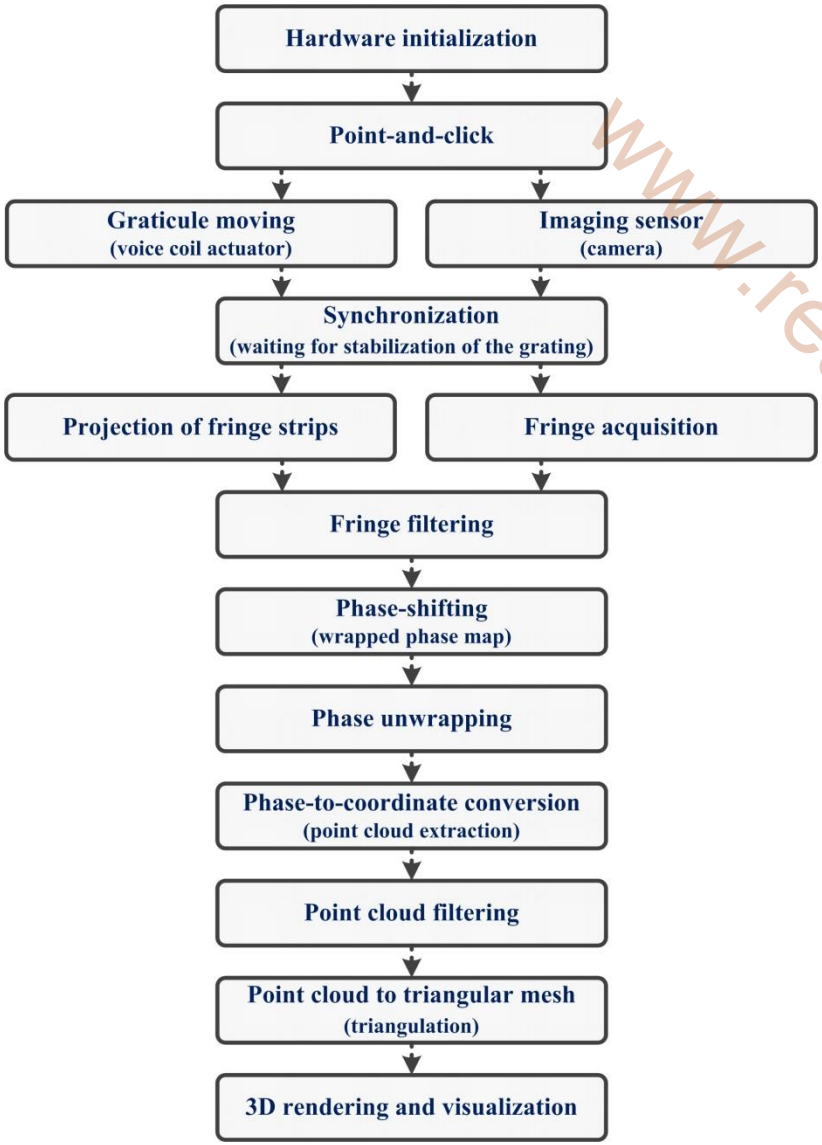




***Measurement results of a plaster model with and without color information.***

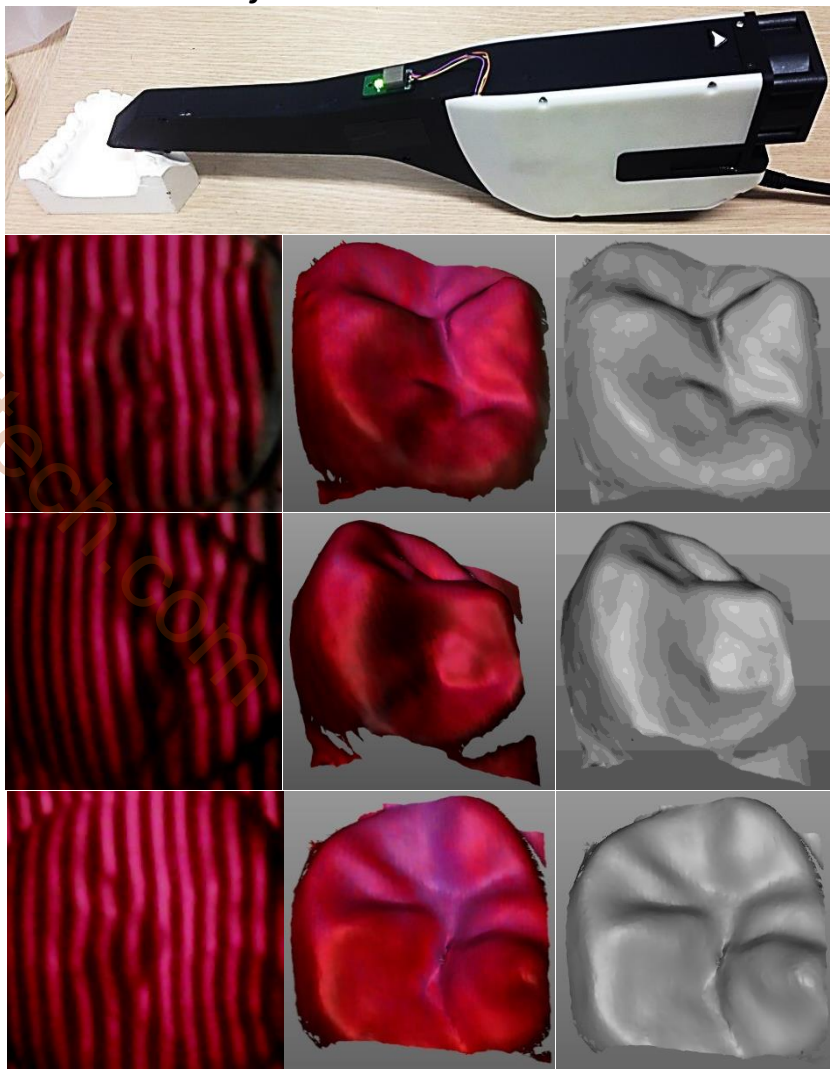

# Articulated Robot Arm



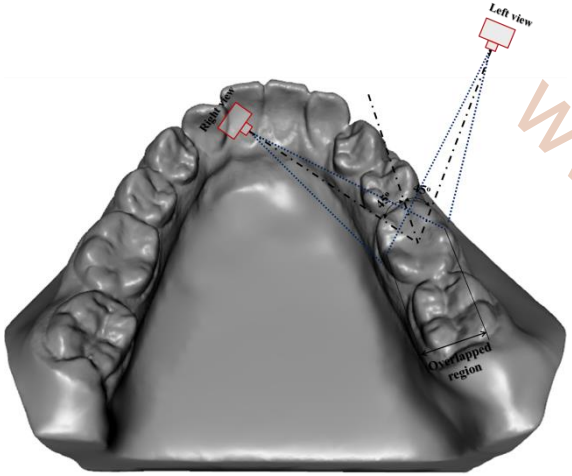


$$D_1 = \frac{{l_1}^2 + {l_2}^2 - {l_3}^2 - x^2 - y^2 - {l_3}^2(xcos\theta + ysin\theta)}{x l_1 l_2}$$

$$D_2 = \left(\frac{x - l_3 cos\theta}{\sqrt{{x_2}^2 + {y_2}^2 + 2l_3(xcos\theta + ysin\theta)}}\right)$$

$$D_3 = \left(\frac{l_2 sin\theta_2}{\sqrt{x^2 + y^2 - 2l_3(xcos\theta + ysin\theta)}}\right)$$

$$\theta_1 = tan^{-1}\left(\frac{\sqrt{1 - D^2{}_2}}{D_2}\right) - tan^{-1}\left(\frac{D_2}{\sqrt{1 - D^2{}_3}}\right)$$

$$\theta_2 = 180 - tan^{-1}\left(\frac{\sqrt{1 - D^2{}_1}}{D_1}\right)$$

$$\theta_3 = \theta - \theta_1 - \theta_2$$

$$\theta_4 = \frac{d}{\pi \times P_{pinion\_dia}}$$

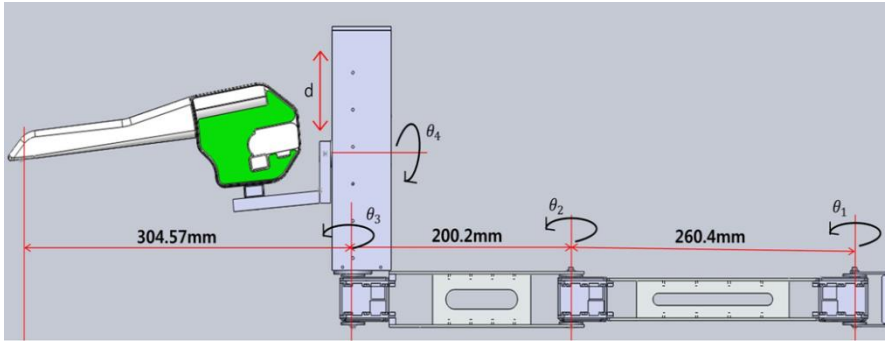


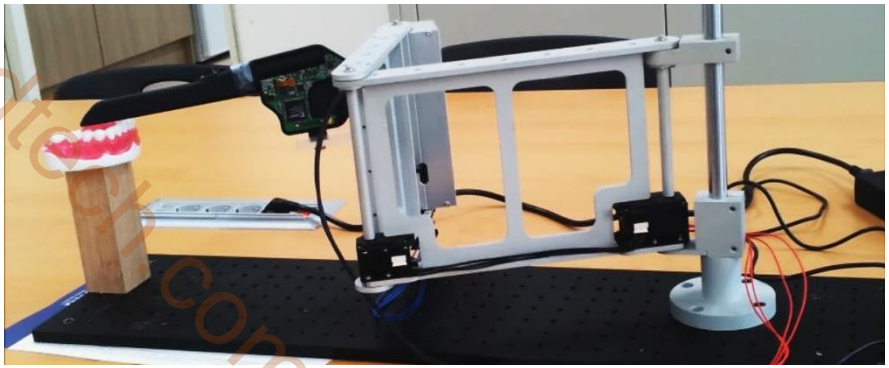

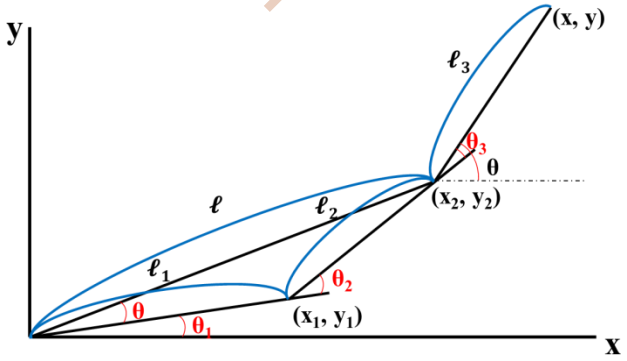

# Registration and Merging

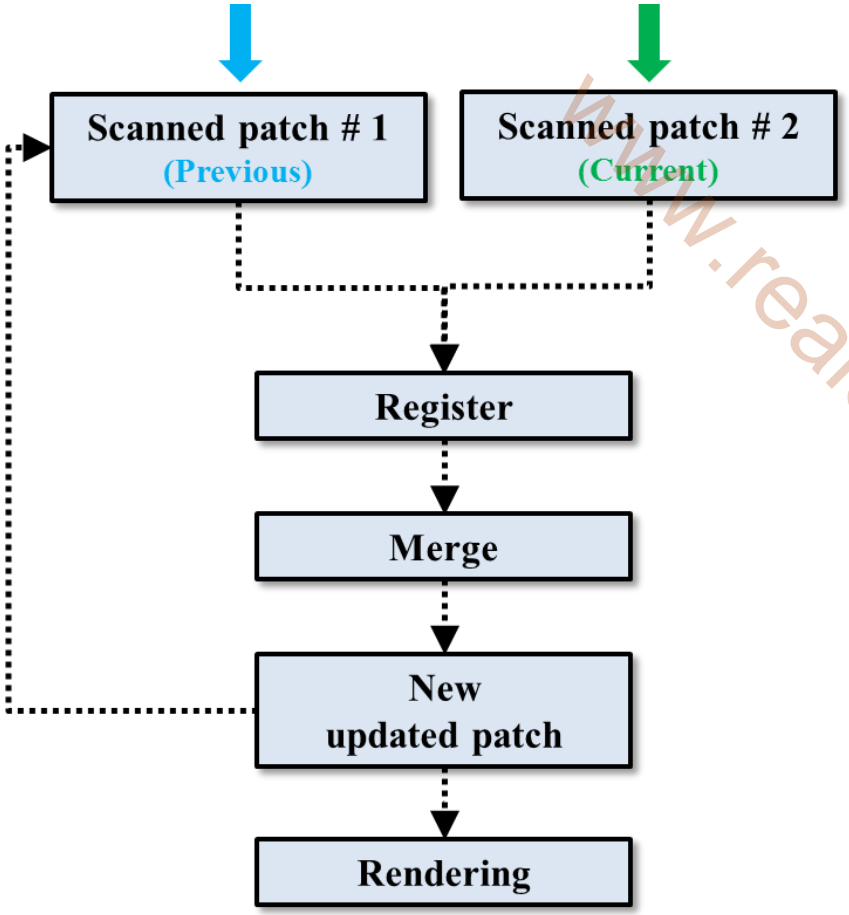


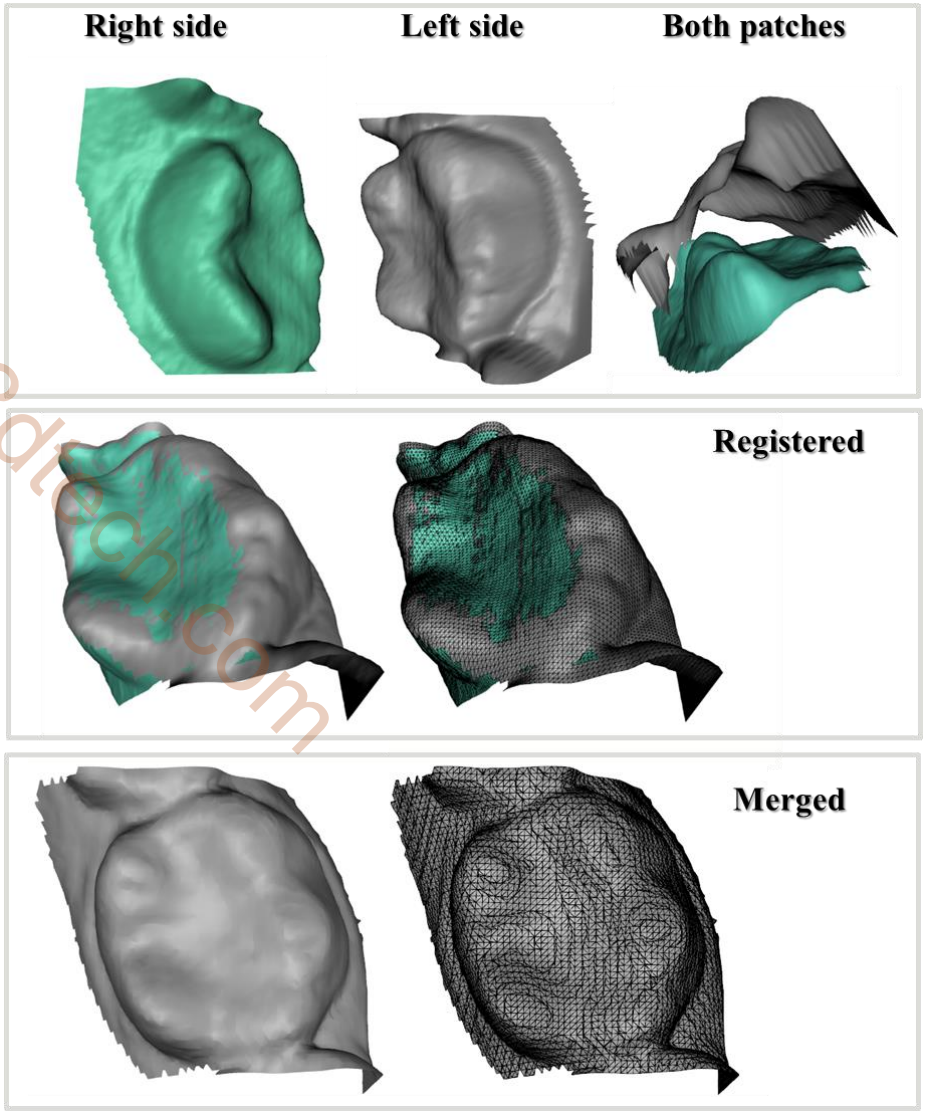




**Registration and merging processes with IOS device are the challenging issues for the future research work.**

# Introduction



***In DFP technique, the fringe patterns are generated by a computer, projected through a digital display device such as DLP projector or LCD projector onto the object and obtained the height of an object from deformed fringe images, which are modulated by the object surface.***

# Setup



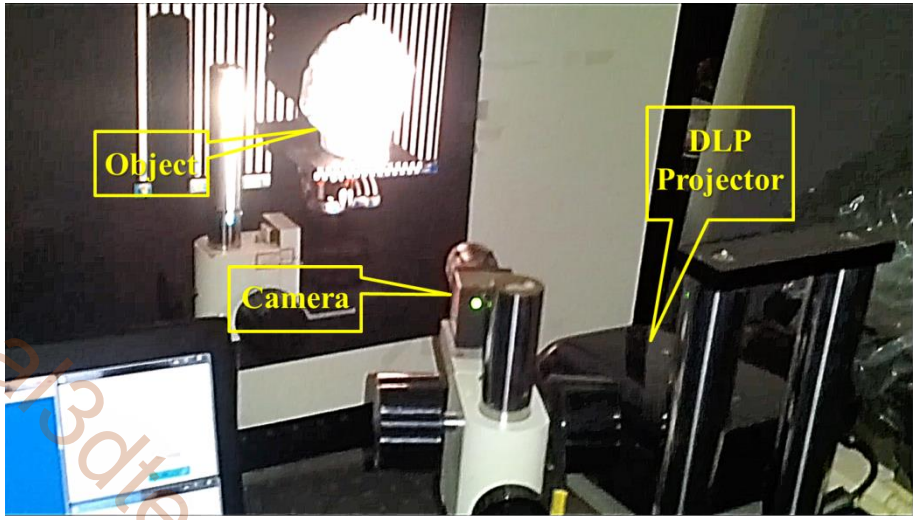


**Features:**

- High resolution reconstruction
- 3,4,5,7-step phase shifting method and can be easily added more.
- Various phase unwrapping algorithms
- Capturing of color and texture information
- Real-time visualization of the scanned object.
- Various kinds of system models can also be adjusted.

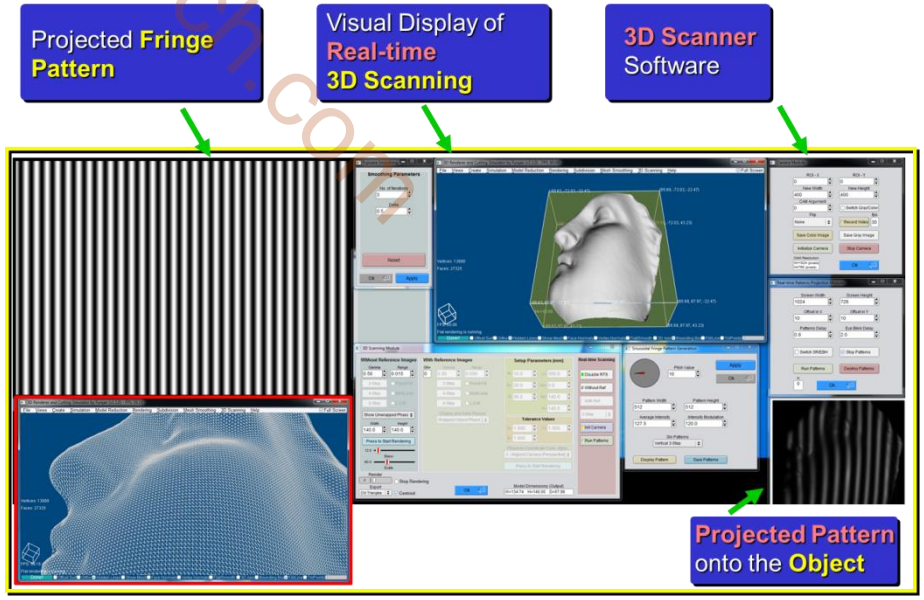

# System Calibration (computer simulation)

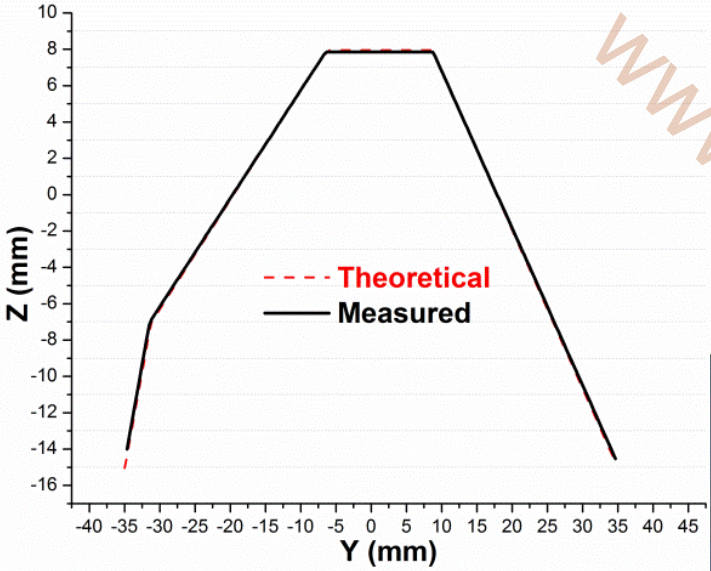


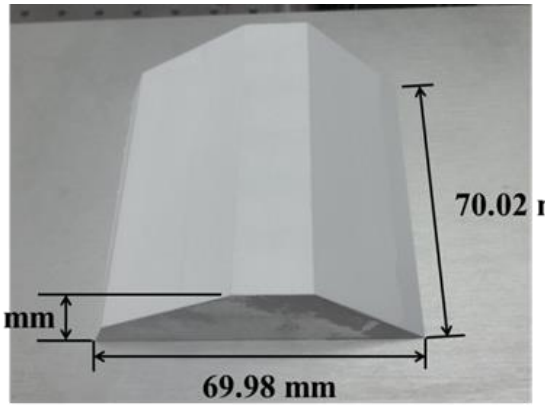


*Reconstruction result of the calibration jig*

**RMS difference = 0.001 mm**

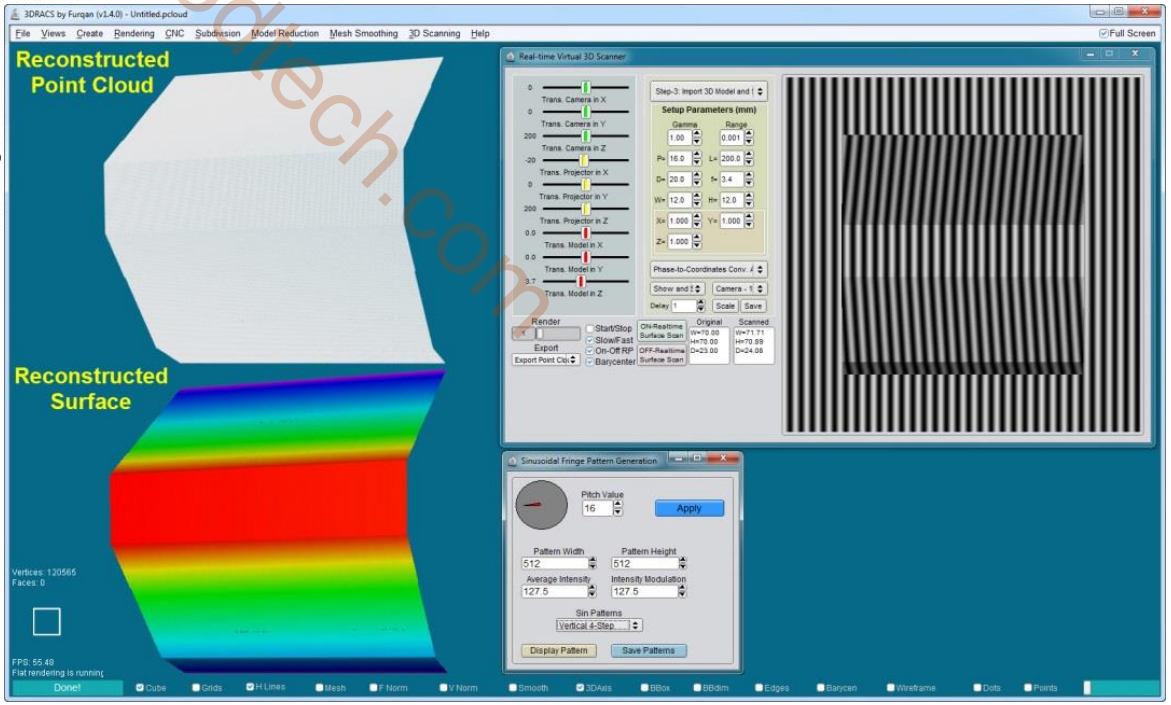

명지대학교
MYONGJI UNIVERSITY

# System Calibration (computer simulation)

*Reconstruction result of complex shapes*

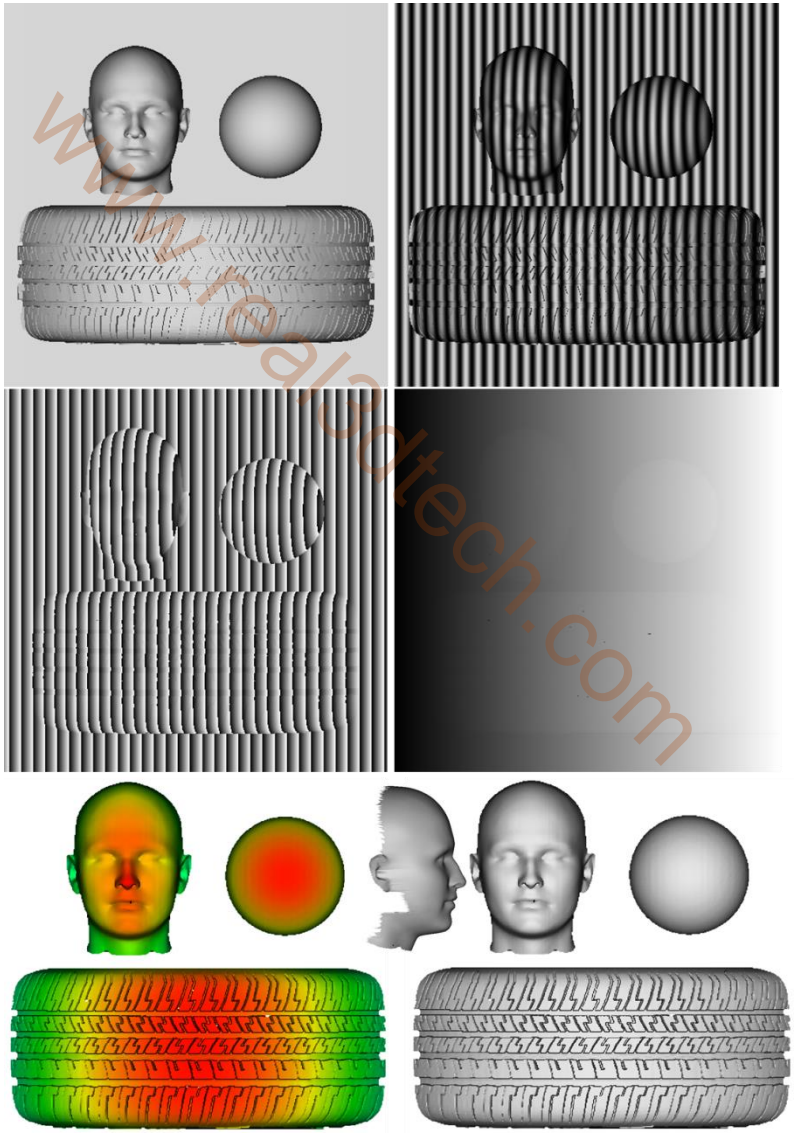

# System Calibration (optical measurement of a jig)

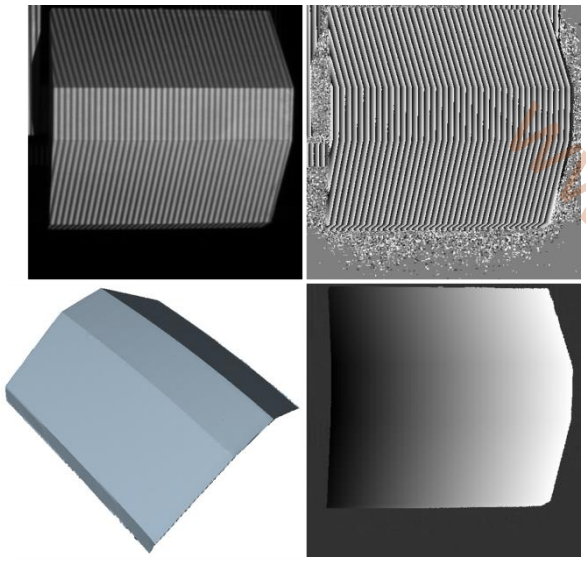

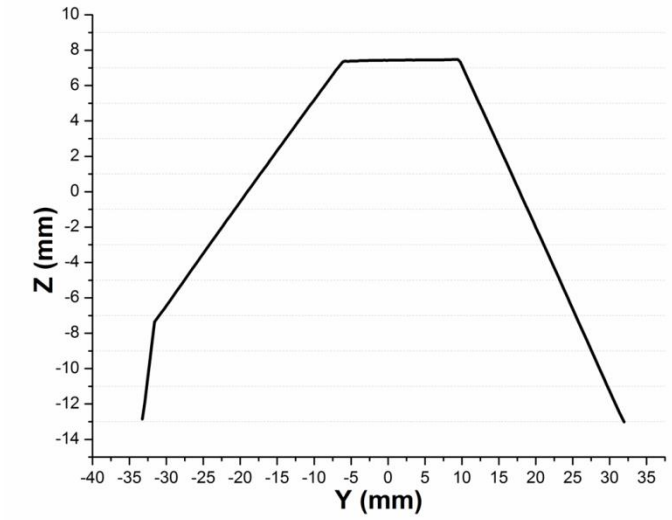


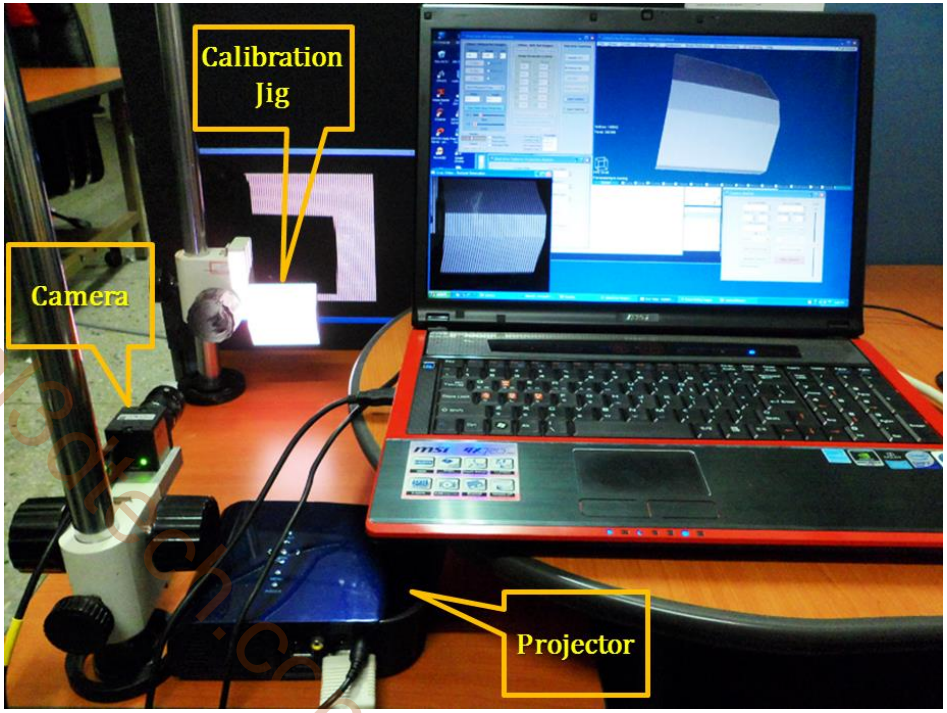


*Setup of the system*

**RMS difference = ±0.036 mm**

# Scanning Procedure

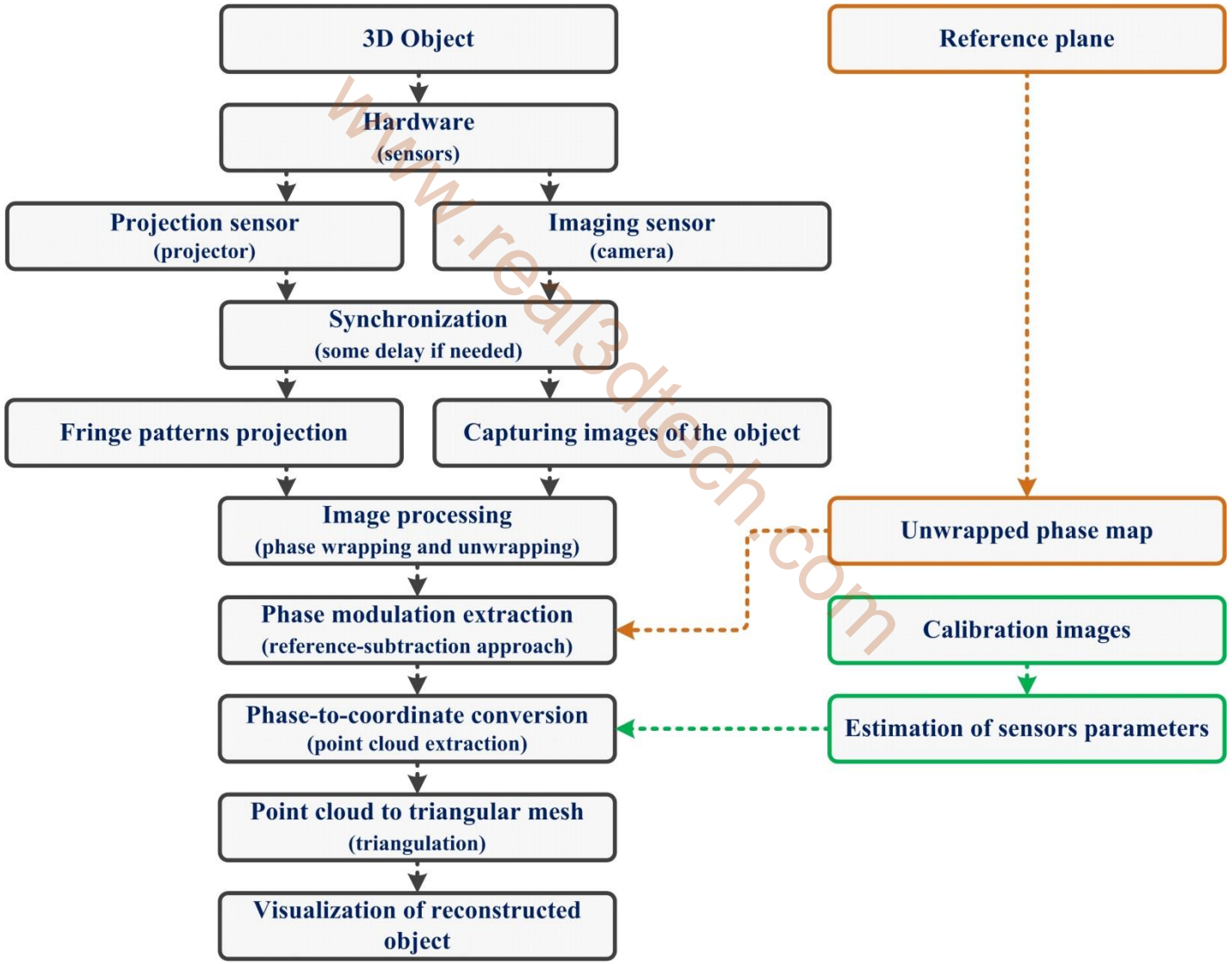

# Optical Measurements of Different 3D Shapes


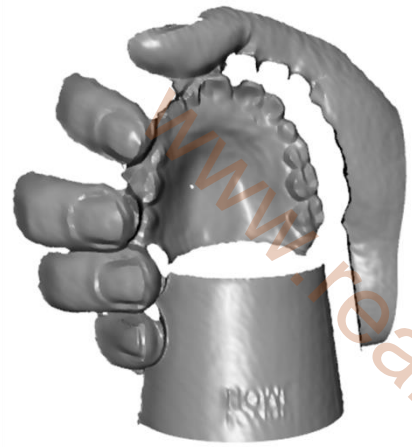


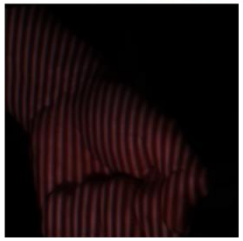
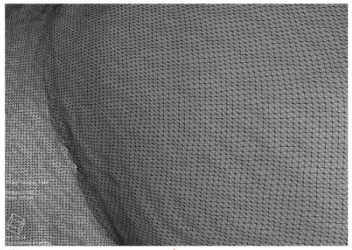



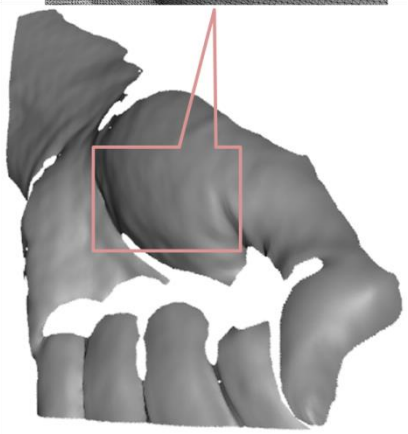

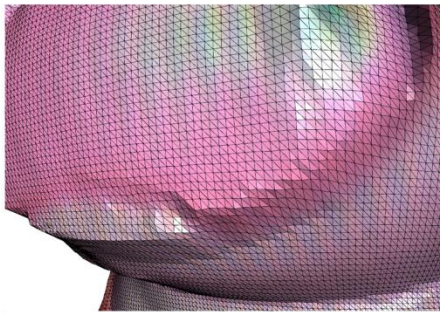

# Optical Measurements of Different 3D Shapes



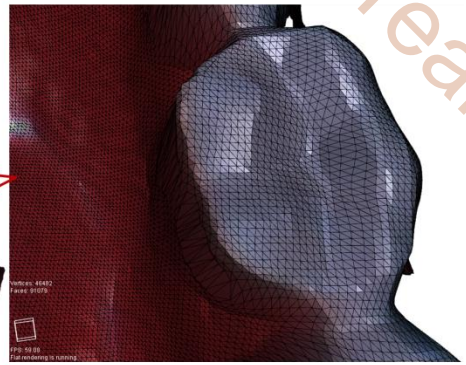

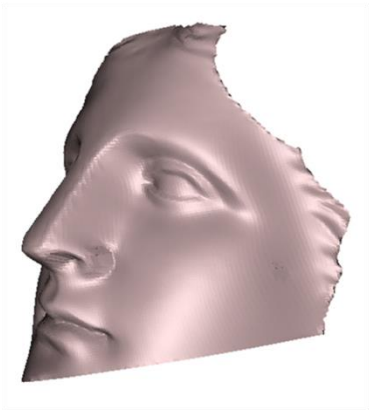

*Approx. 235K triangles*

# Optical Measurement of a Human Hand

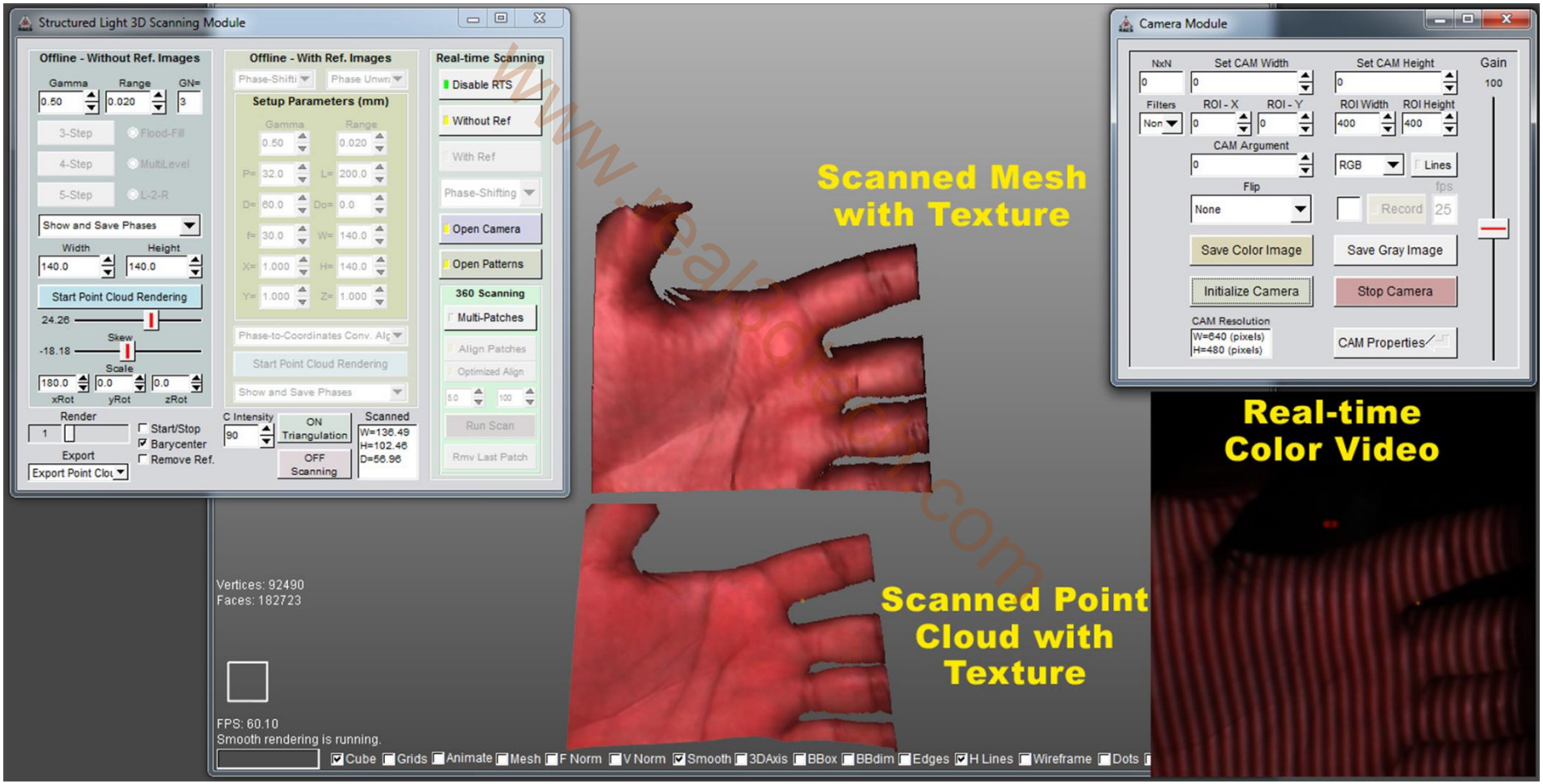


*Real-time scanning is being performed of a human hand with color and texture information*

# Introduction

***Real-time virtual 3D scanner is a high resolution DFP technology based virtual scanner that scans virtual/CAD objects in the virtual environment.***

***It performs projection of computer generated fringe patterns onto the virtual 3D object, images capturing, point cloud acquisition, reconstruction, color texturing, and display processes, simultaneously.***

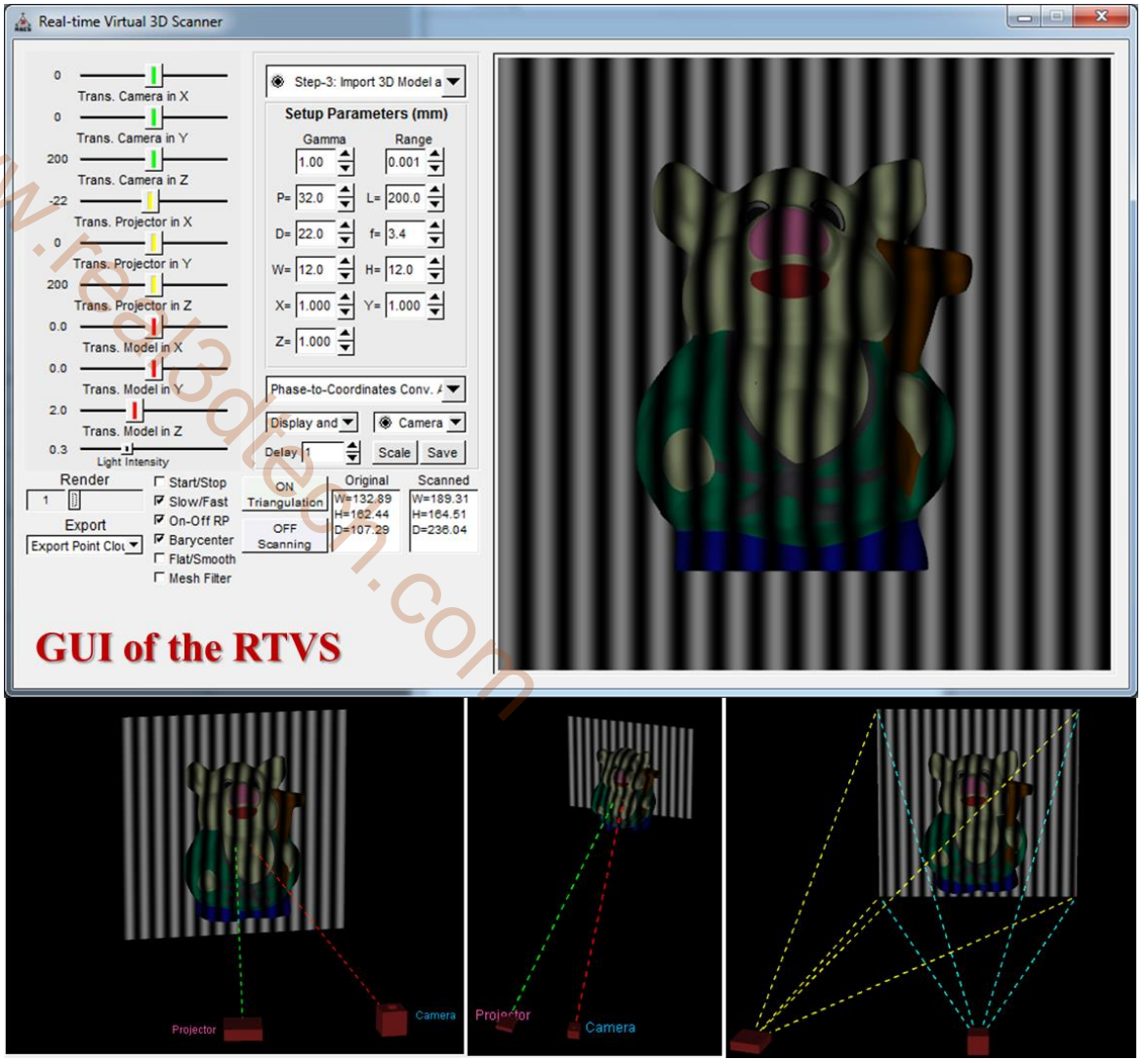

# Relationship of algorithms

$$M_e = \begin{bmatrix} 0.5 & 0 & 0 & 0 \\ 0 & 0.5 & 0 & 0 \\ 0 & 0 & 0.5 & 0 \\ 0.5 & 0.5 & 0.5 & 1.0 \end{bmatrix}_{bias\ from [-1,1] to [0,1]} M_l M_v$$

***$M_e$ = eye linear texgen homogenous matrix***

***$M_l$ = light projection homogeneous matrix***

***$M_v$ = light view homogenous matrix***

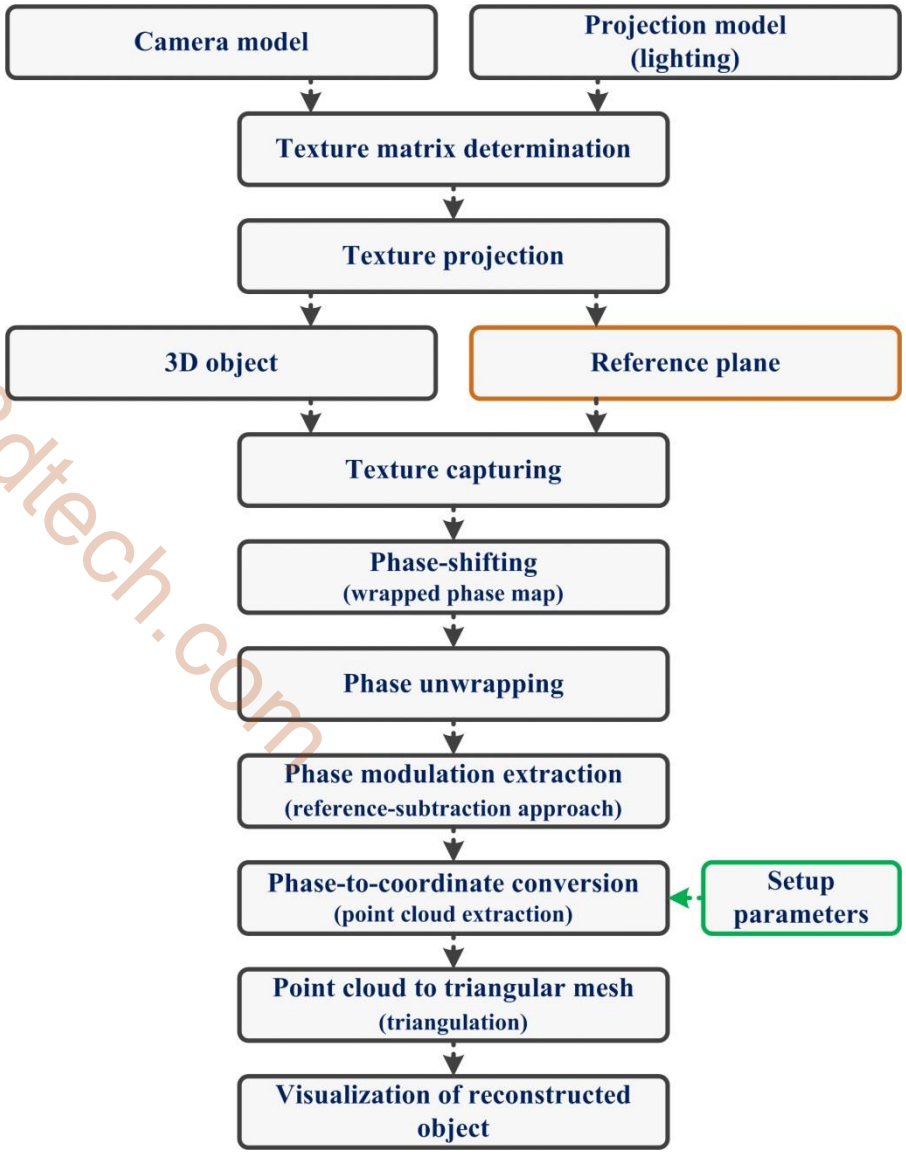

# Experiments

**Features:**

- High resolution reconstruction
- 3,4,5,7-step phase shifting method and can be easily added more.
- Various phase unwrapping algorithms
- Capturing of color and texture information
- Real-time visualization of the scanned object.
- Various kinds of system models can also be adjusted.

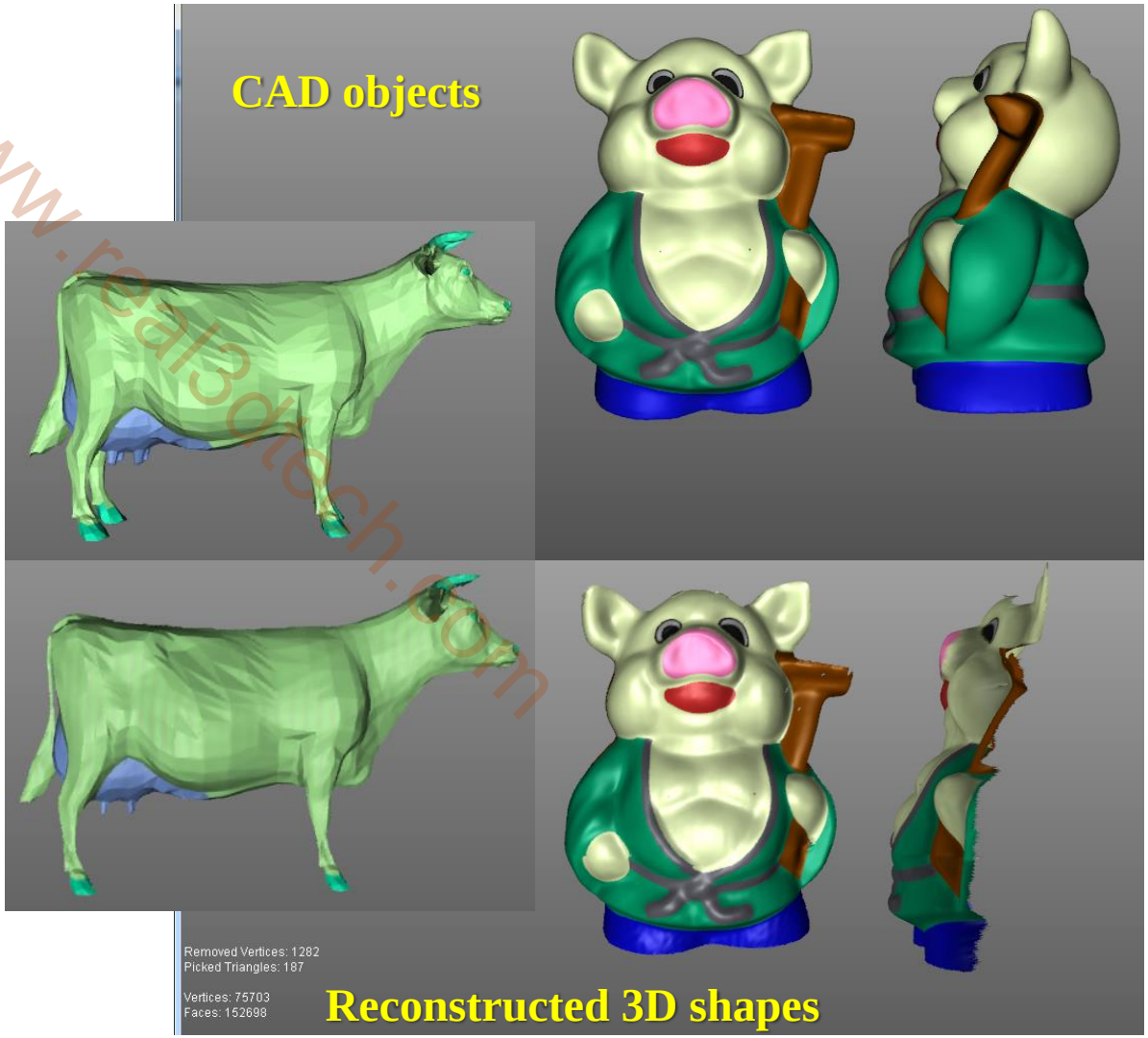

# Virtual Reconstruction of different 3D Shapes

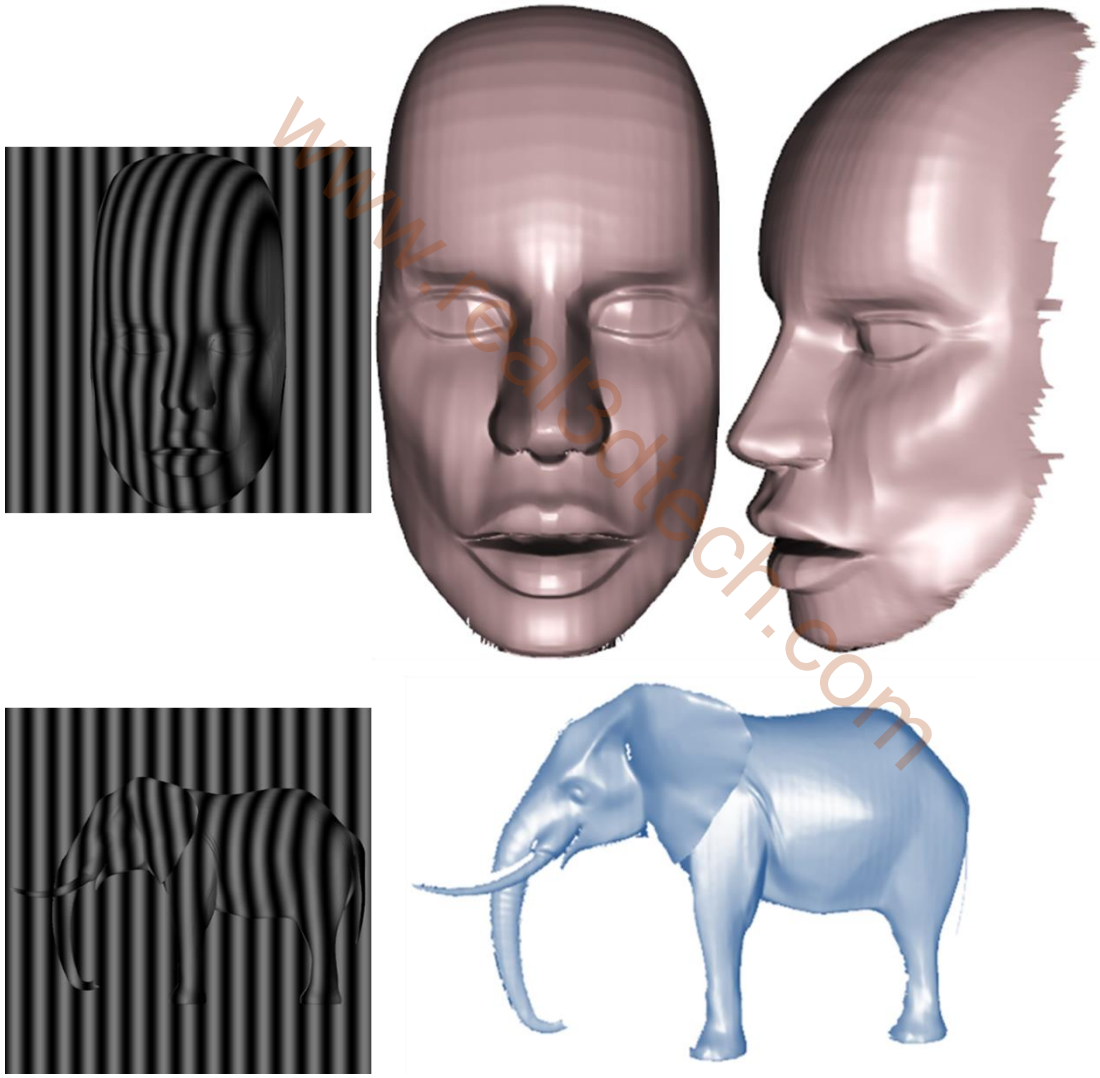



*Fringe patterns onto the CAD objects and reconstructed 3D shapes*

# Virtual Reconstruction of different 3D Shapes

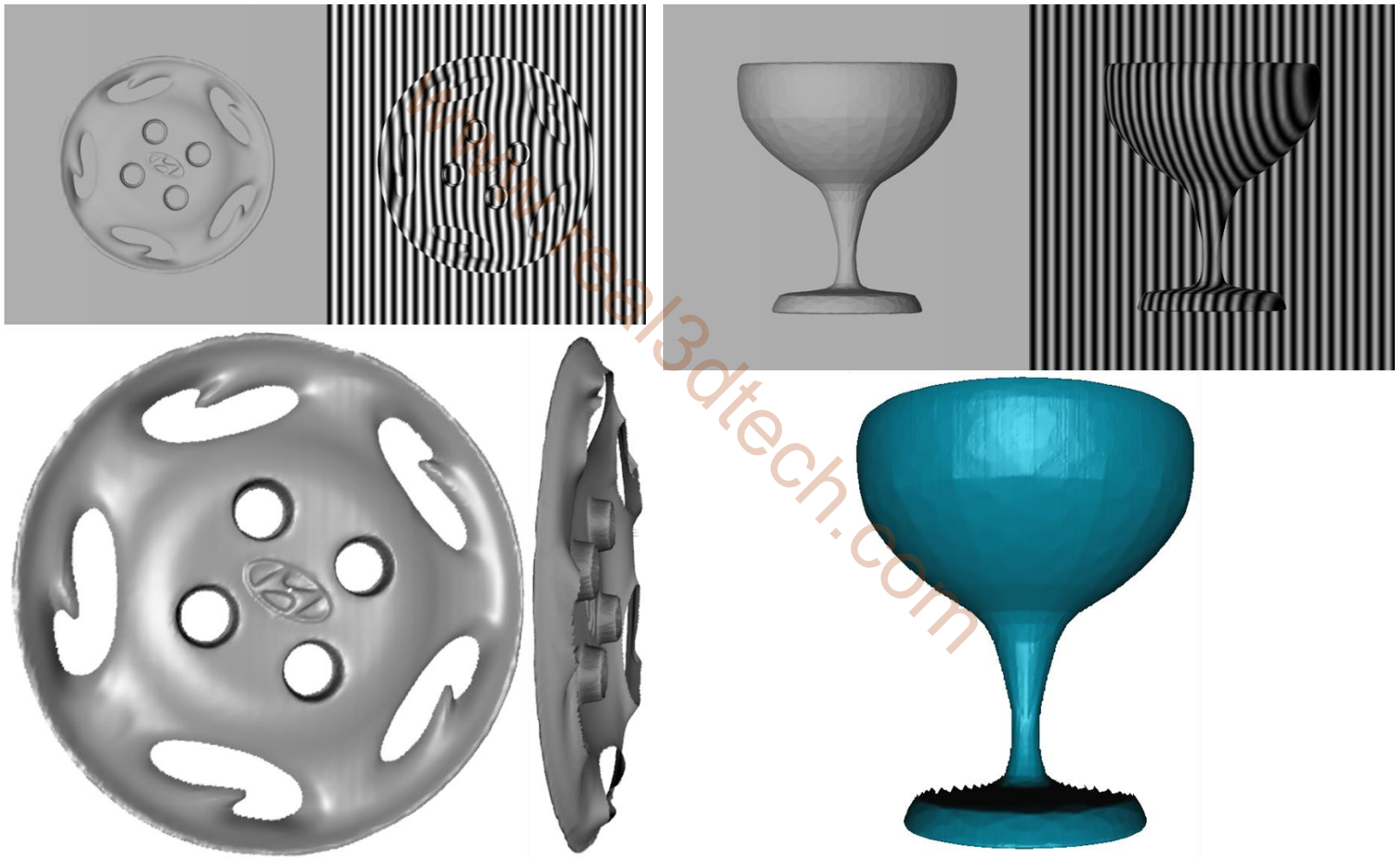



*Cad objects with reference planes and reconstructed 3D shapes*

# Introduction



***The important portion of the research work of this dissertation is to design and develop a computer software.***

***The system software is developed based on C/C++ object oriented, OpenCV, and OpenGL programming languages. The software is based on Windows and FLTK GUI and can be executed on Microsoft Windows XP/Vista/7/8.1 operating systems.***

# GUI

명지대학교
MYONGJI UNIVERSITY

**Projected Fringe Pattern**

**Visual Display of Real-time 3D Scanning**

**3D Scanner Modules**

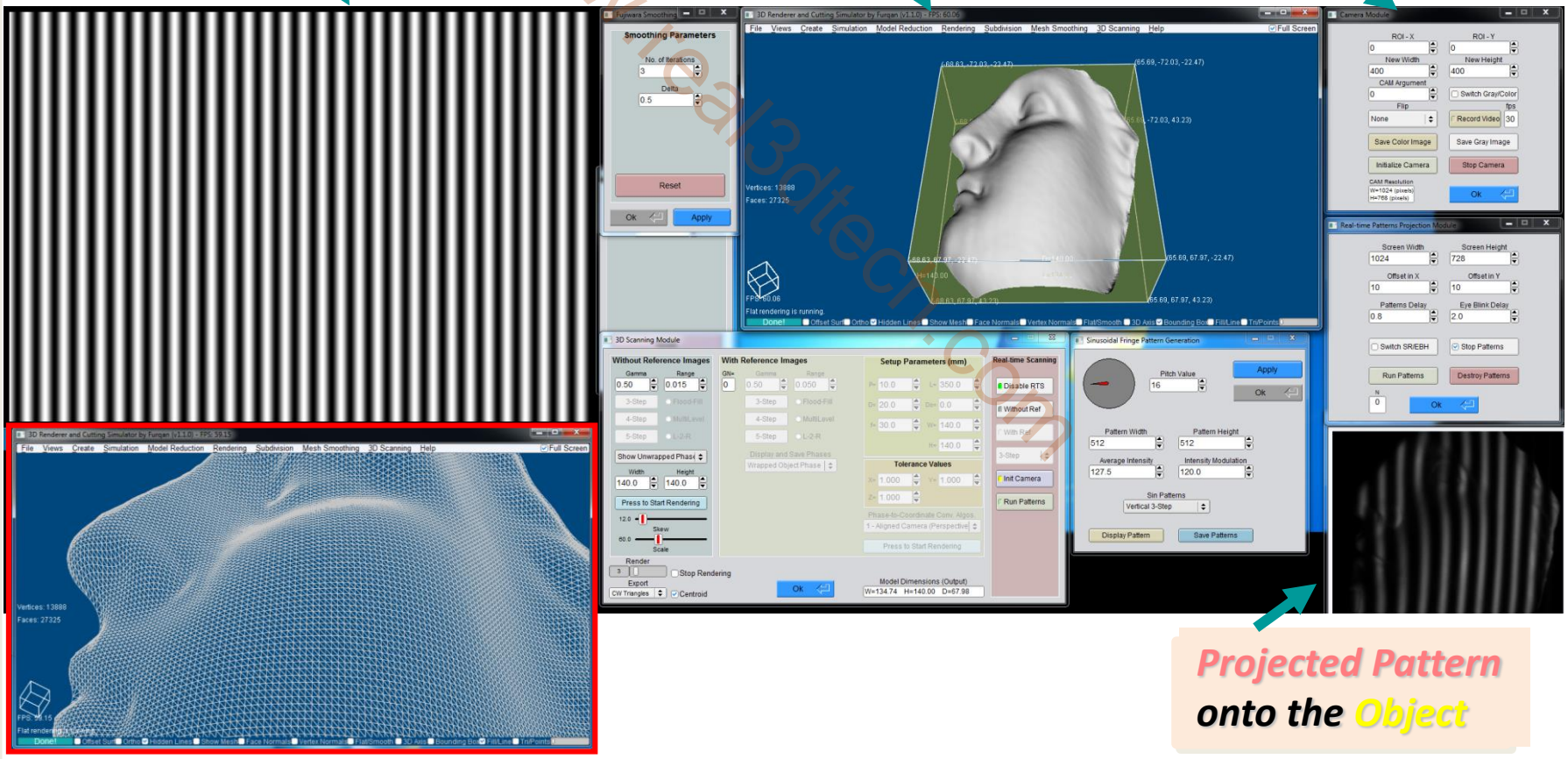


**Projected Pattern onto the Object**

# Features

**General image Processing:**

- Import and export
- Display
- Noise reduction and smoothing filters
- Color adjustment (brightness, contrast, equalize, etc.)
- Resize
- Rotate
- Zoom in and zoom out
- Filters for edge detection

**General 3D Processing:**

- Import and export of point clouds and triangular meshes
- 3D visualization with rotate, zoom, and pan using mouse and keyboard
- Point clouds and meshes filtering and smoothing
- Lightings and color adjustments
- Sectioning
- Translate, rotate, and scale
- Texturing
- Animation
- Mesh reconstruction, subdivision, smoothing, decimation, normal
- Point cloud and mesh registration
- Batch processing for more than one point clouds and meshes

명지대학교 MYONGJI UNIVERSITY

# Features

**Simulation for real-time 3D scanning:**

- Real-time 3D scanning using 3-step, 4-step, and 5-step phase shifting methods
- Phase unwrapping using quality-guided, flood-fill, multilevel, and linear algorithms
- Real-time 3D scanning with any image resolution
- Adjustable system parameters for camera, projector, and object
- Display of virtual scene from different angles
- Real-time visualization of reconstructed point cloud and mesh
- Various system models for collimating and non-collimating illumination
- Display and save wrapped, unwrapped, phase modulation, and color map images
- Real-time point cloud and mesh filtering
- Real-time reconstruction resolution adjustment
- Delay in real-time scanning
- Import of CAD/virtual objects
- Export of reconstructed point clouds and meshes

**Real-time and Offline 3D scanning:**

- Processing of 3-step, 4-step, and 5-step phase shifted images
- Unwrap the wrapped image
- Display and save the processed images
- Reconstruction of point clouds using various algorithms
- Point cloud to triangulation conversion with real-time visualization
- Real-time camera control
- Real-time projection of fringe patterns control
- 3D Reconstruction with and without reference plane
- Point-and-click scanning with multi-patches visualization
- Texture capturing and visualization
- Export of reconstructed point clouds and meshes

# Controls for IOS device

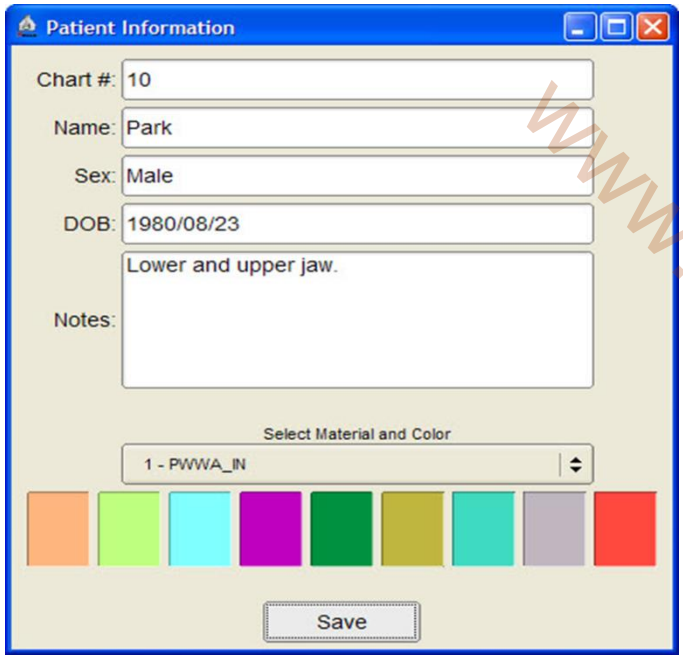


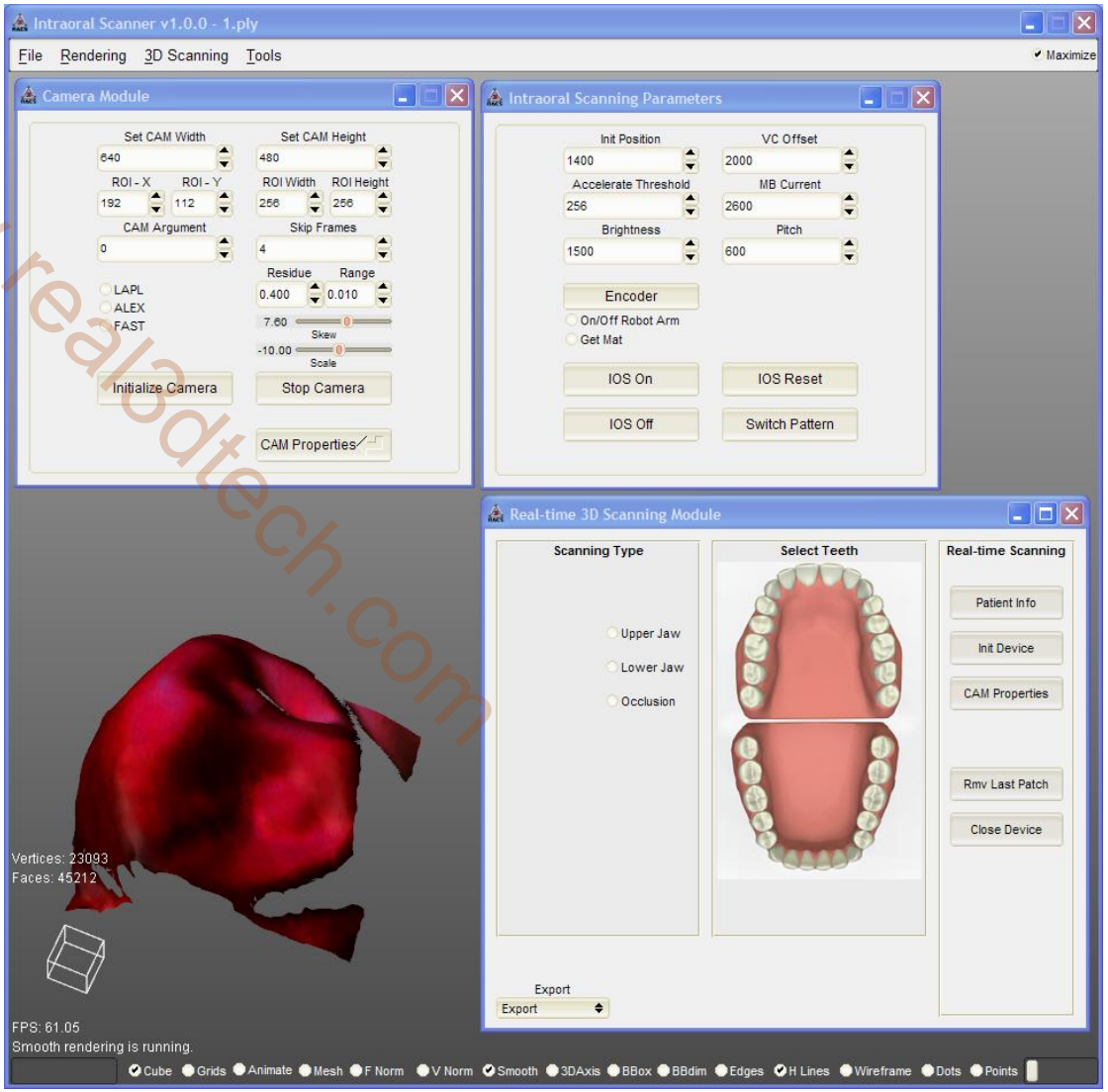

# Contributions

1. *Two mathematical system models for SMFP for calculating the x, y, and z coordinates of the object profile.*

2. *Development of a 3D intraoral scanner based on structured light fringe projection technology.*

3. *Development of a SMDFP system which is capable of performing small and large scale measurements in real-time and can be applied to various applications.*

4. *Development of a real-time virtual 3D scanner based on DFP which will be very effective in the future development of new algorithms, and performance analysis of new 3D shape measurement systems.*

5. *The important contribution of this dissertation is the development of a 3D CAD and Scanning software with various fast and improved algorithms. The algorithms include triangulation, filtering, smoothing, registration, merging, etc.*

# Industrial Benefits

1. *3D shape measurement is becoming increasingly important in many industrial applications, e.g. precision shape measurement for production control, reverse engineering, volume measurement, skin surface measurement for cosmetics and medicine, body shape measurement, intraoral dental measurement, forensic science inspections, microscale measurements, and entertainment, etc.*

2. *The research results reported in this dissertation can be used to develop new methods, algorithms, and improve the performance of existing 3D shape measurement systems to ensure their wide spread use in industry.*

3. *The new mathematical models presented in this dissertation provide a rigorous theoretical base for the practical applications of fringe projection profilometry, thus improving the shape measurement accuracy.*

# Industrial Benefits



3. *This dissertation presented a detailed development procedure of a 3D intraoral scanning device that could solve some of the issues associated with cast production, and it could also provide a digital workflow with digital output data. The presented intraoral scanner is a very effective addition in the industry of dentistry and we believe that this research will open a new way to develop such micro-scale devices.*

4. *This dissertation also presented a low-cost real-time 3D SMDFP system that uses only one camera and a projector, and can be applied to various industrial applications for small and large scale measurements. We believe that the low cost of the systems ensures the wide deployment of this technique in industry.*

# Future Work

- **Improvement in IOS device:**
  - *The calibration of the PZT or VCA for accurate phase shift*
  - *There is still room for improvement in the device to achieve better performance*
  - *It is desired to seek for other ideas and methods which are easier to develop, handle, and operate rather than Articulated Robot Arm.*
  - *Video-scanner should be developed that register multiple 3D images in real-time*

- **Improvement in SMDFP system:**
  - *It is desired to seek for other non-linear methods which should provide better performance and easiness in the calibration process.*
  - *Full body or 360$^{o}$ shape*

# Videos

명지대학교
MYONGJI UNIVERSITY



- Real-time IOS Scanning using 1st IOS Device
- Point-and-click scanning using 3rd IOS Device
- Working of Articulated Robot Arm

- Real-time 3D Scanning using SMDFP system

- Real-time Virtual 3D scanning

# References


1. Gorthi, S. S., Rastogi, P., "Fringe projection techniques: whither we are?," Opt. Lasers Eng. Vol. 48, pp. 133-140, 2010.
2. Mark L. Kimber, "Development of a Virtually Calibrated Projection Moiré Interferometry Technique Capable of Inaccessible Surface Measurements," 2004.
3. Huntley, J. M., "Optical shape measurement technology - past, present, and future," Proc. SPIE 4076, pp. 162-173, 2000.
4. Chen, L., Huang, C., "Miniaturized 3D surface profilometer using digital fringe projection," Meas. Sci. Techn. Vol. 16, No. 5, pp. 1061-1068, 2005.
5. Moore, C. J., Burton, D. R., Skydan, O., Sharrock, P. J., Lalor, M., "3D body surface measurement and display in radiotherapy part I: Technology of structured light surface sensing," Proc. Int. Confe. Medical Information Visualisation - BioMedical Visualisation (1691277), pp. 97-102. 2006.
6. Chen, X., Xi, J. t., Jiang, T., Jin, Y., "Research and development of an accurate 3D shape measurement system based on fringe projection: Model analysis and performance evaluation", Precision Engineering, Vol. 32, pp. 215–221, 2008.
7. Zhang, S., "Recent progresses on real-time 3D shape measurement using digital fringe projection techniques," Opt. Lasers Eng. Vol. 48, pp. 149–158, 2010.
8. Furqan U., Gun S. L., Kang P., " Development of a Real-time 3D Intraoral Scanner based on Fringe-Projection Technique," Transactions of the Society of CAD/CAM Engineers, Vol. 17, No. 3, pp.156-163, 2012.
9. Furqan U., Gun S. L., Kang P., "Analysis and Performance Comparison of 3D Measurement Systems based on Fringe Projection Profilometry," 2012 International Conference on Information Science and Applications, pp. 62-67, 23-25 May 2012.
10. Shouhong T., Tucson, AZ., "Non-linear phase shift calibration for interferometric measurement of multi surfaces," US Patent No. 6856405 B2, Feb. 15, 2005.
11. Hui D., Xiangnan W., Jianqi L., Xianli L., "Online calibration of PZT driven fiber Fabry–Perot filter nonlinearity using FBG array and PSO algorithm," Measurement, Vol. 42, pp. 1059-1064, 2009.
12. Yeou Y., Cheng and James C. Wyant, "Phase shifter calibration in phase-shifting interferometry," Applied Optics, Vol. 24, No. 18, 1985.
13. K. Kinnsta¨tter, A. W. Lohmann, J. Schwider, and N. Streibl, "Accuracy of phase shifting interferometry," Appl. Opt. 27, 5082–5089, 1988.
14. C. P. Brophy, "Effect of intensity error correlation on the computed phase of phase-shifting interferometry," J. Opt. Soc. Am.A7, 537–541, 1990.
15. L. A. Selberg, "Interferometer accuracy and precision," in Optical Fabrication and Testing, D. R. Campbell, C.W. Johnson, and M. Lorenzen, eds., Proc. Soc. Photo-Opt. Instrum. Eng.1400, 24–32, 1990.
16. P. de Groot, "Predicting the effects of vibration in phase shifting interferometry," in Optical Fabrication and Testing Workshop, Vol. 13. of 1994 OSA Technical Digest Series 1Optical Society of America, Washington, D.C., 19942, pp. 189–192.
17. Rusinkiewicz, S., Hall-Holt, O., Levoy, M., "Realtime 3D model acquisition," In Proceedings of Siggraph, pp. 438-446, July 2002.
18. Huang, P. S., Zhang, C., Chiang, F., "High-speed 3-D shape measurement based on digital fringe projection," Opt. Eng. Vol. 42, No. 1, pp. 163-168, 2003.
19. Guan, C., Hassebrook, L. G., Lau, D. L., "Real-time 3-D data acquisition for augmented reality man and machine interfacing," Visualization of Temporal and Spatial Data for Civilian and Defense Applications V, SPIE's AeroSense, vol. 5097, A-5, 2003.
20. Koninckx, T. P., Gool, L. V., "Real-time range acquisition by adaptive structured light," IEEE Trans. Pattern Analy. Mach. Intell., Vol. 28, No. 3, pp. 432-445, 2006.
21. Breuckmann, B., Halbauer, F., Klaas, E., Kube, M., "3D-metrologies for industrial applications," In Proceedings of SPIE 3102, pages 20–29, 1997.
22. Wicher, J., Meer, V. D., Andriessen, F. S., Wismeijer, D., Ren, Y., "Application of Intra-Oral Dental Scanners in the Digital Workflow of Implantology," PLoS ONE, Vol. 7, No. 8, August 2012.
23. Riehemann, S., Palme, M., Kuehmstedt, P., Grossmann, C., Notni, G., Hintersehr, J., "Microdisplay-Based Intraoral 3D Scanner for Dentistry," Journal of Display Technology, Vol. 7, No. 3, pp. 151-155, 2011.
24. Hart DP., Lammerding J., Rohaly J., " 3-D Imaging System," US Patent 2004/0155975 A1, Aug 12, 2004.
25. Trissel RG., "Polarizing multiplexer and methods for intra-oral scanning," US Patent 2007/0047079 A1, Mar 01, 2007.
26. Ernst MM., Neta U., Cohen C., Geffen M., "Three-dimensional modeling of the oral cavity," US Patent 2008/0273773 A1; Nov 6, 2008.
27. Dillon RF., Zhao B., Judell NHK., "Intra-oral three-dimensional imaging system," International Publication WO 2009/058656 A1, May 7, 2009.
28. Silvia L., Giordano F., Ari K., Michele C., Lapo G., Luciano B., "A Comparative Analysis Of Intraoral 3d Digital Scanners For Restorative Dentistry," The Internet Journal of Medical Technology, Vol. 5, No. 1, 2011.
29. E. Hu and Y. He., "Surface profile measurement of moving objects by using an improved π phase-shifting Fourier transform profilometry," Optics and Lasers in Engineering, 47(1):57-61, 2009.
30. M.T.K. Takeda M, Mutoh, "Fourier transform profilometry for the automatic measurement of 3-D object shapes," Appl. Opt, 22:3977–3982, 1983.
31. H.M. Yue, X.Y. Su, and Y.Z. Liu. "Fourier transform profilometry based on composite structured light pattern," Optics and Laser Technology, 39(6):1170–1175, 2007.
32. L. Zhang, B. Curless, and SM Seitz. "Rapid shape acquisition using color structured light and multi-pass dynamic programming," In 3D Data Processing Visualization and Transmission, 2002. Proceedings. First International Symposium on, pages 24–36, 2002.
33. J. H. Bruning, D. R. Harriott, J. E. Gallagher, D. P. Rosenfeld, A. D. White, D. J. Brangaccio, Appl. Opt. 13, 2693 (1974).
34. Wyant, J. C., "Phase-Shifting Interferometry," Technical Report. Optical Sciences Center, University of Arizona, 1998.
35. Buckland, J. R., Huntley, J. M., and Turner, J. M., (1995), Unwrapping noisy phase maps by use of a minimum-cost-matching algorithm, Applied Optics, vol. 34, pp. 5100-5108.
36. Chavez, S., Xiang, Q. and An, L., (2002), Understanding phase maps in MRI: a new cutline phase unwrapping method, IEEE Transactions on Medical Imaging , vol. 21, no. 8, pp. 966-977.
37. Chen, C. and Zebker, H., (2000), Network approaches to the two-dimensional phase unwrapping: intractability and two new algorithms, Applied Optics, vol. 17, pp. 401-414.
38. Cho, B., (2004), Quality map extraction for radar interferometry using weighted window," Electronic Letters, vol. 40, no. 8.
39. Collaro, A., Fornaro, G., Franceschetti, G., Lanari, R., Sansosti, E. and Tesauro, M., (1997), Local, global and unconventional phase unwrapping techniques, 1997 International Geoscience and Remote Sensing Symposium. Remote Sensing - A Scientific Vision for Sustainable Development, pp. 433-435.
40. T., (1996), Consistent 2-D phase unwrapping guided by a quality map, in IEEE Proceeding of the 1996 International Geoscience and Remote Sensing Symposium, Lincoln, vol. 4, pp. 2057-2059.
41. Flynn, T., (1997), Two-dimensional phase unwrapping with minimum weighted discontinuity, Applied Optics, vol. 14, pp. 2691-2701.
42. Fornaro, G. and Franceschetti, G., (1995), Two dimensional phase unwrapping based on the Laplace and Eikonal equations, 1995 International Geoscience and Remote Sensing Symposium, IGARSS '95. Quantitative Remote Sensing for Science and Applications, vol. 3, pp. 1828-1830.
43. Fornaro, G., Franceschetti, G. and Lanari, R., (1996), Interferometric SAR phase unwrapping using Green's formulation,'' IEEE Transaction Geoscience Remote Sensing, vol. 34, pp. 720–727.
44. Fornaro, G., Franceschetti, G., Lanari, R., Sansosti, E., and Tesauro, M., (1997), Global and local phase-unwrapping techniques: a comparison, Applied Optics, vol. 14, No. 10, pp. 2702-2708.
45. Ghiglia, D. C. and Romero, L. A., (1994), Robust two-dimensional weighted and unweighted phase unwrapping that uses fast transforms and iterative methods, Applied Optics, vol. 11, no. 1, pp. 107-117.
46. Ghiglia, D. C., and Romero, L. A., (1996), Minimum Lp-norm two-dimensional phase unwrapping, Applied Optics, vol. 13, No. 10, pp. 1999-2013.
47. Xu, W. and Cumming, I., (1996), A region growing algorithm for InSAR phase unwrapping, Proceedings of the 1996 International Geoscience and Remote Sensing Symposium, Lincoln, NE, May 27-31, IEEE, pp. 2044-2046.
48. 3. M. Arevalillo Herráez, D. R. Burton, M. J. Lalor and M. A. Gdeisat, "A Fast two dimensional phase unwrapping algorithm based on sorting by reliability following a non-continuous path," Applied Optics, Vol. 41, No. 35, pp 7437-7444, 2001.
49. K. Itoh, "Analysis of the phase unwrapping problem," Applied Optics, Vol. 21, No. 14, p. 2470, July 15, 1982.
50. Dennis Ghiglia and Mark Pritt, Two-dimensional phase unwrapping theory, algorithms and applications, John Wiley & Sons, 1998.

# References


51. Quan, C., Tay, C. J., Chen, L. J., "A study on carrier-removal techniques in fringe projection profilometry," Optics and Laser Technology Vol. 39, No. 6, September, 2007. p. 1155-1161.
52. Li J. L, Su X. Y, Su H. J, Cha S. S. Removal of carrier frequency in phase-shifting techniques. Opt Lasers Eng 1998; 30: 107-15.
53. Srinivasan V, Liu HC, Halioua M. Automated phase-measuring profilometry: a phase mapping approach. Appl Opt 1985, 24, 185-8.
54. Chen L, Quan C. Fringe projection profilometry with nonparallel illumination: a least-squares approach. Opt Lett. 2005, 30, 2101-3.
55. Chen L, Tay CJ. Carrier phase component removal: a generalized least-squares approach. J Opt Soc. Am A 2006, 23, 435-43.
56. Srinivasan, V., Liu, H. C., Halious, M., "Automated phase-measuring profilometry of 3-D diffuse objects," Appl Opt 1984, 23, 3105-8.
57. C. Quan, X. Y. He, C. F. Wang, C. J. Tay, and H. M. Shang. Shape measurement of small objects using LCD fringe projection with phase shifting. Optics Communications, 189(1–3):21–29, 2001.
58. Takeda M, Ina H, Kobayashi S., "Fourier-transform method of fringe pattern analysis for computer-based topography and interferometry," J Opt Soc Am 1982;72:156–60.
59. W. Schreiber, G. Notni, Theory and arrangements of self-calibrating whole-body three-dimensional measurement systems using fringe projection technique, Opt. Eng. 39 (1) (2000) 159–169.
60. Y. Y. Hung, L. Lin, H. M. Shang, B. G. Park, Practical three-dimensional computer vision techniques for full-field surface measurement, Opt. Eng. 39 (1) (2000) 143–149.
61. H. Liu, W. Su, K. Reichard, S. Yin, Calibration-based phase-shifting projected fringe profilometry for accurate absolute 3D surface profile measurement, Opt. Commun. 216 (1-3) (2003) 65–80.
62. X. Zhang, Y. Lin, M. Zhao, X. Niu, Y. Huang, Calibration of a fringe projection profilometry system using virtual phase calibrating model planes, J. Opt. A: Pure Appl. Opt. 7 (4) (2005) 192–197.
63. L. Zhongwei, S. Yusheng, W. Congjun, W. Yuanyuan, Accurate calibration method for a structured light system, Opt. Eng. 47 (5) (2008) 053604.
64. R. Anchini, G. Di Leo, C. Liguori, A. Paolillo, A new calibration procedure for 3-D shape measurement system based on phase-shifting projected fringe profilometry, IEEE Trans. Instrumentation and Measurement 58 (5) (2009) 1291–1298.
65. E. Zappa, G. Busca, Fourier-transform profilometry calibration based on an exhaustive geometric model of the system, Opt. Laser Eng. 47 (7-8) (2009) 754–767.
66. X. Chen, J. Xi, Y. Jin, J. Sun, Accurate calibration for a camera-projector measurement system based on structured light projection, Opt. Laser Eng. 47 (3-4) (2009) 310–319.
67. Z. Wang, H. Du, H. Bi, Out-of-plane shape determination in generalized fringe projection profilometry, Opt. Express 14 (25) (2006) 12122-12133.
68. H. Du, Z. Wang, Three-dimensional shape measurement with an arbitrarily arranged fringe projection profilometry system, Opt. Lett. 32 (16) (2007) 2438–2440.
69. X. Mao, W. Chen, X. Su, Improved Fourier-transform profilometry, Appl. Opt. 46 (5) (2007) 664–668.
70. D. Feipeng, G. Shaoyan, Flexible three-dimensional measurement technique based on a digital light processing projector, Appl. Opt. 47 (3) (2008) 377–385.
71. T. A. Clarke and J. G. Fryer. The development of camera calibration methods and models. Photogrammetric Record, 16(91):51–66, 1998.
72. J. G. Fryer and D. C. Brown. Lens distortion for close-range photogrammetry. Photogrammetric Engineering and Remote Sensing, 52(1):51–58, 1986.
73. J. Salvi, X. Armangu ́e, and J. Batlle. A comparative review of camera calibrating methods with accuracy evaluation. Pattern Recognition, 35(7):1617–1635, 2002.
74. Besl, P., Mckay, N., "A Method for Registration of 3-D Shapes," Trans. PAMI, Vol. 14, No. 2. 1992.
75. D. A. Field, "Laplacian smoothing and delaunay triangulations," Communications in Numerical Methods in Engineering, vol. 4, pp. 709–712, 1988.
76. [4] J. Vollmer, R. Mencl, and H. M ̈uller, "Improved laplacian smoothing of noisy surface meshes," Computer Graphics Forum, vol. 18, no. 3, pp. 131–138, 1999.
77. M. Desbrun, M. Meyer, P. Schr ̈oder, and A. H. Barr. Implicit fairing of irregular meshes using diffusion and curvature flow. Proceedings of ACM SIGGRAPH 99, pages 317–324, 1999.
78. L. Kobbelt, S. Campagna, J. Vorsatz, and H.-P. Seidel. Interactive multiresolution modeling on arbitrary meshes. In Proceedings of ACM SIGGRAPH 98, pages 105–114, 1998.
79. G. Taubin. A signal processing approach to fair surface design. In Proceedings of ACM SIGGRAPH 95, pages 351–358, 1995.
80. A. Belyaev and Y. Ohtake, "A comparison of mesh smoothing methods," in Proceedings of Israel-Korea Bi-National Conference on Geometric Modeling and Computer Graphics, 2003, pp. 83–87.
81. Jones TR, Durant F, Desbrun M. Non-iterative, feature-preserving mesh smoothing. Proceedings of the 30th Annual Conference on Computer Graphics and Interactive Techniques, 2003; 943–949.
82. Fleishman S, Drori I, Cohen-Or D. Bilateral mesh denoising. Proceedings of the 30th Annual Conference on Computer Graphics and Interactive Techniques, 2003; 950–953.
83. Mao, Z., Ma, L., Zhao, M., Xiao, X., "SUSAN structure preserving filtering for mesh denoising,", Vol. 22, No. 4, pp 276-284, April 2006.
84. Pfeiffer, J., Cerec 10 Year Anniversary Symposium (Chicago, IL: Quintessence), 1996.
85. Chen, L., Huang, C., "Miniaturized 3D surface profilometer using digital fringe projection," Meas. Sci. Techn. Vol. 16, No. 5, pp. 1061-1068, 2005.
86. Riehemann, S., Palme, M., Kuehmstedt, P., Grossmann, C., Notni, G., Hintersehr, J., "Microdisplay-Based Intraoral 3D Scanner for Dentistry," Journal of Display Technology, Vol. 7, No. 3, pp. 151-155, 2011.
87. Hart DP., Lammerding J., Rohaly J., " 3-D Imaging System," US Patent 2004/0155975 A1, Aug 12, 2004.
88. Trissel RG., "Polarizing multiplexer and methods for intra-oral scanning," US Patent 2007/0047079 A1, Mar 01, 2007.
89. Ernst MM., Neta U., Cohen C., Geffen M., "Three-dimensional modeling of the oral cavity," US Patent 2008/0273773 A1; Nov 6, 2008.
90. Dillon RF., Zhao B., Judell NHK., "Intra-oral three-dimensional imaging system," International Publication WO 2009/058656 A1, May 7, 2009.
91. Silvia L., Giordano F., Ari K., Michele C., Lapo G., Luciano B., "A Comparative Analysis Of Intraoral 3d Digital Scanners For Restorative Dentistry," The Internet Journal of Medical Technology, Vol. 5, No. 1, 2011.
92. ThorLabs, http://www.thorlabs.de/thorproduct.cfm?partnumber=DCC1645C. Accessed September 26, 2012.
93. Lanics Laser Electronics, http://www.lanics.com/products/diode-laser-dot.php. September 26, 2012.
94. Malacara, D., Servin, M., Malacara, Z., "Interferogram Analysis for Optical Testing," Second Edition. Taylor & Francis Group, 2005.
95. Greivenkamp, J. E., Bruning, J. H., "Phase Shifting Interferometry. Optical Shop Testing," Third Edition, D. Malacara, ed., (John Wiley, 2007), pp. 547–655, 2007.
96. Zhang, Z., "A flexible new technique for camera calibration," IEEE Trans. Pattern Anal. Vol. 22, pp. 1330–1334, 2000.
97. Huang PS, Hu Q, Jin F, Chiang F; Color-encoded digital fringe projection technique for high-speed three-dimensional surface contouring. Opt. Eng. 0001;38(6):1065-1071.
98. Bernardini, F.; Martin, I.M.; Rushmeier, H., "High-quality texture reconstruction from multiple scans," Visualization and Computer Graphics, IEEE Transactions on , vol.7, no.4, pp.318,332, Oct-Dec 2001.
99. B. Curless and M. Levoy. A volumetric method for building complex models from range images. In Proceedings of SIGGRAPH 96, ACM SIGGRAPH, Computer Graphics Proceedings, Annual Conference Series. pp. 303–312. August, 1996.
100. G. Turk and M. Levoy. Zippered polygon meshes from range images. In A. Glassner (ed), Proceedings of SIGGRAPH 94, Computer Graphics Proceedings, Annual Conference Series. pp. 311–318. July, 1994.
101. M. Soucy and D. Laurendeau. A general surface approach to the integration of a set of range views. IEEE Transactions on Pattern Analysis and Machine Intelligence, 17(4):344–358, April, 1995.
102. F. Bernardini, J. Mittleman, H. Rushmeier, C. Silva and G. Taubin. The ball-pivoting algorithm for surface reconstruction. IEEE Transactions on Visualization and Computer Graphics, 5(4):349–359, October-December, 1999.
103. M. Wheeler, Y. Sato and K. Ikeuchi. Consensus surfaces for modeling 3D objects from multiple range images. In Sixth International Conference on Computer Vision, IEEE. pp. 917–924. 1998.
104. A. Hilton, A. Stoddart, J. Illingworth and T. Windeatt. Reliable surface reconstruction from multiple range images. In Fourth European Conference on Computer Vision, pp. 117–126. 1996.
105. W. Lorensen and H. Cline. Marching cubes: a high resolution 3D surface construction algorithm. Computer Graphics, 21(4):163–170, 1987.
106. Lance Williams. Casting curved shadows on curved surfaces. In Proceedings of SIGGRAPH '78, pages 270-274, 1978.
107. Mark Segal and Kurt Akeley. The OpenGL Graphics System: A Specification (Version 1.2.1). www.opengl.org

# Q & A

명지대학교
MYONGJI UNIVERSITY

# Comments from Review Committee

명지대학교
MYONGJI UNIVERSITY

- ✓ Title should be focused
- ✓ Goals should be focused
- ✓ Contents should connected to each other
- ✓ Development word of the entire chapters should be reviewed
- ✓ Comparison with other Intraoral Scanners if possible.
- ✓ Some errors in the references, should be corrected

# Comments from Review Committee

명지대학교
MYONGJI UNIVERSITY



- ✓ Page 51 and 28 should be fixed
- ✓ Fig. 46 should be modified
- ✓ Fig. 1 should be rotated 90 deg
- ✓ Chapter 3 should be Comparison of Mathematical 3D Scanning System Models
- ✓ Chapter 6 should be Development of an Intraoral Scanner

# Special Thanks

I would also like to thank my dearest professor

Kang Park, Ph.D.,

the chair Kye Han Rhee, Ph.D.,
and the other members in my dissertation review committee,

Soo Jin Lee, Ph.D.,
Seungjae Min, Ph.D.,
Ji Hyun Yang, Ph.D.,

for their valuable time and suggestions.

명지대학교
MYONGJI UNIVERSITY

# THE END



*Furqan Ullah*
*furkan@mju.ac.kr*
*Myong Ji University,*
*South Korea*